Reports

1970

Utilization of physical and mathematical models in marine water resources research, planning and management : a final report

Willliam J. Hargis Jr.
Virginia Institute of Marine Science

UTILIZATION OF PHYSICAL AND MATHEMATICAL MODELS IN MARINE WATER RESOURCES

RESEARCH, PLANNING AND MANAGEMENT

(CONTRACT NO. 14-01-0001-1597, C-1214 AND CONTRACT NO. 14-01-0001-1983, C-1428)

A FINAL REPORT

(Covering the period 1 September 1967 - 30 September 1969)

by

William J. Hargis, Jr.

Project Director

Virginia Institute of Marine Science
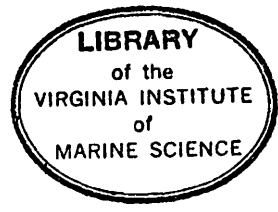
Gloucester Point, Virginia 23062

June 1970

TABLE OF CONTENTS

ABSTRACT

During the period 1 September 1967 to 30 September 1969, Virginia Institute of Marine Science personnel were engaged in hydraulic model studies, mathematical and computer studies, and instrument and technique development.

An investigation was made into the stability and reproducibility of an estuarine hydraulic model. Studies were made of the dispension of point-source dye releases in an estuarine hydraulic model, and of the applicability of the results to the release of disease-resistant seed oysters.

Analytical studies were made of diffusion in estuaries and of the integro-differential equations for estuarine flow. Computer studies were made of two-dimensional estuarine circulation and of solution of the one-dimensional equations by analogue simulation.

Development was carried out on an automated recording salinometer and on a miniaturized current meter for hydraulic models. Computer techniques were developed for use in hydraulic model work.

iv

UTILIZATION OF PHYSICAL AND MATHEMATICAL MODELS IN MARINE WATER RESOURCES

RESEARCH, PLANNING AND MANAGEMENT

(CONTRACT NO. 14-01-0001-1597, C-1214 AND CONTRACT NO. 14-01-0001-1983, C-1428)

A FINAL REPORT

(Covering the period 1 September 1967 - 30 September 1969)

by

William J. Hargis, Jr.

Project Director

Virginia Institute of Marine Science

Gloucester Point, Virginia 23062

INTRODUCTION

Estuarine and coastal waters are generally the most complex in
the hydrosphere. Chemically, physically, biologically and geologically
they are a dynamic mix of many variables. This complexity is compounded by
the pressures of man and his societal activities which increase alarmingly
in number and scope.

Estuarine and coastal waters also are the most useful to man and
in demand. While explaining the increasing pressures for uses, some
destructive and some not, mounting and diversifying demand coupled with our
strong dependence on a reasonably clean and productive marine environment
makes active concern for maintenance of the quality of that environment of
paramount importance.

To preserve the quality and utility of coastal and estuarine
waters and their resources we must develop a thorough understanding of the

complexities involved and their subordinate variables. We also must develop techniques for acquiring requisite scientific knowledge, for making sound engineering studies and for using the information thus obtained in development and operation of sound planning and management programs. Planning and management of the resources of the coastal zone require, in addition to knowledge--ability to evaluate, predict and manipulate.

Among the techniques that will be of great aid in this complicated and important work are those of a) physical modeling and b) mathematical modeling. Both techniques are in use for these purposes. Both are undergoing development and refinement. Each has its weaknesses; each its champions; and, each its potentials. To determine and evaluate the strengths, the weaknesses and potentials involved and to improve their capabilities and utility were among the original goals of this project. This work, still in progress when the OWRR funding terminated, is being continued.

VIMS was in a fortunate position to undertake this work because of a) previous experience with both physical and mathematical modeling techniques, b) ownership, with the Corps of Engineers, of an hydraulic model of the tidal James River, a major tributary of the mighty Chesapeake Bay system, and c) access to intermediate- and high-speed computers, software and programmers. In addition, our scientists have actually participated in design, construction, verification and use of hydraulic models. This use involved actual solution of scientific questions and practical problems relating to evaulation, planning and management of estuarine resources (Hargis, W.J., Jr. 1966).

Beginning in late 1967 and early 1968, through auspices of this Office of Water Resources Research (OWRR) grant, an extensive program involving models was undertaken. Of major importance in this OWRR program was ability to develop mathematical models from "prototype" data, i.e., from nature, and to test determinations and predictions made mathematically by use of the physical or hydraulic scale model. We planned also to utilize experimental results from the scale model to develop mathematical and verbal concepts of the physical features of the tidal James.

We planned further to investigate existing Froudian hydraulic models to determine their physical limitations and potentials and to develop improvements where possible. Included in the program, as it subsequently developed, were plans to improve utility of mathematical and hydraulic models by critically applying them to as wide a variety of planning and management problems as possible.

NARRATIVE HISTORY OF THE PROGRAM

(A complete list of people involved in the program is attached, Appendix I.)

From 1 September 1967 to April 1968, when the two hydraulics mechanics specialists Dr. Yee-chang Wang and Dr. Paul V. Hyer who worked in this program joined the staff, the project was hampered by lack of personnel. Delay in inception of the program from spring to fall when personnel are traditionally hard to find made recruiting difficult.

Despite serious lack of key, full-time specialists, it was possible to undertake certain work during this early period, namely:

1. Preliminary planning of mathematical and hydraulic
   modeling studies designed to examine the hydraulic
   model, itself.

2. Development of model research agreements and schedules
   with U. S. Waterways Experiment Station (hereafter WES)
   at Vicksburg, Mississippi where the James River hydraulic
   model is located.

3. Study of the relationship between salinity in the estuarine
   portion of the James, as determined at the recording
   salinometer station near the James River Bridge (Miles
   Watch House - Newport News), and freshwater inflow into
   the system at the fall line at Richmond (and the Susquehanna
   River). (MacIntyre and Ruzecki)

4. Attempts to develop a mathematical model of the tidal
   James using the Ketchum technique.

5. Evaluation, using available prototype and hydraulic
   model data and mathematical predictive techniques, of
   the probable effects of a proposed tidal exclusion dam
   (at Jamestown Island) on the hydraulics of the estuary--
   a practical problem.

Results of the research efforts are described and/or discussed
below. Though not a part of this project, it is of interest to note that
during this period the hydraulic model of the James also was used to:

1. Establish a suitable location of the outfall of the
   Jail Point treatment plant of the Hampton Roads
   Sanitation District Commission and evaluate its
   effects. (Cooperative program between VIMS and WES
   and the Hampton Roads Sanitation District Commission).

2. Study the effects of a proposed waterfront development and landfill project at Newport News Point on circulation and sedimentation of the nearby Hampton Roads area and examine different possible project designs (City of Newport News-VIMS project).

3. Examine existing sediment characteristics of the Norfolk Harbor Reach of Hampton Roads (U.S. Navy and the Corps of Engineers, WES).

4. Consider possible environmental effects of heated-water effluent from the proposed Hog Island (Surry County) nuclear power generating plant. Also examined were alternate locations and designs of intakes and outfalls for this installation (Virginia Electric and Power Company).

After Dr. Wang and Dr. Hyer joined the staff in April 1968 to devote full attention to the program, operations increased markedly and, despite difficulties of scheduling caused by high demand for use of the hydraulic model by FWPCA, the Corps of Engineers, the Navy and others, considerable work has been possible. Involved have been:

1. Hydraulic Model Studies

    a. Examination of the ability of an estuarine hydraulic model to attain steady states and reproduce them (Mr. Hyer, see below).

    b. Studies of dilution, dispersion and trajectory of simultaneous point-source dye releases (Mr. Ruzecki and Moncure, see below).

c. Consideration of the significance of the findings determined by study b (above) to production of seed and market oysters in the biologically and economically important middle James and to develop plans for management and improvement of those biological resources (W. J. Hargis, Jr., See resumé presented below in narrative form).

2. Mathematical and Computer Studies

a. Theoretical studies on diffusion in estuaries (Dr. Wang, see below).

b. The integro-differential equations for estuarine flow, (Dr. Wang, see below).

c. Further studies on the integro-differential equations for estuarine flow, (Dr. Wang, see below).

d. Estuarine computer models: 1) a preliminary two-dimensional computer study of the boundary-value problem for advective-diffusive estuarine circulation, and 2) preliminary attempts at development of techniques for analogue computer simulation on a digital machine, (Dr. Hyer, see below).

3. Instrument and Technique Development

a. Development of an automated recording salinometer for use in hydraulic scale models (Dr. MacIntyre, see below).

b. Development of a miniaturized current meter for use in hydraulic scale models, (Mr. Ruzecki, see below).

c. Comparative studies of automation in hydraulic models elsewhere, (Dr. Hyer, Dr. Nichols and Dr. Hargis, preliminary report in narrative below).

d. Development of computer technology for use in hydraulic

model work (Dr. Hyer, Mr. Moncure and Dr. MacIntyre,

preliminary report in narrative below).

During the course of this OWRR sponsored research project,

personnel have undertaken, by request, several advisory activities growing

directly out of their mathematical and hydraulic modeling experiences and

capabilities. Additionally, plans for future studies in this continuing

program have been formulated.

RESULTS

As indicated immediately above, activities carried out under this

OWRR program may be roughly classified into a) hydraulic model studies,

b) mathematical model studies, c) instrument and technique development

projects, and d) prediction and advisory efforts. For convenience, they

are so presented.

Due to the broad nature of this cooperative effort between the

Office of Water Resources Research and VIMS, it must be considered and

treated as a program consisting of a number of projects and activities,

each designed to contribute to the objectives of the overall effort. The

projects have been undertaken individually and/or collectively within the

framework of the program and after considerable discussion and thought de-

signed to establish priorities and operational feasibility.

A central purpose of the program was to evaluate the capabilities

and potentialities of estuarine hydraulic models, specifically the James

River Model and to improve them where necessary and·possible. Development

and refinement of mathematical models of estuarine circulation was another.
Also, it was proposed to use hydraulic modeling capabilities in development
and testing of mathematical models. We also planned to consider the utility
of mathematical and scale modeling techniques and capabilities developed in
this work in scientific research and engineering developments on estuarine
and coastal waters and in practical activities relating to planning and
management.

Some, but not all, of these objectives have received fruitful
attention as will be shown. We have made significant progress in evaluating
hydraulic models and in developing mathematical concepts. Practice advisory
activities have taken place and improvements in hydraulic modeling instru-
mentation and data handling techniques have ensued.

Though the subprojects reported below are integral parts of the
large or master project, they were conducted separately.

HYDRAULIC MODEL EXPERIMENTS

Steadiness and Repeatability in an Hydraulic Model

Paul V. Hyer[1]

ABSTRACT

Experiments were run on the James River hydraulic model to
determine its ability to reach a steady state and to repeat it. Aberration
of the tide generator prevented the reaching of a truly steady state, and
uncertainty of the freshwater inflow limited the ability to approach
the same steady state twice. Tidal salinity variations can be viewed
as a cyclic translation of an otherwise stationary salinity distribution.

---

[1]Associate Marine Scientist, Virginia Institute of Marine Science,
Gloucester Point, Virginia.

LIST OF SYMBOLS

The following symbols are used in this paper:

A = cross sectional area of an estuary.

$|\ |$ = absolute value.

CFS = cubic feet per second.

D.F. = degrees of freedom.

DLT = longitudinal dispersion.

dQ = uncertainty in river discharge rate.

$\dfrac{d\ S}{d\ x}$ = rate of change of salinity with distance from river mouth upstream.

dZ = uncertainty in measured height of water in weir.

Δt = aberration in length of tidal period.

ΔS = fluctuation salinity caused by abberation in length of tidal period.

L = distance from river mouth to upstream limit of saline intrusion.

N = total number of salinity observations at a station and tidal stage.

$^o/oo$ = parts per thousand. Measure of salinity of an aqueous solution.

P = pressure.

Q = river discharge rate.

ρ = density.

S = salinity.

SBE, SBF - tidal stages; slack before ebb, and slack before flood, respectively.

S_i = an individual salinity sampling of a station and tidal stage.

$\overline{S}_{j\ to\ N}$ = the average of the salinity samplings at a station and tidal stage, starting with the jth and proceeding to the last.

S_o = the mean salinity at the river mouth, used as a reference value.

S_R = the tidal range of salinity.

Σ = summation.

T = duration of a tidal period, temperature, index of statistical significance of observed difference.

t_r = ratio of scale time length in the prototype to that in the model.

X = distance upstream from river mouth.

X_r = ratio of prototype horizontal scale to that of the model.

y_r = ratio of prototype vertical scale to that of the model.

INTRODUCTION

To be useful as a research tool, an hydraulic model must be capable of being brought to a steady state. As used here, "steady state" signifies the condition wherein the current, tidal height, and salinity at any point in space remain the same from one tidal cycle to the next at any given state of the tide. An hydraulic model must also be capable of being brought to the same steady state in separate experimental runs under identical operating conditions. It was felt that a study should be made to find out if an hydraulic model could satisfy these elementary demands. (As far as could be determined, there has been no other investigation of this sort.) Accordingly, the author investigated this subject, using the James River hydraulic model housed at the Waterways Experiment Station in Vicksburg, Mississippi.

DESCRIPTION OF TESTS

Model Operation - The James River hydraulic model is a Froude model; that is, a model designed to reporduce the flow occurring under the influence of gravity in a natural system, or prototype (Ippen, 1963).

The physical quantity modeled is the square of the ratio of the horizontal speed of water motion to the propagation speed of shallow-water waves. The formula expressing this correspondence is:

$$(1) \quad \frac{Xr^2}{tr^2} \quad \frac{1}{yr} \quad = \quad 1$$

where Xr is the ratio of river horizontal length scale to that of the model, yr is the ratio of depth scales, and tr the ratio of time scales. The horizontal and time scales for the model are chosen for convenience, leaving the depth scale to be determined from the above equation. It can be seen from Table 1 that the model is distorted, i.e., the horizontal scaling factor is different from the vertical one. A Froude model will not reproduce turbulent mixing, because it is impossible to preserve both the Reynolds number and the Froude number in a model using water as the working fluid (Von Arx, W.S., 1962). Model turbulence is therefore generated artificially in the wakes of tabular roughness elements, which extend upward from the floor of the model. The roughness elements are bent up or down until they produce the proper degree of local turbulence to make the model function similarly to the river under similar conditions of flow and tide. Descriptions of model operation are to be found elsewhere (American Society of Civil Engineers, 1942 and U. S. Army Corps of Engineers, 1966).

Fresh water is introduced at the fall line at Richmond (Figure 1) and at the headwaters of the Chickahominy, Appomattox, and Nansemond rivers. There is a tide-generating mechanism at the "Atlantic Ocean" end of the model. Prior to starting the model for the experiments reported herein, one dam was placed at the river mouth, and another far upstream (Figure 1). Below the downstream dam, the model was filled with water having a salinity of 24 ^{o}/oo (parts per thousand). Between the two dams, the basin was filled

with water having a salinity of $6\ ^o/oo$. Above the upstream dam the water was fresh. At the start of an experiment, the dams were removed and the tide generation and freshwater inflow begun.

Experimental Procedure - Because salinity was the fluid property which could be most satisfactorily measured with the available equipment, water samples were taken at several points along the model (Figure 1). The number of sampling stations varied from test to test because the spatial extent of salinity intrusion depended on the volume discharge of the river. The sampling points and discharge rates for the various tests are summarized in Table 2.

Samples were taken periodically along the model at local high-water slack and again at the low-water slack occurring 1.5 tidal cycles later. "Slack water" refers to the short period of time when the surface water is relatively motionless and the tidal current is about to reverse.

There are several advantages in choosing these tidal stages for sampling: first, these times are clearly defined in the tidal cycle; second, because the water is nearly motionless, the length of time taken to draw a sample is not critical; third, the salinity at these times is close to one extreme or the other, so that fluctuations may be readily observed. This choice has also a practical advantage. The slack water tidal stage propagates upstream from the river mouth, so that only two investigators are required to reach all stations along the river in time to sample at local slack water.

A sampling run proceeded as follows: water samples were drawn off by means of a rubber syringe at local high water slack from both surface and bottom and were then stored in 100 ml sample bottles. After the entire length of the model had been sampled, the bottles were capped

and identified according to depth, station, tidal stage, and tidal cycle number. For the last three tests, samples were taken again at the low water slack coming 1.5 tidal cycles after the high water slack. This procedure was repeated periodically beginning early in the test so that both the initial transient process and the smaller fluctuations occurring later in the test could be observed.

Analysis - At the end of a test, the water samples were stored under constant $\pm^{o}C$) temperature conditions. The salinity of each sample was measured using a Beckman RS7-A inductance salinometer, to an accuracy of ± 0.05 $^{o}/oo$.

SUMMARY OF MODEL TESTS

Steadiness - Figures 2 through 6 summarize the results for surface salinity for the first three of the tests. Generally there is an initial transient period in which the initially discontinuous spatial distribution of salinity approaches a continuous distribution.

If one chooses as a criterion for steadiness that the salinity at a point in space at a given tidal stage be held constant ± 0.1 $^{o}/oo$, a steady state is never reached in the James River hydraulic model. Given the typical values of longitudinal salinity gradient extant in the model, this resolution in salinity corresponds to a longitudinal spatial resolution in the location of an isohaline of ± 1 km (prototype). (The vertical dashed line appearing in Figures 3 through 6 represents a point in time at which the model was disturbed greatly. The discussion of steadiness relates to events prior to this point in time.) At best the performance is "steady" only in the sense that there is a span of time in which the salinity shows no trend. The quantitative requirement is that the ensemble of partial averages for a sequential group of samples from N' to N, i.e.:

$$\overline{S}_{j\,to\,N} = \frac{1}{N-j+1} \sum_{i=j}^{N} S_i \quad , \quad j = N, N+1, \cdots N$$

be held constant ± 0.1 ^{o}/oo for at least 75 tidal cycles. Seventy-five tidal cycles is, to an integral number of sampling intervals, equivalent to a month's lapse of time in the prototype. A month is about as long as the prototype itself exhibits any sort of steady behavior. This criterion is sometimes met and sometimes not. In Figures 2 through 6, brackets delineate the limits of the "steadiness" span of time for a given station. Where there are no brackets for a station, a net trend existed in the measured salinity.

It is instructive to consider the various factors which would cause fluctuations of the observed salinity even long after the experiment was started, and to weigh their relative importance.

One begins by distinguishing between errors involved with the testing program and sources of fluctuation intrinsic to the apparatus.

A. Errors in testing program

    1. Error in position from which sample drawn

    2. Error in tidal stage at which sample drawn

    3. Error of salinity measuring instrument.

B. Fluctuations in model operation

    1. Fluctuation of sump salinity

    2. Fluctuations of river discharge

    3. Aberrations of tide generator

Concerning factor A1, the rate of change of salinity with distance upstream, even early in the experiment, is less than 0.4 ^{o}/oo m^{-1}, and the vertical rate of change is less than 0.3 ^{o}/oo cm^{-1}. The latter

could conceivably be important for surface samples because a rubber
syringe was used to draw the samples, and the depth from which the surface
sample was taken depended somewhat on the judgment of the investigator.
Correlation coefficients were calculated between the surface and bottom
salinities at the same stage of the tide at the same station, however,
and these coefficients were in almost all cases 0.75 or more, suggesting
that this factor is of minor importance as a cause of salinity fluctuation.

Correlation coefficients were also used to evaluate factor A2
as a cause of the observed fluctuation. The correlation between surface
salinities at two adjacent stations proved to be quite high, ranging from
.80 to .96. Since adjacent stations are in practice sampled by different
people this factor is relatively unimportant in explaining the observed
fluctuations.

The accuracy of the inductance salinometer has already been
stated to be much smaller than the range of fluctuation actually observed.
Factor A3 is the least important of those to be considered.

The sump salinity does fluctuate, but is not a major cause of
the fluctuations of salinity at other points on the model. This con-
clusion is based on the fact that the correlation coefficient between the
sump salinity and the salinity at the river mouth is quite low for each
test.

The normal tidal variation of salinity over a tidal cycle can
be viewed, to a first approximation, as a cyclic translation of an other-
wise stationary pattern of isohalines (Preddy, W.S., 1954). One can see
by comparing Figure 3 with Figure 5 that the extreme position of advance of the
salinity pattern depends on the river discharge: the fresh water serves
to "drive back" the ocean water. Hence, factors B2 and B3 would tend to
produce the same effects on the measured salinity, i.e.:

Positive salinity deviation is caused by:

1. Excessive duration of flood tide;

2. insufficient duration of ebb tide;

3. decrease in river discharge.

Negative salinity deviation is caused by:

1. Excessive duration of ebb tide;

2. insufficient duration of flood tide;

3. increase in river discharge.

The flow meters used at the Waterways Experiment Station for freshwater input are Van Leer weirs, i.e., short channels having a water height gauge and a semi-circular cross section (U.S. Army Corps of Engineers, 1966). The water volume flow through the channel varies only with the measured height of water in the channel. The water input to the flow meter is controlled by a faucet so that once the freshwater inflow for a test is set it is unlikely to change accidentally for the duration of that test.

Relatively small fluctuations in the duration of the ebb or flood tide will produce measurable variations in the salinity at a point at a slack water. An appropriate formula based on an order of magnitude argument is:

$$(2) \quad \Delta t = \Delta S \ \frac{T}{2S_R} \ , \text{ where } \Delta S \text{ is an aberration}$$

in measured salinity at a station, Δt is the change in duration of ebb or flood needed to produce that effect, S_R is the range of salinity at the point, and T is the duration of the tidal cycle in seconds. For $\Delta S = 0.1 \ ^o/oo$ and $S_R = 4 \ ^o/oo$, one obtains $\Delta t = 5$ sec.

This much of a time error is entirely possible given the design of the tide generator used for the James River hydraulic model. Under

the present system, an operator monitors the action of the tide generator by comparing visually the actual tide record with a curve of the desired tidal height (U.S. Army Corps of Engineers, 1966). If the two disagree, he adjusts the tide height by manipulating the relay switches controlling the tide generator.

Reproducibility - Two experimental runs were made under the same conditions, with freshwater input set at 3,200 cfs. Neither test achieved a truly steady state, but the two tests agreed fairly well with one another. Statistical analysis was required to ascertain the significance of the measured difference in mean salinity between the two tests at various sampling stations. As can be seen from Table 3, the difference in mean salinity between the two tests is statistically significant at the 5% level in fewer than half the cases. The "T" shown is the standard index of statistical significance, i.e., the ratio of the difference in measured means to the pooled standard error (Snedecor, G.W., 1956).

There are two regions in the model where the differences in mean salinity are statistically significant: the first is in the mid-stream portion, where the differences between the mean salinities are maximal; the other is the extreme upstream end of the model, where the variances of the measured salinities are extremely small.

The difference in salinity distribution in the mid-stream portion of the model may be caused by a difference in freshwater input between the two tests.

The flow meters in use at the Waterways Experiment Station have already been described. The channels are sections of pipe having a diameter of 4", 2" or 1". For the experiments in question, the 2"

diameter weir was the largest used. The accuracy of the height gauge used is 0. 001' (American Society of Civil Engineers, 1942).

To obtain an estimate of the uncertainty in the freshwater input, one can, with fair reliability, use the formula appropriate for a V-notch weir (Streeter, V.L., 1961).

$$(3) \quad \frac{dQ}{Q} = \frac{5}{2} \frac{dZ}{Z}$$, where $\frac{dQ}{Q}$ is the relative uncertainty in the discharge and $\frac{dZ}{Z}$ is the relative uncertainty in the depth. For a 2" diameter weir nearly filled,

$$(4) \quad \frac{dQ}{Q} = 3\%$$

For estimating the relationship between an uncertainty in freshwater inflow and an uncertainty in mid-stream salinity distribution, one uses a one-dimensional, steady equation (Hansen, D.V.)

$$(5) \quad S = D_{LT} \frac{A}{Q} \frac{dS}{dx}$$, where D_{LT} is the longitudinal dispersion coefficient and $\frac{Q}{A}$ is the freshwater discharge per unit cross sectional area. If one assumes that, to a first approximation, a change in Q affects S but does not alter D_{LT} or $\frac{dS}{dx}$, then

$$(6) \quad \frac{dS}{S} = \frac{-dQ}{Q}$$, so that the uncertainty in S is also 3%.

It can be seen in Table 1 that the discrepancies between the two tests in the midstream portion of the model (stations 5, 18, and 22) are, with one exception, less than 5%, so that allowance for a possible systematic difference in freshwater input between the two tests will reduce the disagreement between the two tests to the point of statistical insignificance.

Concerning the discrepancies observed in the extreme upstream end of the model, it can be seen from Table 1 that there was a salinity inversion in the freshest water sampled, and that the stratification varied between tests. These effects appear to have been caused by a lack of equilibration in temperature between the .freshwater inflow (tap water) and the water already in the model, whose temperature was measured to be 25°C. ±1.5°C. The tap water temperature was not measured, but is estimated to be less than 20°C. Because density is a function of temperature, salinity, and pressure, a change in density $d\rho$ is

$$(7) \quad d\rho = \frac{\partial \rho}{\partial T}\bigg|_{S,P} dT + \frac{\partial \rho}{\partial S}\bigg|_{T,P} dS + \frac{\partial \rho}{\partial P}\bigg|_{T,S} dP$$

where ρ is the density, T the temperature, S the salinity, and P the pressure. Ignoring the pressure term and evaluating the other partial derivatives from a table (Neumann, G. and W.J. Pierson, Jr., 1966) using T = 25°C and S = 0 °/oo, one finds that a drop in temperature of 1°C is equivalent to an increase in salinity of 0.35 °/oo. Hence, relatively cool tap water could easily underride the more saline water in the model, thereby altering greatly the stratification in upstream regions.

Other Observations on the Experiments - Figures 3 through 6 show an abrupt drop in salinity at a certain time. These perturbations came about because of an unavoidable modification of the experimental setup for subsequent tests. The area above Weyanoke Pt. (Figure 1) was dammed off and flushed out. The original flow was then re-established, but in each case a charge of excess fresh water came downstream and depressed the salinity along the entire model. This occurred at cycle 285 for the first 3,200 cfs test, and at cycle 320 for the 1,000 cfs test. In neither case did the model recover completely from this flushing.

If the mean steady surface salinity profiles are plotted to the same horizontal and vertical scales in Figure 7, the resulting curves appear quite similar. The same is true for the third curve shown, which was drawn by Hansen (Hansen, D.V. and M. Rattray, 1965) from data obtained from the Delaware River hydraulic model by Pritchard (Pritchard, 1954). The empirical curve shown in the three graphs results from the equation

$$(8) \quad \frac{S}{S_o} = \text{Sin}^2 \left(\frac{\pi}{2} \left(1 - \frac{X}{L} \right) \right), \text{where} \quad \frac{S}{S_o}$$

is the salinity relative to the salinity at the river mouth, and $\frac{X}{L}$ is the distance from the river mouth divided by the scale length. This curve has the same general features as the gaussian curve obtained by Harleman (Ippen, A.T., 1963) assuming an x^{-1} functional dependence for the dispersion coefficient. It can be shown that if the sinusoidal form is put into equation (5), the longitudinal dispersion coefficient can be deduced:

$$(9) \quad D_{LT} = \frac{QL}{\pi A} \left[\csc \left(\pi \left(1 - \frac{x}{L} \right) \right) + \cot \left(\pi \left(1 - \frac{x}{L} \right) \right) \right].$$

This form has the same difficulty as the x^{-1} form considered by Harleman, namely that it becomes infinite.

These results suggest that there is an underlying similarity in longitudinal salinity distribution among estuaries, and that the topography, tidal current amplitude and discharge rate of a particular estuary affect only the scale length of the salinity distribution.

Figure 8 shows the range of surface salinity plotted againt distance upstream for two different values of river flow. Range is defined as the salinity at slack before ebb minus the salinity at slack before flood. These are not exactly the maximum and minimum values of salinity (Shidler, J.K. and W. G. MacIntyre, 1967) because of horizontal diffusion. Consider the one-dimensional equation for salinity in an estuary when the periodic variation of salinity is included:

$$(10) \quad \frac{\partial S}{\partial t} + U \frac{\partial S}{\partial x} = \frac{\partial}{\partial x} \left(D_{LT} \frac{\partial S}{\partial x} \right) .$$

The tide turns when

$$(11) \quad U = 0,$$

while the salinity reaches an extremum, when

$$(12) \quad U = \left(\frac{\partial}{\partial x} \left(D_{LT} \frac{\partial S}{\partial x} \right) \right) \left(\frac{\partial S}{\partial x} \right)^{-1} .$$

Instrumentation other than that employed in these tests would be required to determine the exact maximum and minimum of salinity. Two things are apparent from Figure 8:

1. the range is greater for the higher flow rate, and

2. the range drops off farther downstream for the higher flow rate.

Both of the observations can be explained by saying that the cyclic variation of salinity is the result of translation of isohalines (Preddy, W.S., 1954). Thus, when the isohalines are more crowded together, as they would be at the higher flow rate, the tidal range of salinity at a fixed point is greater. The central depression in salinity range at the lower flow rate appears to be caused by the mixing of waters from the Chickahominy, which meets the James between stations 27 and 21.

CONCLUSIONS

1. It has been shown that, given a reasonable set of starting conditions, the James River hydraulic model will achieve a state which is "steady," but only in the special sense that the salinity at a point in space and tidal stage shows no long-term tendency to increase or decrease. The salinity at a point in space and tidal stage was generally not held constant $\pm$ 0.1 ^{o}/oo.

2. The main reason for the observed fluctuation of salinity is aberrations of the tide generator, because this device is monitored and adjusted by a human operator who cannot correct an error in tide height quickly enough to prevent a measurable deviation in salinity.

3. Two experimental runs under the same starting conditions and operating conditions can produce similar "steady" state salinity distributions. The uncertainty of the freshwater inflow limits the degree of correspondence between the two experiments. The disagreement in measured salinity between the two tests is more often than not insignificant compared to the fluctuations observed in each individual test.

4. The far upstream salinity shows a salinity inversion, and the magnitude of this inversion varies from test to test. This effect seems to be caused by failure to equilibrate the temperature of the fresh-water inflow. The equipment for such an equilibration would not necessarily be elaborate or expensive.

5. An empirical model has been put forth in which a constant salinity distribution moves back and forth under tidal action, thereby producing the cyclic salinity variation seen at a point fixed in space. The surface salinity profile has a characteristic shape independent of the river discharge, which establishes the characteristic length only of the salinity intrusion.

ACKNOWLEDGMENTS

REFERENCES

American Society of Civil Engineers, Committee of the Hydraulics Division on Hydraulic Research, July 1942. Hydraulic Models.

Hansen, D. V. Salt balance and circulation in partially mixed estuaries, pp. 45-51, In G. H. Lauff, Estuaries, Washington, D. C., AAAS

Hansen, D. V. and M. Rattray, Jr. Gravitational circulation in straits and estuaries. J. Mar. Res. v. 23, No. 2, May 1965 pp. 104-122.

Ippen, A. T. 1963. ed. Estuary and Coastline Hydrodynamics. Cambridge Massachusetts. (Dept. of Civil Engineering, M.I.T.).

Neumann, G. and W. J. Pierson, Jr. 1966. Principles of Physical Oceanography. Englewood Cliffs, N.J. (Prentice Hall).

Preddy, W. S. 1954. The mixing and increment of water in the estuary of the Thames. J. Mar. Biol. Assoc. U.K. 33, p. 645-662.

Pritchard. 1954. A study of flushing in the Delaware model. Technical Report. C.B.I. No. 7, ref. 54-4.

Shidler, J. K. and W. G. MacIntyre. 1967. Hydrographic data collection for operation James River - 1964. Data Report No. 5. Virginia Institute of Marine Science.

Snedecor, G. W. 1956. Statistical Methods Applied to Experiments in Agriculture and Biology. Ames, Iowa (Iowa State College press.)

Streeter, V. L. 1961. ed. Handbook of Fluid Dynamics. New York (McGraw-Hill)

U. S. Army Corps of Engineers, September 1966. Effects of a proposed 35-foot channel to Richmond on currents and salinities over the seed oyster beds in the James River. Summary Report, Waterways Experiment Station, Vicksburg, Mississippi.

Von Arx, W. S. 1962. An Introduction to Physical Oceanography. Reading, Massachusetts. (Addison-Wesley).

TABLE 1. - Scaling factors used in the James River hydraulic model.

Quantity	Scaling Factor
Horizontal Distance	10^3
Vertical Distance	10^2
Salinity	1
Time	10^2

TABLE 2. – Summary of experimental conditions and sampling locations for the experiments.

Experiment	Richmond Discharge (CFS)	Total Discharge (CFS)	Station Designation	Distance Upstream from River mouth (km)
I	11,000	14,961	Sump	---
			H	0
			5	20
			18	38
			22	44
II, IV	3,200	4,168	Sump	---
			H	0
			5	20
			18	38
			22	44
			27	68
			21	85
III	1,000	1,297	Sump	---
			H	0
			5	20
			18	38
			22	44
			27	68
			21	85
			26	112
			31	125

TABLE 3

Station	Tide Stage	Depth	D.F.	T	First Test Mean	Variance	Second Test Mean	Variance
Sump	SBE	-----	6	0.667	25.30	.0047	25.39	.0786
Sump	SBF	-----	10	0.626	25.28	.0188	25.39	.1081
H	SBE	Surface	6	0.792	23.03	.0074	22.91	.0883
		Bottom	12	0.513	24.12	.0364	24.21	.0693
	SBF	Surface	6	1.720	21.40	.0820	21.67	.0137
		Bottom	12	0.147	22.98	.2358	23.03	.2570
5	SBE	Surface	6	1.048	20.21	.0075	20.35	.0652
		Bottom	6	1.5392	20.39	.0167	20.80	.1024
	SBF	Surface	12	0.6436	16.49	.0442	16.44	.0503
		Bottom	12	4.0768	19.41	.0089	19.88	.0448
18	SBE	Surface	12	2.6148	14.67	.0275	15.14	.0953
		Bottom	12	2.9200	15.54	.0467	16.02	.0591
	SBF	Surface	12	3.4906	10.57	.0167	11.07	.0619
		Bottom	6	0.3662	12.92	.0691	13.05	.4558
22	SBE	Surface	6	4.8580	10.26	.0065	11.06	.1248
		Bottom	6	2.6137	11.20	.0178	11.66	.1114
	SBF	Surface	6	3.7298	7.58	.0077	8.01	.0489
		Bottom	12	1.1633	7.85	.1262	8.15	.1067
27	SBE	Surface	6	2.2531	3.90	.0118	4.29	.1277
		Bottom	6	1.8151	4.76	.0113	5.02	.07215
	SBF	Surface	6	2.9466	2.68	.0038	2.92	.0220
		Bottom	12	0.8586	2.85	.0070	2.83	.0200
21	SBE	Surface	12	5.4996	0.50	.0023	0.72	.0030
		Bottom	12	1.2650	0.47	.0052	0.53	.0028
	SBF	Surface	6	7.2764	0.24	.0001	0.36	.0012
		Bottom	12	1.9391	0.22	.0002	0.23	.0001

TABLE 3. T-Test results for comparison of the two experiments run at 3,200 cfs.
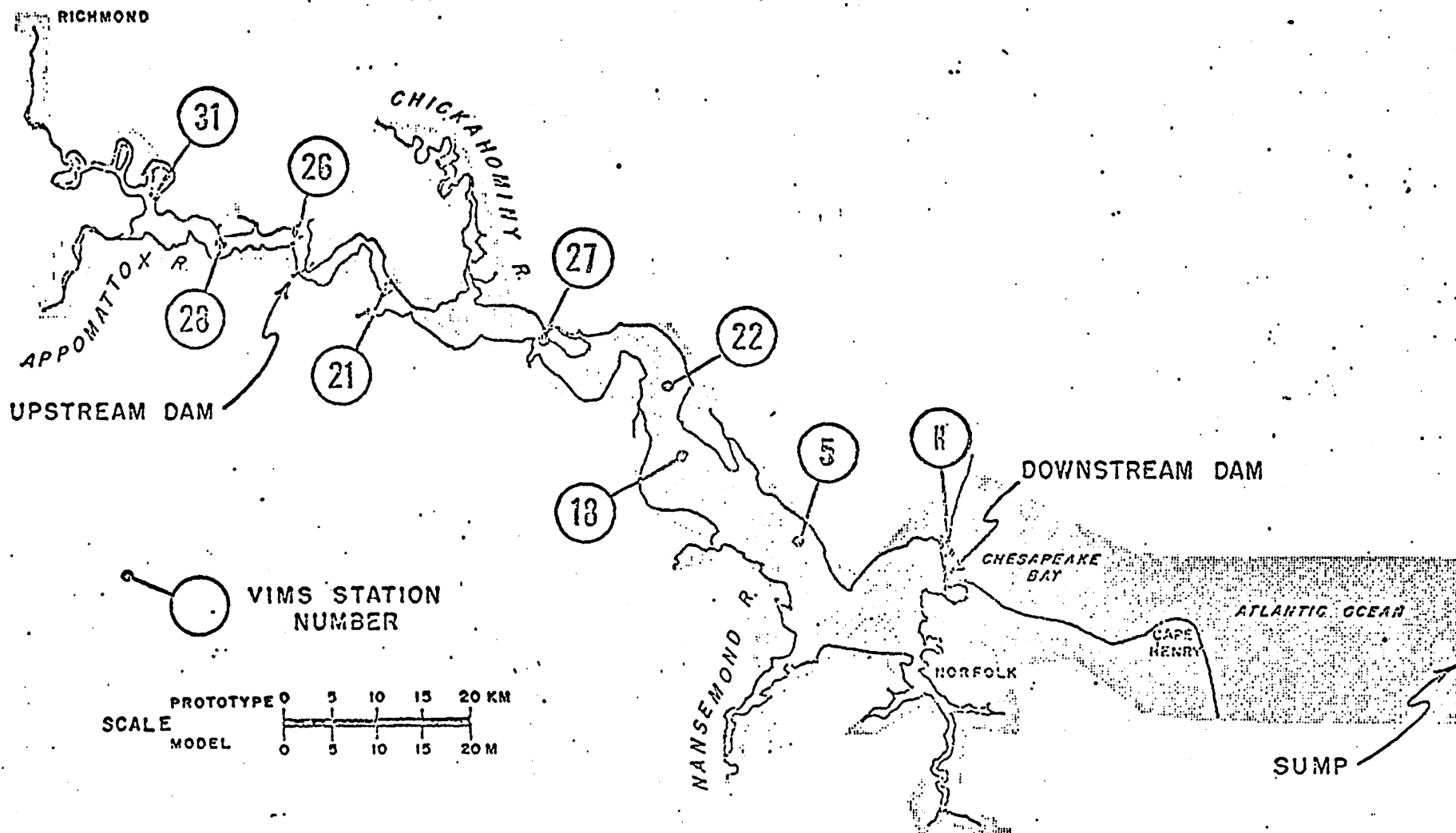
Figure 1.

Figure 2.

11,000 cfs.   SLACK BEFORE EBB

SUMP

RIVER MOUTH
(STA. H)

20 km. UPSTREAM   (STA. 5)

38 km. UPSTREAM   (STA. 18)

44 km. UPSTREAM   (STA. 22)

SALINITY, ‰

24

20

16

12

8

4

0

15   25   50   75   100   125

- 28 -

Figure 3.   - 29 -

3200 cfs, SLACK BEFORE EBB

SUMP

RIVER MOUTH   (STA. H)

20 km UPSTREAM   (STA. 5)

38 km UPSTREAM   (STA. 18)

44 km UPSTREAM   (STA. 22)

68 km UPSTREAM   (STA. 27)
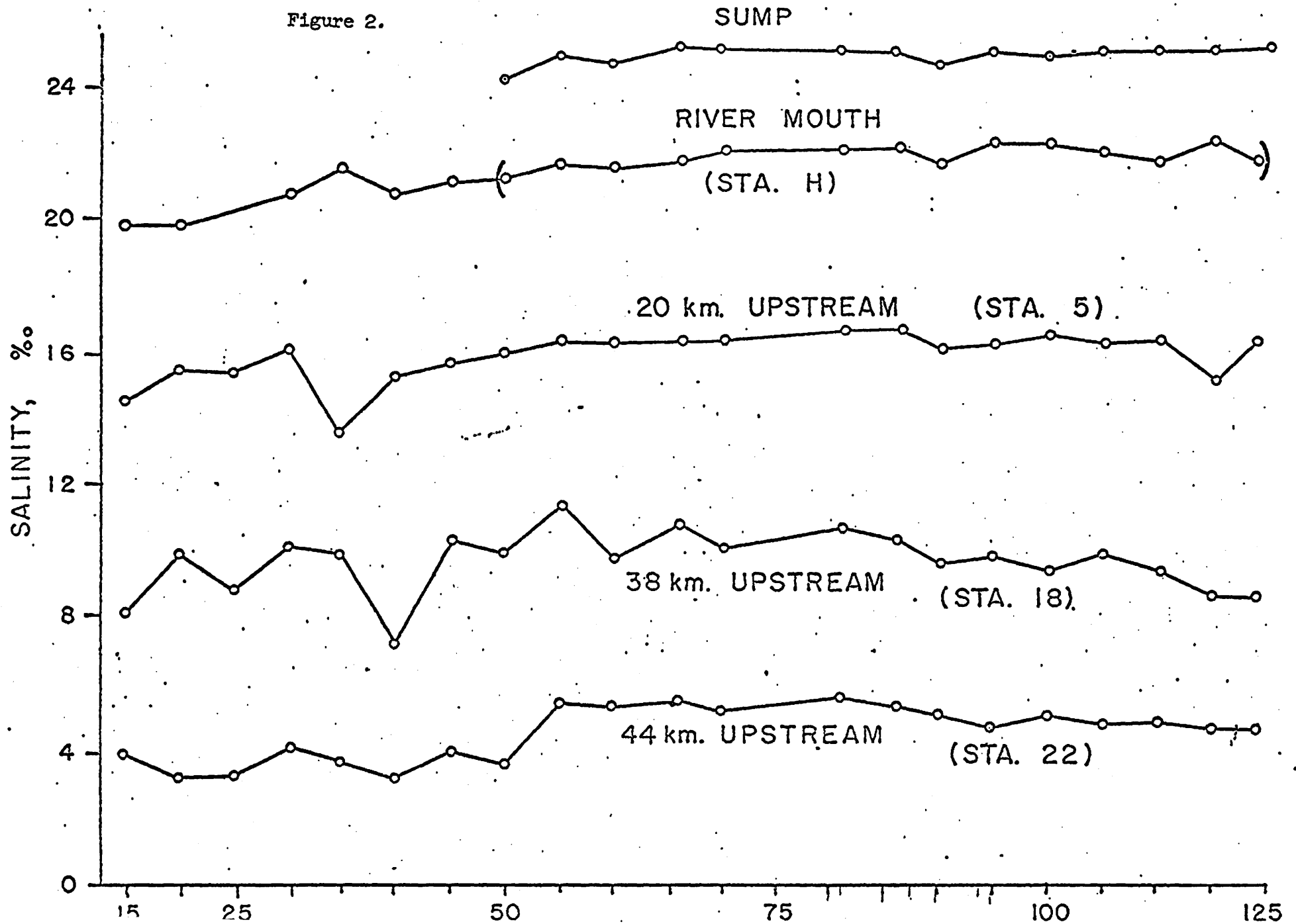
SALINITY ‰
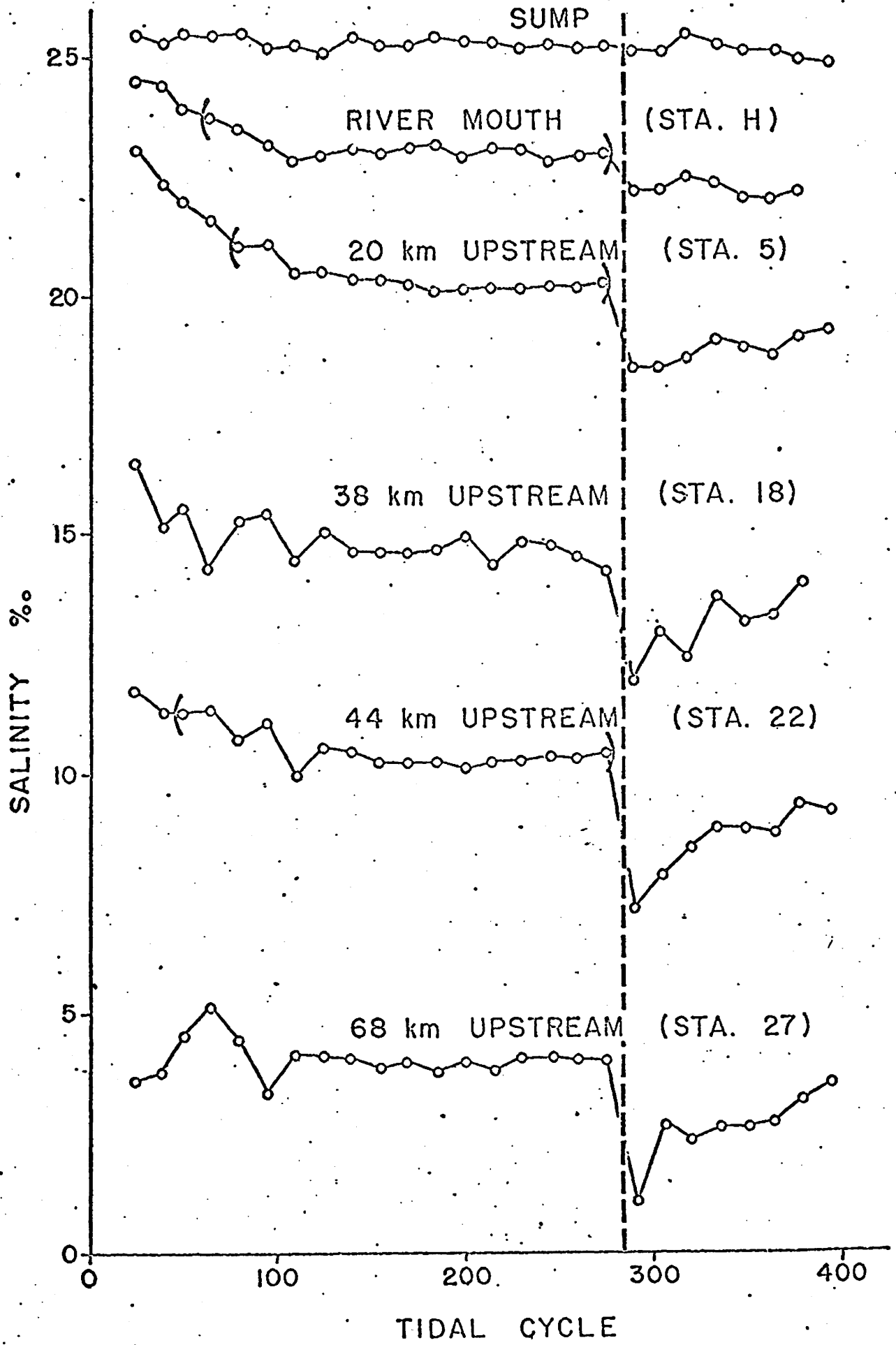
TIDAL CYCLE

Figure 4.

3200 cfs, SLACK BEFORE FLOOD

SUMP

RIVER. MOUTH (STA. H)

20 km UPSTREAM (STA. 5)

38 km UPSTREAM (STA. 18)

44 km UPSTREAM

(STA. 22)

68 km UPSTREAM (STA. 27)

SALINITY, ‰
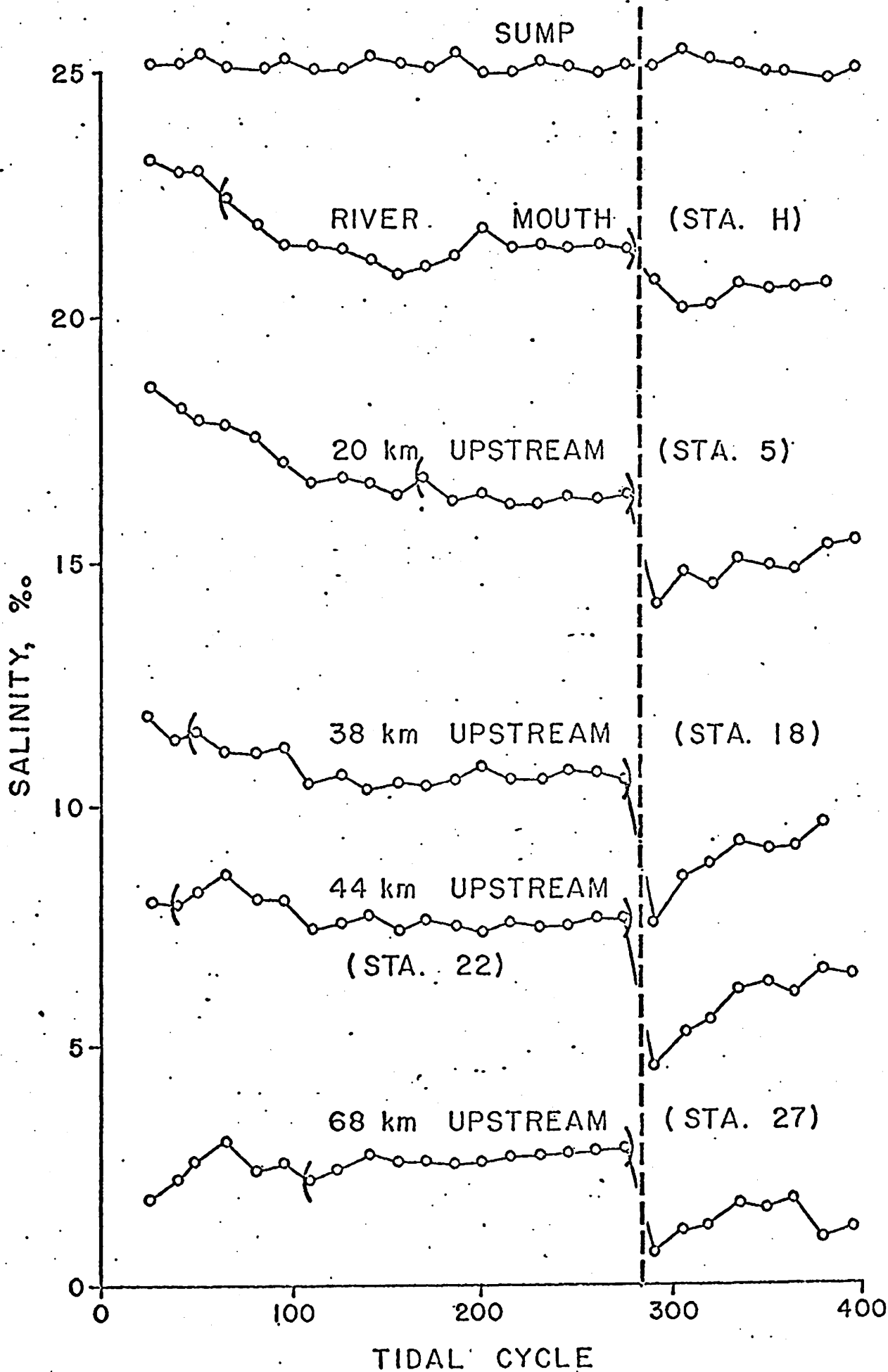
TIDAL CYCLE

Figure 5.

1000 cfs, SLACK BEFORE EBB

SUMP

RIVER

MOUTH (STA. H)

20 km UPSTREAM (STA. 5)

38 km UPSTREAM (STA. 18)

68 km UPSTREAM (STA. 27)

125 km UPSTREAM (STA. 31)

SALINITY, ‰

TIDAL CYCLE
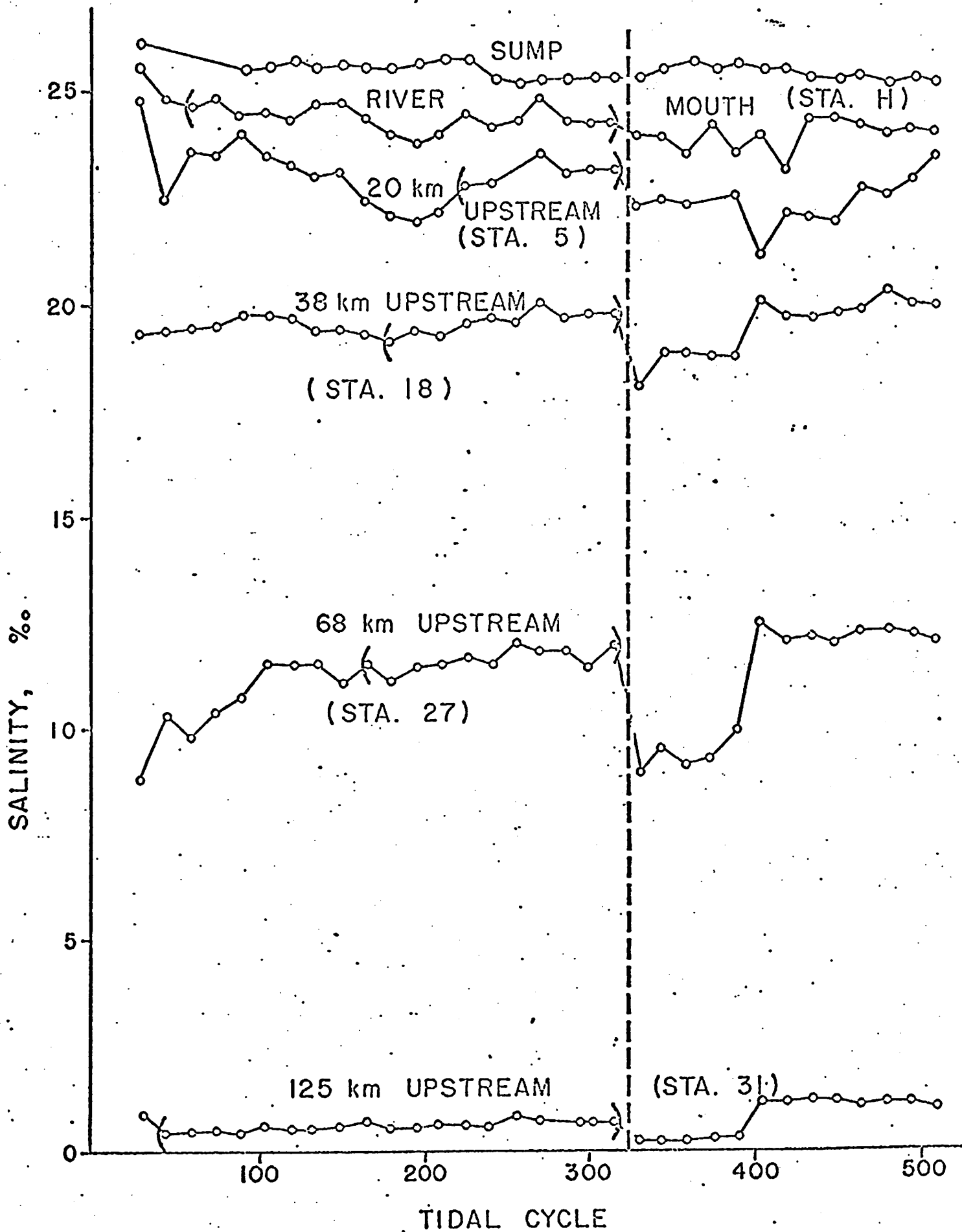
Figure 6.   - 32 -

Figure 6. 1000 cfs, SLACK BEFORE FLOOD
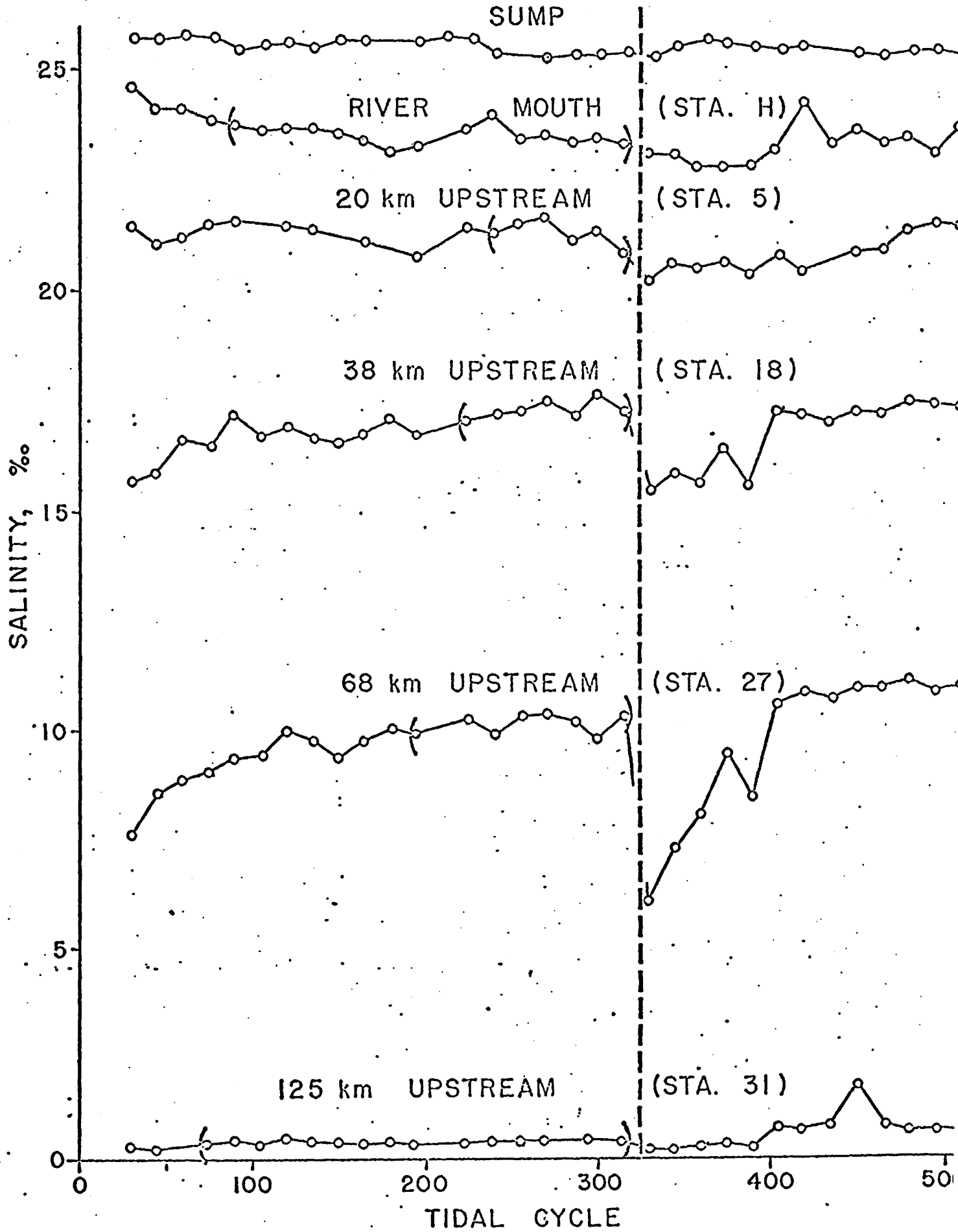
Figure 7.

AVERAGE SURFACE SALINITY
(·········· EMPIRICAL CURVE)

3200 cfs test

1000 cfs test

DELAWARE RIVER
MODEL
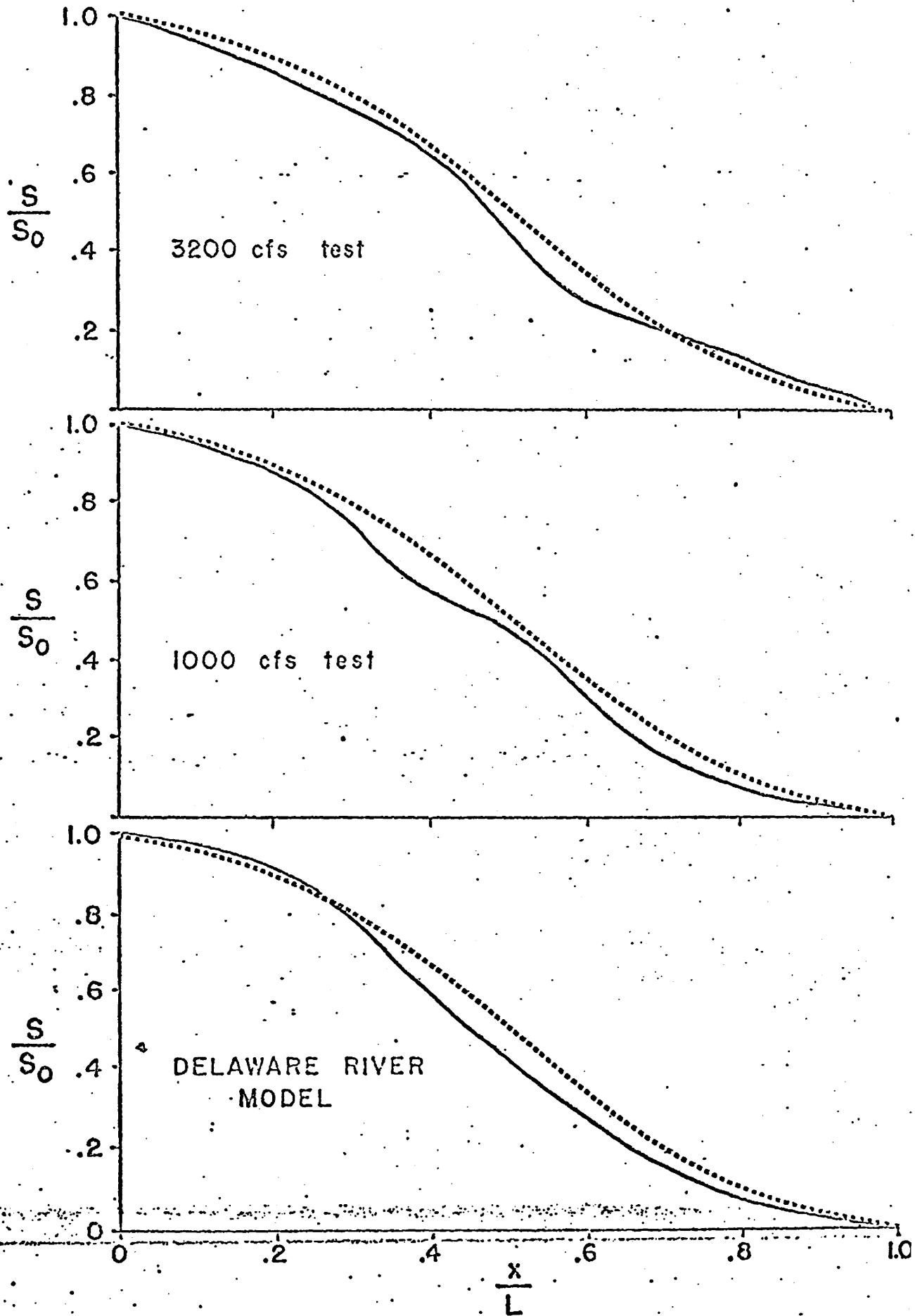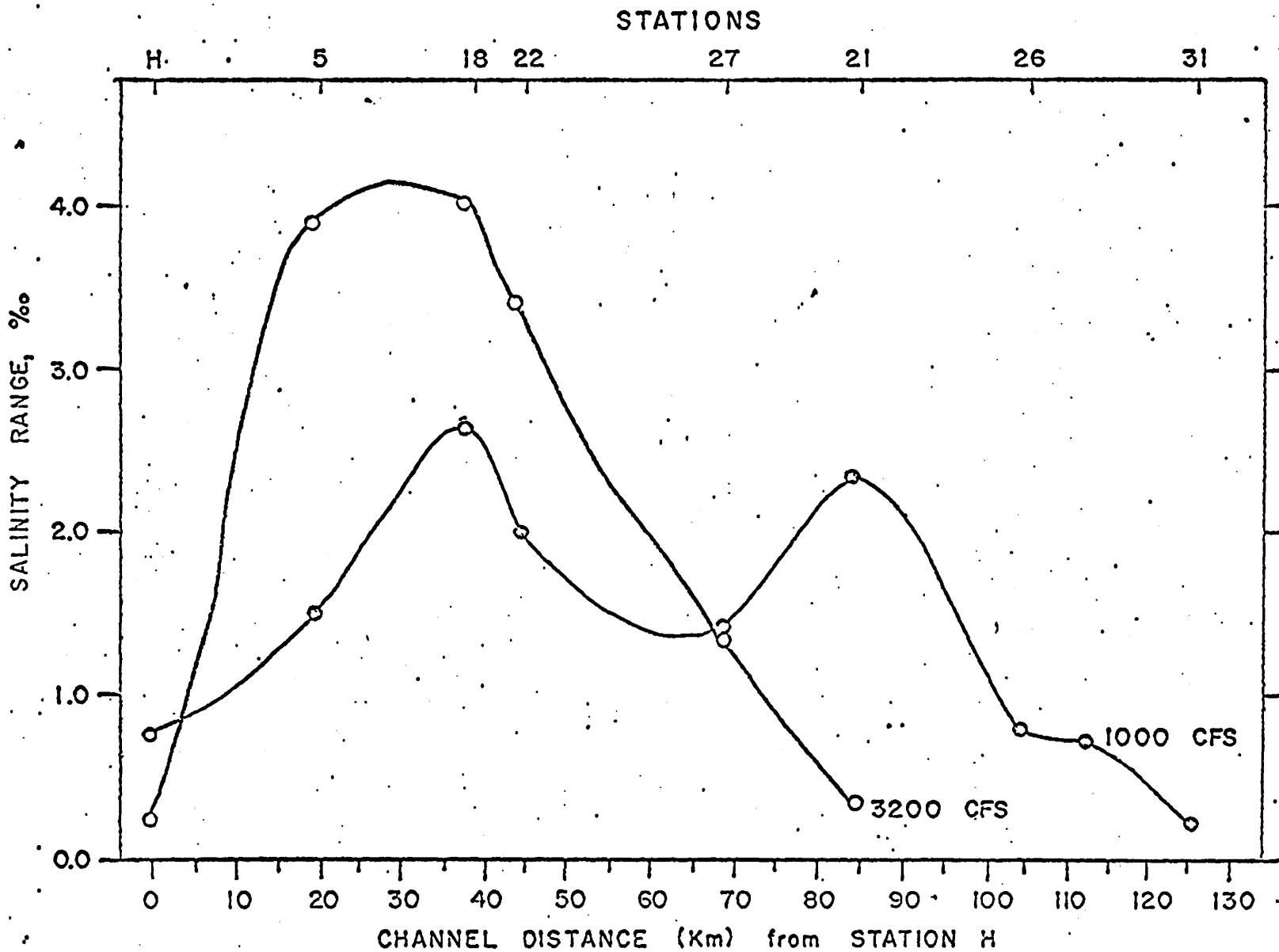
STATIONS

Figure 8. Range of Salinity During a Tidal Cycle vs Distance From Station H.

Dye Distribution Resulting from Point Releases

in the James River Model

E. P. Ruzecki[2] and R. W. Moncure[3]

INTRODUCTION

A quantitative experiment was conducted in the James River hydraulic model to determine the distribution of suspended particulate matter introduced at selected locations. The experiment was designed to aid in determining the best location for placement of disease resistant brood stock oysters in the James River to achieve the greatest concentration of larvae over oyster producing areas during the setting period (approximately thirty tidal cycles after spawning). Dye molecules were used to simulate oyster larvae in the model.

Two basic assumptions were made:

1. The James River hydraulic model will adequately duplicate the advection and turbulence of the real river under similar conditions of source salinity and freshwater inflow.

2. Oyster larvae behave as free-floating particulate matter in the real river and can therefore be simulated by dye molecules in the model.

[A complete description of the experimental procedure and results was included in the contract report, (Hargis, W. J., 1968).]

---

[2]Associate Marine Scientist, Virginia Institute of Marine Science,
Gloucester Point, Virginia

[3]Computer Systems Analyst, Virginia Institute of Marine Science,
Gloucester Point, Virginia

EXPERIMENTAL PROCEDURE

Solutions of the fluorescent dyes Pontacyl Brilliant Pink, and Fluorescene were injected at two locations within the model during each of three separate model runs. This resulted in a total of six distinct release points as shown in Figure 9. Dye releases were made at the bottom and consisted of twenty-five 50 ml injections over one tidal cycle.

Spatial and temporal fluctuations in the concentrations of each dye were determined by fluorometric analysis of samples removed from 108 locations as shown in Figure 10. The number of levels sampled at each location ranged from one to three depending on water depth. Samples were taken at local high and low slack water from twenty to forty tidal cycles after release for the first model run and from six to forty cycles after release for the second and third runs. Model conditions for each run were as follows: Source salinity and freshwater input were held constant at multi-annual summer mean values; a mean tide was generated.

Steady state was achieved by imposing these conditions on the model for 140 tidal cycles prior to dye injection. Final dye distributions throughout the entire model were determined by segmenting the model with dams, mixing the water within each segment, and analyzing twenty samples taken from each segment. This procedure was followed after the last samples were removed for each model run. Dam locations and segments are shown in Figure 11.

RESULTS

Dye Distribution - Two methods were used to determine the release location which would produce the most desirable dye distribution within the estuarine portion of the model.

In the first method (A) mean dye concentrations were determined for specific areas in the model over the period 25 to 35 cycles after injection. The areas chosen corresponded to known oyster producing areas in the James estuary. The second method (b) determined the percent of dye retained in various reaches of the model as a result of each release.

Method A used integrated (surface to bottom) dye concentrations for stations within each of five selected areas (designated as Regions of Particular Interest in Figure 9) for each set of samples. These values were used to calculate the average quantity of dye within each of the five areas for the period of time between 25 and 35 cycles after release. The averages were then used to determine the effectiveness of each release point in distributing dye over the selected areas during the setting period for oyster larvae. Release points were ranked according to effectiveness. Results, shown in Table 4, indicate that release point 2 (off Mulberry Island) was the most effective.

TABLE 4

Mean quantity of dye per unit horizontal area (relative units) for particular areas of interest for each of six dye release points.

Release Point

AREA OF INTEREST	1	2	3	4	5	6
A	2700	3370	1097	1658	1690	1570
B	3732	5690	2736	4039	2160	2170
C	2190	3500	1189	2413	1020	1064
D	3530	5360	1310	3030	1196	1131
E	2820	4890	859	3135	732	1176

Method B was used to determine which release point resulted in maximum retention of dye within both the estuarine portion of the model and the region of the model representing the oyster producing portion of the real river (that portion between Newport News Point and Mulberry Point).

o

Table 5 shows the percent of dye from each release retained in these portions of the model 40 cycles after injection. Release point 2 is once again the most efficient location.

TABLE 5

Percent of injected dye retained in portions of the James River model for various release points 40 tidal cycles after release.

Portion of Model Considered	Release Point 1	2	3	4	5	6
All above Hampton Roads Tunnel	85.1	99.0	56.5	68.2	49.1	36.7
Segments VI and VII	21.6	38.5	15.8	25.8	13.2	12.9

General Circulation - Dye movements were observed visually for the first five cycles after release. The position of what appeared to be the maximum concentration was recorded and general circulation patterns for the surface and deep layers of the model were plotted. These plots are shown in Figures 12 and 13.

Gross circulation features within the model appear to be as follows:

1. There was a general upstream movement of water over the northeastern shoals from Newport News to Mulberry Point. This upstream surface flow branches at Mulberry Point with a slight intrusion upstream around the point while the bulk of the surface water turned cyclonically in the Burwell's Bay region and then moves downstream across the southwest shoals. The general downstream movement of waters over the southern shoals persisted throughout the middle and lower estuarine portion (Mulberry Point to Hampton Roads).

2. The deeper waters exhibited a net upstream motion through-
out the model except in the region immediately downstream
from Mulberry Point where the circulation was somewhat
similar to surface motion, some cyclonic movement was
observed. Entrainment of deeper water into the surface
layer was particularly evident in the shoal areas on both
sides of the channel between the James River Bridge and
Mulberry Island.

Small Scale Circulation Features - During the six tidal cycles
between dye injection and the start of sampling, pellets of potassium per-
manginate (a non-fluorescent dye) were distributed at several locations
within the model to aid in observing small scale circulation features. Such
small scale features were of particular interest in the Burwell's Bay region
where no flooding of bottom waters was observed. Pellets placed in the
vicinity of the circled station in Burwell's Bay (Figure 10) produced plumes
that were transported downstream on the local ebb but appeared to stagnate
when the tide was flooding. The net result appeared to be a unidirectional
pumping action in this region rather than the normal oscillatory tidal flow
observed elsewhere in the model. Although the physical implications of such
small scale features have not been pursued, their importance to the overall
circulation should be investigated.

ANALYSIS IN PROGRESS

Data from these experiments is presently undergoing additional
analysis. They are:

1. Spatial and temporal fluctuations of dye concentration over
the entire area sampled are being re-evaluated with sampling
locations grouped to form horizontal and vertical segments
which will allow a more difinitive statement on dye movement
and distribution.

2. A mathematical diffusion model will be developed based

   on data from the experiments. The mathematical model will

   then be used to predict dye concentrations resulting from

   releases at various points within the hydraulic model.

Results of both these analyses should be available within one

year.

REFERENCES

Hargis, William J., Jr.
     Utilization of Physical and Mathematical Models in Marine Water
     Resources Research, Planning and Management (Contract No. 14-01-0001-
     1597, C-1214). A report for the period 1 September 1967 - 31
     December 1968).
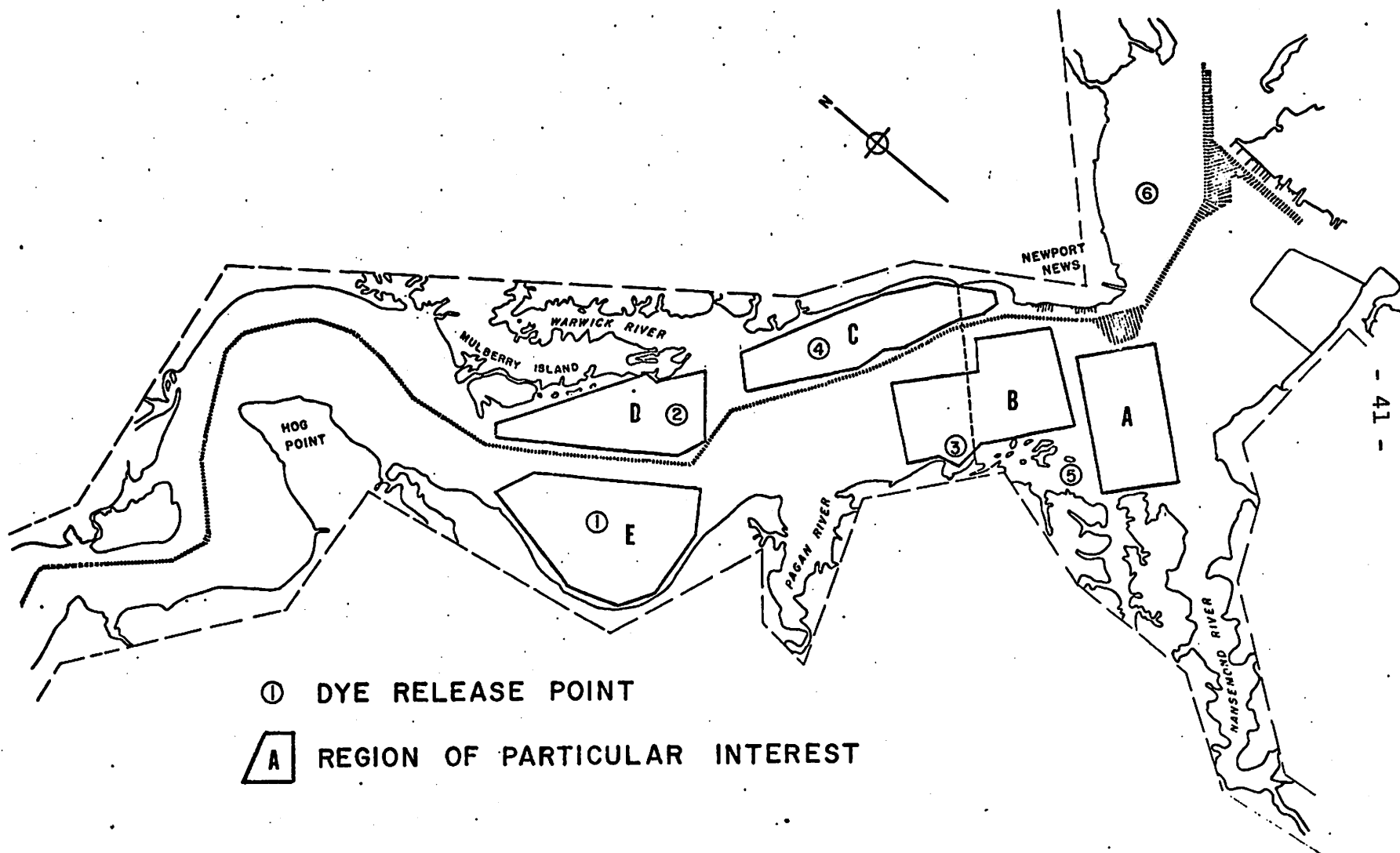
Figure 9. Section of James River hydraulic model showing dye release points and regions of particular interest pertaining to VIMS dye tests.
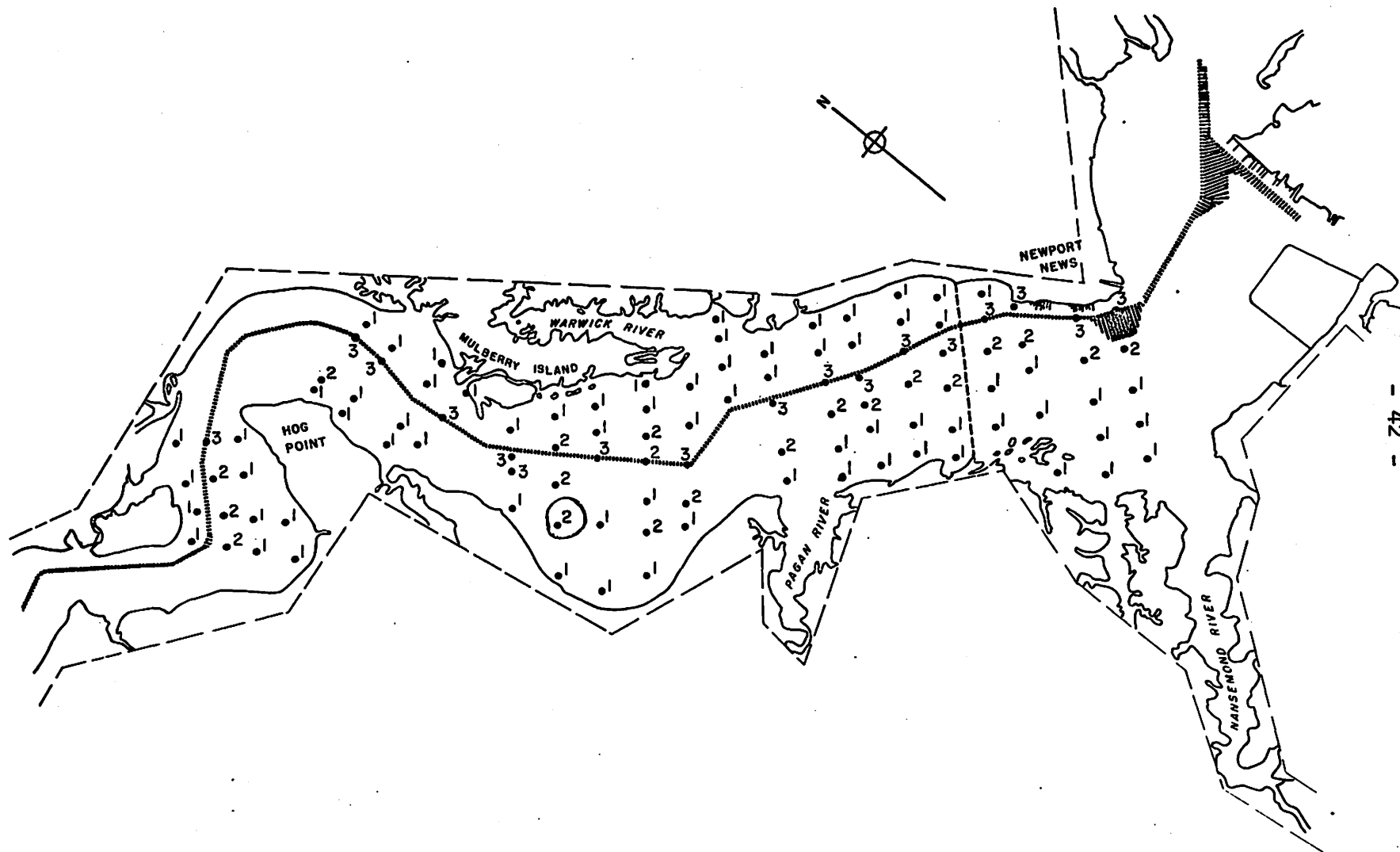
Figure 10. Section of James River hydraulic model showing stations sampled during VIMS dye tests. ⊙2 Location in Burwell's Bay where unidirectional "pumping" of bottom water was observed.
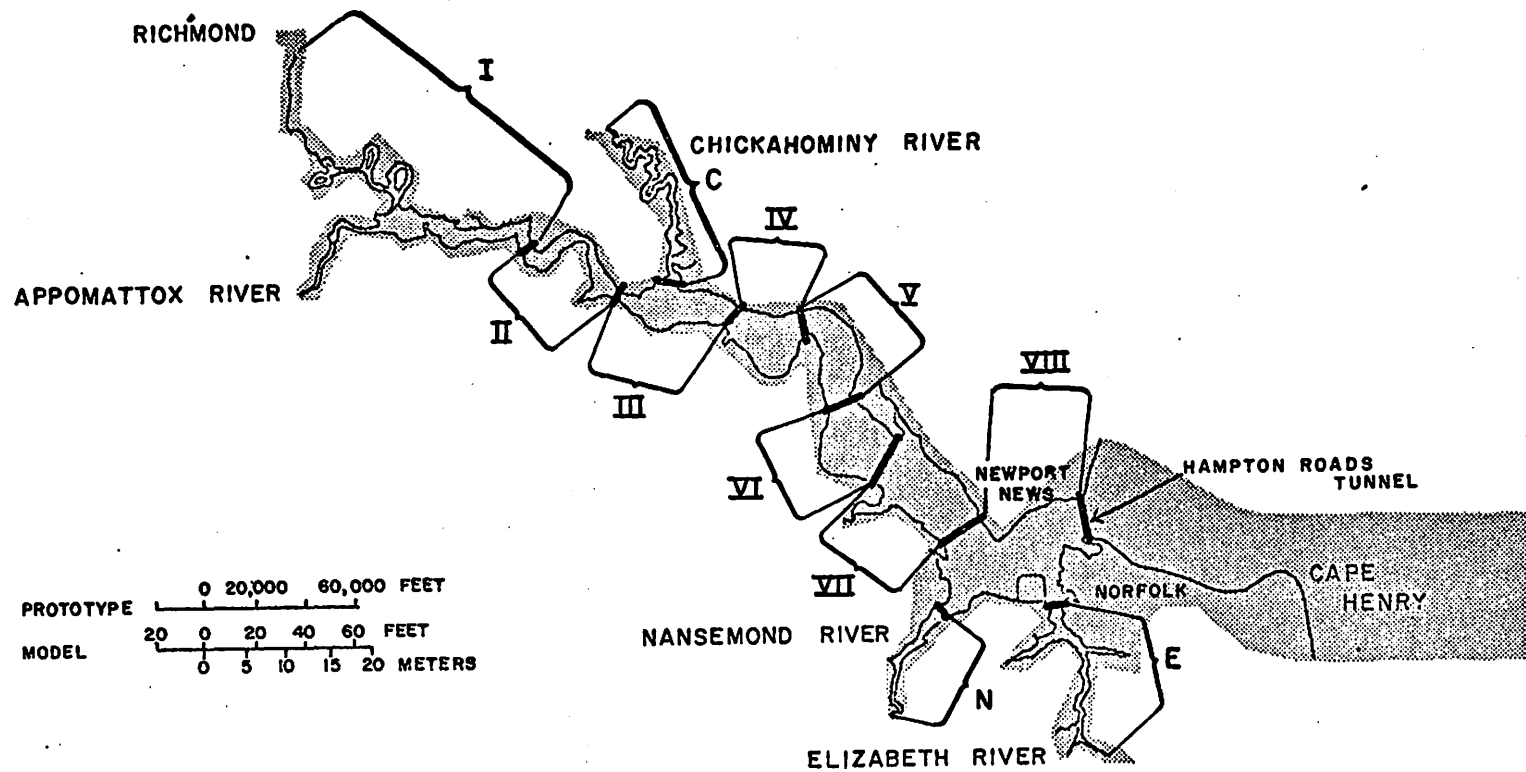
Figure 11. Chart of James River hydraulic model showing the locations of dams used to segment the model after each dye test and segment numbers.
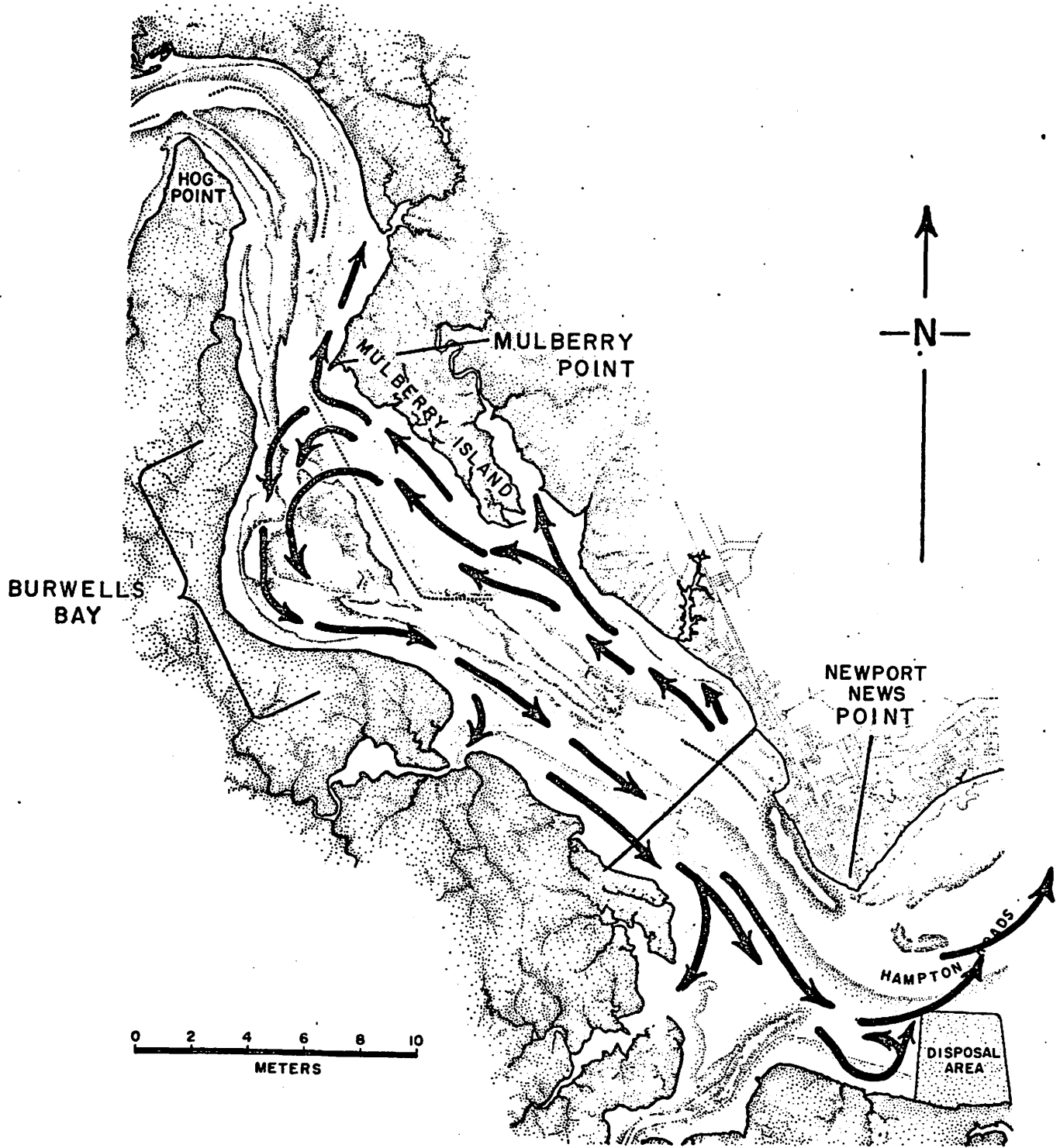
Figure 12. General surface circulation in James River hydraulic model resulting from dye releases.
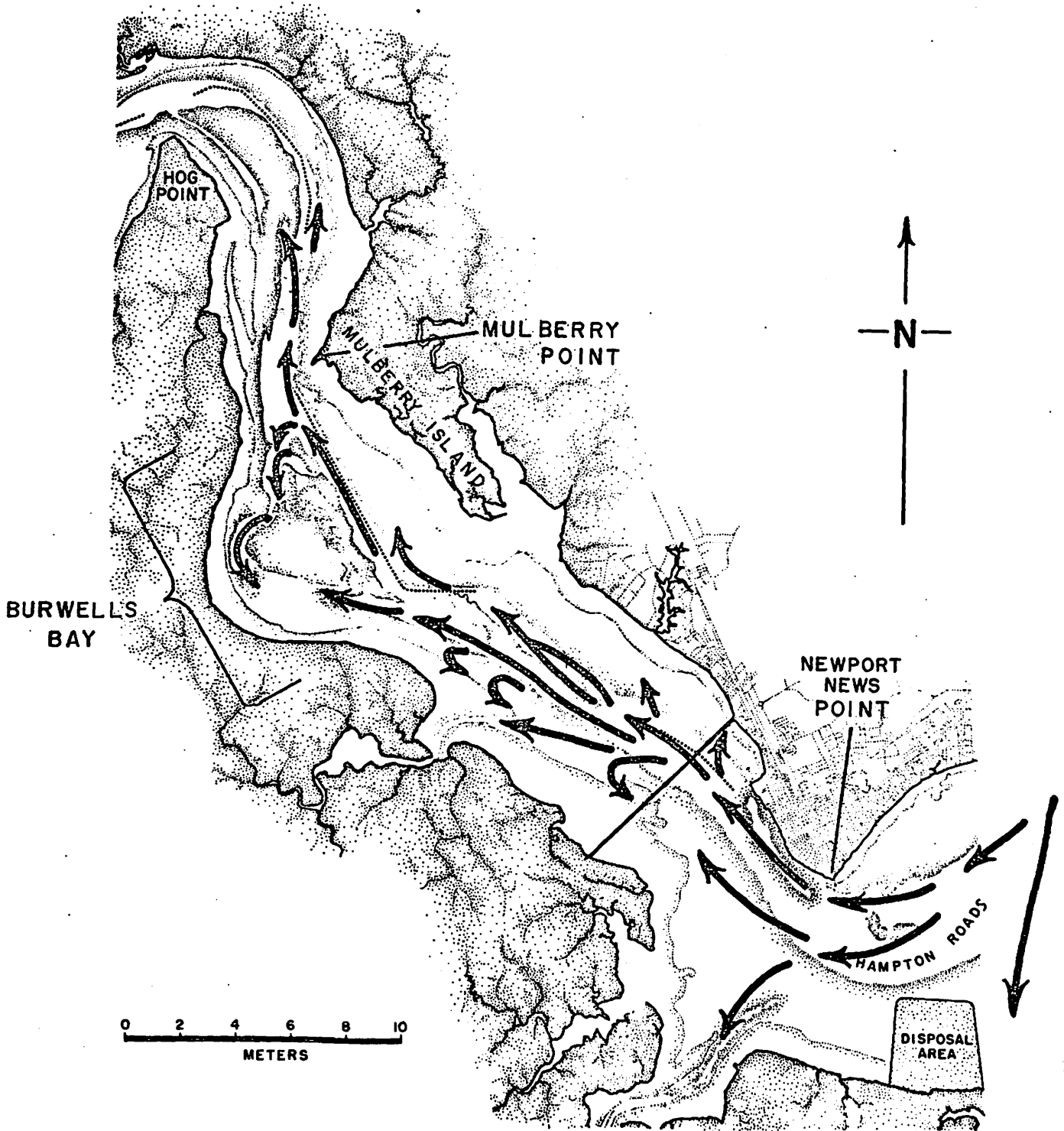
Figure 13. General bottom circulation in James River hydraulic model resulting from dye releases.

Significance of Certain Circulatory Patterns

as Determined in Hydraulic Model Studies to Production

of Seed and Market Oysters in the James Estuary

and to Their Rehabilitation

William J. Hargis, Jr.[4]

The most important seed oyster producing area in the lower

Chesapeake Bay region has been the estuary of the tidal James, which in

normal years produced 80 - 85 percent of all seed used in lower Chesapeake

Bay and its tributaries. Significant supplies of market oysters have also

been produced there. Formerly seed oysters were overwhelmingly important

but in recent years market oyster production has increased relatively.

For some time the factors causing this tremendous productivity

have been under investigation (Andrews 1951, 1955; Hargis 1962a, b and

1966; Pritchard 1953). Oyster biologists have learned that the success

of the James River seed beds (extending normally from above the James

River Bridge off Newport News to Mulberry Point in the Burwell's Bay

area off Mulberry Island (Figure 9) has been due to large, regular sets

and good-survival. The latter is due to exclusion of predators and

diseases by salinity levels which they cannot tolerate and the seed oysters

can. The high sets have been thought to be due to "funnelling" of oyster

larvae into the areas with suitable setting characteristics by the upstream

moving lower, higher salinity layer in this conceptually, horizontally-

stratified estuary (Pritchard 1953 and Hargis, 1966 and others). Recently,

in attempting to explain good setting areas here and elsewhere in lower

Chesapeake Bay, Andrews (personal communication) has postulated that there are

---

[4]Director, Virginia Institute of Marine Science, Gloucester Point,
Virginia

"open" and "closed-setting systems" primarily based upon prevailing
hydrographic patterns. In the latter, larvae originating locally and/or
nearby are concentrated and retained in the vicinity of suitable "cultch"
or setting surfaces until a large number can set. In the former, larvae
are swept away from otherwise suitable setting areas and/or diluted before
they can set. To examine these factors and theories the hydraulic model
group was asked by the Project Director to undertake the series of dye
experiments described above.

A further reason for these studies was to determine the best
site or sites to introduce oyster larvae or brood stocks for purposes of
enhancing setting (and the feasibility thereof) which has dropped
markedly since 1960, and rehabilitating the seed beds. It has been
thought that the parasite <u>Minchinia</u> <u>Nelsoni</u> (MSX) which has raged in
Hampton Roads, in river around and below Newport News Point, (Figure 9)
has been responsible for destroying the brood-stock of older oysters
whose larvae were carried into the above-Bridge seed areas by prevailing
currents in the upstream moving higher salinity, bottom layers. The
possibility of reseeding these beds with disease-resistant oysters has been
considered. To do so effectively and economically would require determination
of the best locations for such introductions and the model seemed the best
possibility for making such determinations.

Accordingly, the experiments were designed to compare the quali-
tative and quantitative fate of dye particles which are here used as
experimental analogues of oyster larvae--in full realization that there
are dissimilarities between dye particles and larvae, from six different
introduction sites or release points (Figure 9). Sampling grids were
established over estuarine reaches which are now or were formerly producing
seed-oyster bars (Figure 10). Primary critical sampling intervals, 10, 15,
and 20 days after release, were chosen to bracket the time in the history of

larval development when past studies (of larval availability, development and setting) indicate that most larvae are ready to set, i.e. around 15 days.

Sampling areas and times and numbers were also limited by availability of the model, costs, and personnel. Because of these factors and the fact that neither the VIMS hydraulic model group nor WES personnel had run as extensive and complex series of dye studies before, it was anticipated that follow-up studies would be necessary later, that this was a preliminary series.

Details of this series of experiments can be determined from the paper by Ruzecki and Moncure presented above. However, these preliminary analyses yielded very interesting results.

First, it appears that the deeper, saltier and more dense layer does move upriver, but that its main pathway is in the deeper layer as would be expected. Secondly, contrary to expectations that dye releases made in Hampton Roads at Hampton Bar (Release Point 6, Figure 9) would concentrate more effectively in the upriver area, these studies indicated that the releases made above the bridge at Release Points 4 (Brown Shoal) 2 (Wreck Shoal) contributed more to the Burwell's Bay area and that concentrations persisted there longer than the other releases.

Releases made at the southerly Release Points 1 (Point of Shoals), 3 (Naseway Shoals) and 5 (Nansemond Ridge) contributed less to the Burwell's Bay area and were flushed downstream and out of the system faster.

Based on earlier theory, we would have predicted that Release Point 6 would have been more effective. This contrary indication should be investigated further in additional dye studies. However, the dye studies must be accompanied by thorough-going current studies in the model which we hope to be able to do.

Further refinement of this work is justified because of its
importance to conservation and rehabilitation of the James River oyster
industry. This is planned for the future.

REFERENCES

Andrews, J.D. 1951. Seasonal patterns of oyster setting in the James
    River and Chesapeake Bay. Ecology 32:752-758. VIMS Contribution
    No. 34.

Andrews, J. D. 1955. Setting of oysters in Virginia. Proc. Natl. Shellfish
    Association 45(1954):38-46. VIMS Contribution No. 53

Hargis, W. J. Jr. 1962a. History and current status James River
    navigation project. VIMS Mimeo. Report 9 p.

Hargis, W. J. Jr. 1962b. Current knowledge on the hydrography and
    biology of the estuarine portion of James River. VIMS Mimeo..
    Report 7 p.

Hargis, W. J. Jr. 1966. Investigation of oyster larvae and spat and
    certain environmental factors in an horizontally stratified estuary
    Final Report on Project 3-7-R, PL 88-309, U.S. Bur. Comm. Fish. 68 p.

Pritchard, D. W. 1953. Distribution of oyster larvae in relation to
    hydrographic conditions. Proc. Gulf Caribbean Fish. Inst. 6:123-132.

MATHEMATICAL MODELING AND COMPUTER STUDIES

Along with the hydraulic model effort a significant part
of this program is devoted to development of more meaningful mathematical
concepts or models of the tidal James, an extensively considered "classical"
horizontally-stratified estuary. It is expected that this work will con-
tribute to development of improved modeling techniques and better under-
standing of estuarine circulation in general. Though it has not been possible
as yet to employ extensively the "bounce" technique of comparing hydraulic
and mathematical model predictions to test the latter extensively, preliminary
indications are that this will be fruitful, and future, more comprehensive
research projects involving this concept are planned for this program.

Results of note, however, have been obtained in the studies
described below.

Theoretical Studies on Diffusion in Estuaries

Yee-chang Wang[5]

ABSTRACT

Assuming a constant longitudinal eddy diffusivity, one-dimensional diffusion in a periodic current is solved mathematically with a view to explaining some basic characteristics of diffusion in estuaries, particularly those in which the tidal effect overwhelms the effect of the river discharge. For a given initial dye distribution $f(x)$, the solution of dye concentration $S(x,t)$ is

$$S(x,t) = \frac{1}{2\sqrt{\pi \kappa t}} \int_{-\infty}^{\infty} f(\delta) e^{-\frac{1}{4\kappa t}\left\{(\delta - x) + \frac{U \sin \omega t}{\omega}\right\}^2} d\delta$$

where t is time, x is the horizontal distance negative in seaward direction, and U and ω are the amplitude and the frequency of the periodic current, respectively.

Based upon the solution, the behavior of dye distribution is studied and numerical analyses are made to further demonstrate the result. The limitation and extension of this theoretical study are discussed.

INTRODUCTION

Diffusion is an ubiquitous phenomenon in nature. In recent years, as natural waters have become seriously polluted, the diffusion in estuaries has demanded attention and study. This theoretical work is undertaken in the hope that it may shed light on the characteristics of diffusion in estuaries and help to explain results of dye-diffusion experiments conducted in the James River model.

---

[5]Formerly Associate Marine Scientist, Virginia Institute of Marine Science, Gloucester Point, Virginia; presently Associate Professor at National Taiwan University, Taipei, Taiwan, Republic of China

There are many works on this subject, notably those of Pritchard (1954), Kent (1958), Harleman (1964), Bowden (1965) and Okubo (1968). For a quasi-steady[6] case, Harleman (1964) introduced a finite difference formula for a "local dispersion coefficient." Following work by Taylor (1953), Bowden (1965) pointed out that effective longitudinal dispersion was produced by transverse gradient of velocity together with transverse turbulent mixing. Later this idea of shear effect on horizontal mixing was further emphasized by Okubo (1968), who, in particular, calculated the variance in the horizontal direction for dye concentration in a shear-diffusion model. However, no direct solutions of the diffusion equation in an alternating current have been reported.

THE PHYSICAL MODEL AND MATHEMATICAL FORMULATION

Assume a given amount of diffusive material to be spread along an estuary at a certain initial time. The material is subject to convection and diffusion by the combined action of river flow and an alternating tidal current. The object is to find how well the material is mixed and how far it is carried up and down stream after a given time interval; in short, what the distribution of concentration is.

Because of the turbulent mixing of salt water and fresh water, the irregular bottom topography and the meandering of the river bed, the diffusion in an estuary is a complicated unsteady three-dimensional problem. In order to simplify the explanation of this intricate physical problem, a mathematical model is formulated for an "ideal" estuary in which the current is periodic sinusoidally, the diffusion is one-dimensional, and the so-called "eddy diffusivity" is assumed constant along the estuary. The problem is mathematically formulated as follows:

---

[6] The concentration of the diffused matter is steady at the same tidal stages.

The governing equation is

$$(1) \quad \frac{\partial S}{\partial t} + U \cos(\omega t) \frac{\partial S}{\partial x} = K \frac{\partial^2 S}{\partial x^2}$$

where S is the concentration of the diffusive material, K is the longitudinal eddy diffusivity, t is time, x is the horizontal distance negative in seaward direction, and U and ω are the amplitude and the frequency of the periodic current, respectively. At all times, the concentration S should satisfy the following two conditions which may be called boundary conditions:

$$(2) \quad S(x,t) \longrightarrow 0 \quad \text{as } x \longrightarrow \pm\infty$$

and

$$(3) \quad \int_{-\infty}^{\infty} S \, dx = \quad \text{constant,}$$

for the conservation of the diffusive material.

The initial condition is

$$(4) \quad S(x,0) = f(x)$$

where f(x) is the given function describing the initial concentration of the diffusive material along the estuary.

Needless to say, this physical model is too simplified to simulate a real estuary. However, the mathematical solution of this ideal physical model can be used to examine and illustrate certain important aspects of the diffusion in an estuary. The limitation of this mathematical study and its possible extension to a better physical model will be discussed later.

THE FORMAL SOLUTION

To find the solution to equation (1) which satisfied boundary conditions (2) and (3) and the initial condition (4), three main steps are

used: a change of independent variable, the reduction of the partial

differential equation (1) into two ordinary differential equations by

separation of variables and the application of Fourier integral theorem for

satisfying the initial condition.

First, a new independent variable ξ defined as

(5) $\xi = e^{\left[\frac{1}{\omega} \sin(\omega t) - x/v\right]}$

is introduced, and the function $S(x,t)$ is assumed to be separable as

(6) $S(x,t) = F(t) G(\xi)$

a priori. Equation (1) then becomes

(7) $\dfrac{F'}{F} = \dfrac{K}{v^2} \left\{ \dfrac{G'' \xi^2 + G' \xi}{G} \right\}$,

where primes denote differentiations. Obviously, since S cannot approach

infinity as t approaches infinity, both sides of equation (7) are equal

to a constant, $-c_1^2$ (a negative real number). Thus, equation (7) implies

two homogeneous ordinary differential equations:

(8) $F' + c_1^2 F = 0$,

and

(9) $G'' \xi^2 + G' \xi + \dfrac{c_1^2 v^2}{K} G = 0$

Equations (8) and (9) can be solved. The general solutions are

$F = e^{-c_1^2 t}$

and

$G = A_1(c_1) e^{\pm \frac{i c_1 v}{\sqrt{K}} \left(\frac{1}{\omega} \sin \omega t - \frac{x}{v}\right)}$

Hence, the solution of (1) is

(10) $S(x,t) = \displaystyle\int_0^\infty e^{-c_1^2 t} \left\{ A(c_1) \cos \frac{c_1 v}{\sqrt{K}} \left(\frac{1}{\omega} \sin \omega t - \frac{x}{v}\right) + B(\xi) \sin \frac{c_1 v}{\sqrt{K}} \left(\frac{1}{\omega} \sin \omega t - \frac{x}{v}\right) \right\} dc_1$

$= \sqrt{K} \displaystyle\int_0^\infty e^{-Kc^2 t} \left\{ A(c) \cos\left(cv\left(\frac{1}{\omega} \sin \omega t - \frac{x}{v}\right)\right) + B(c) \sin\left(cv\left(\frac{1}{\omega} \sin \omega t - \frac{x}{v}\right)\right) \right\} dc$

where $A(c)$ and $B(c)$ are arbitrary functions of c, and $C = \dfrac{c_1}{\sqrt{K}}$

Then arbitrary functions A(c) and B(c) are determined by the

initial condition (4). At $t=0$ the general solution (10) reduces to

$$(11)\quad S(x,0) = \sqrt{K} \int_0^\infty \{A(c)\cos(cx) - B(c)\sin(cx)\}\, dc .$$

According to the initial condition (4), $S(x,0)$ should be equal to f(x),

i.e. $f(x) = \sqrt{K} \int_0^\infty \{A(c)\cos(cx) - B(c)\sin(cx)\}\, dc .$

By the Fourier integral theorem, arbitrary functions A(c) and B(c) are

determined in terms of f(x) as

$$(12)\quad A(c) = \frac{1}{\pi\sqrt{K}} \int_{-\infty}^\infty f(\delta)\cos(c\delta)\, d\delta ,$$

and

$$(13)\quad B(c) = \frac{1}{\pi\sqrt{K}} \int_{-\infty}^\infty f(\delta)\sin(c\delta)\, d\delta .$$

Substituting (12) and (13) into (10), the solution (10) becomes

$$(14)\quad S(x,t) = \frac{1}{\pi} \int_0^\infty e^{-Kc^2 t} \left\{ \int_{-\infty}^\infty f(\delta)\cos(c(\delta-x) + \frac{cU}{\omega}\sin\omega t)\, d\delta \right\} dc$$

The expression of (14) can be much simplified if the order of the double

integration is reversed and the integration in δ is carried out first.

We therefore write (14) as

$$(15)\quad S(x,t) = \frac{1}{\pi} \int_{-\infty}^\infty f(\delta) \left\{ \int_0^\infty e^{-Kc^2 t}\cos\left[c(\delta-x) + \frac{cU}{\omega}\sin\omega t\right] dc \right\} d\delta$$

and define a new function H(u) as

$$(16)\quad H(u) = \int_0^\infty e^{-Kc^2 t}\cos\left(cu + \frac{cU}{\omega}\sin\omega t\right) dc ,$$

where u = δ -x. It can be shown that the function H(u) satisfies the

following equation

$$(17)\quad H' + \frac{u + \frac{U}{\omega}\sin\omega t}{2Kt} = 0 ,$$

with the solution

$$H(u) = \frac{\sqrt{\pi}}{2\sqrt{Kt}} e^{-\frac{1}{4Kt}\left(u + \frac{U\sin\omega t}{\omega}\right)^2} .$$

Therefore, the final solution of (15) is

$$(18)\quad S(x,t) = \frac{1}{2\sqrt{\pi Kt}} \int_{-\infty}^\infty f(\delta) e^{-\frac{1}{4Kt}\left\{(\delta-x) + \frac{U\sin\omega t}{\omega}\right\}^2} d\delta$$

This can be easily checked as a formal solution to the mathematical problem.

THE PHYSICAL INTERPRETATIONS OF THE FORMAL SOLUTION

The behavior of dye diffusion in the one-dimensional physical model should be described by the solution (18) for a given initial dye distribution $f(x)$. In this physical model, the dye concentration of a specific point at a specific time can be regarded as the sum of contribution of dye to this point at this time due to dye put initially at each separate point. The behavior of dye diffusion becomes clear in a particular case when the initial dye is a patch of dye at one point, that is where $\zeta(\delta - o)$ is a Dirac-delta function which is equal to a if $\delta = 0$ and vanishes if $\delta \neq 0$. Under these conditions, the solution (18) becomes

$$(19) \quad \zeta(x,t) = \frac{a}{2\sqrt{\pi K t}} e^{-\frac{1}{4Kt}\left\{-x + \frac{U \sin \omega t}{\omega}\right\}^2}.$$

An interpretation of this is that the center of mass of the dye patch is transported with the periodic current while the dye patch itself diffuses outwards from the center. With a strong enough current, a point in the dye patch upstream from the initial dye location will have a higher concentration at slack before ebb than at slack before flood. The converse will be true for a point downstream from the initial dye location. For both upstream and downstream locations, concentrations at like tidal stages will initially increase to a maximum value and then decrease with time. For the dye release point, the concentration at the same tidal stages decreases with time.

Numerical analyses have been carried out on a digital computer (IBM/1130) to further demonstrate the above explanation. For $K = 5 \text{ m}^2/\text{sec}$, $U = 0.75 \text{ m/sec}$ and $\omega = \frac{2\pi}{12.42} /hr$[7], the quantity $\frac{S}{a}$, the ratio of concentration ζ to the amount of dye, a, initially at the release point, is calculated from the solution (19) for stations -5400 m, -2700 m, 0 m,

---

[7]These values are taken to fit the James River data in the mean, though the value of K may be underestimated.

+2700 m, +5400 m, +8100 m, +10800 m, +13500 m, +16200 m, +18900 m, and +21600 m over the first five tidal cycles. The numerical analyses were programmed by Mr. R. W. Moncure. The variations of $\frac{S}{a}$ vs. time at the stations located where the release was made and +5400 are plotted on semi-logarithmic graph paper (shown in Figure 14 and Figure 15). The dotted lines on these two graphs are curves describing the variation of $\frac{S}{a}$ at the same tidal stages.

Another numerical study is made to show the variation of the concentration in case that the dye is released at the same amount, a, over a full tidal cycle. Since the governing equation of S is linear, the solution for this case is simply

$$(20) \quad S(x,t) = \int_{0}^{\frac{2\pi}{\omega}} \frac{a}{2\sqrt{\pi\kappa(t+\theta)}} \, e^{-\frac{1}{4\kappa(t+\theta)}\left\{-x + \frac{U\sin\omega(t+\theta)}{\omega}\right\}^2} \, d\theta$$

Again, the quantity $\frac{S}{a}$ is calculated for stations at -5400 m, -2700 m, 0 m, 2700 m, 5400 m, 8100 m and 10800 m over the first five tidal cycles. The variation of $\frac{S}{a}$ at the station +5400 m is plotted in Figure 16. Some features of the curves are interesting:

1. There are abrupt drops in $\frac{S}{a}$ which occur in the first quarter of each tidal cycle.

2. The drops become less abrupt as the number of tidal cycles increases.

3. The spreading of the dye patch is reflected from the computer result.

4. The dotted line in Figure 16 describes qualitatively the variation in concentration at the same tidal stage for certain stations shown in the data of dye-diffusion tests in the James River model.

The first two features are explained as follows: These sudden decreases in $\frac{S}{Q}$ are due to the fact that front of the dye is not well-mixed in the first few tidal cycles. Due to diffusion, the front of dye gradually loses its sharpness that is shown by feature 2. As it can be expected, if K is increased, the front of the dye mass will become less sharp.

DISCUSSION

Though some interesting results are obtained from this mathematical analysis of a simple physical model, the limitation of the model and its possible extension require some elaboration. The possible extension is that, assuming a constant longitudinal and vertical eddy diffusivity, the above mathematical analysis can be generalized for two-dimensional diffusion in an alternating current with a net seaward flow averaged over a tidal period. However, the most serious limitation of this model is that the eddy diffusivity is assumed constant. Since the turbulent mixing, in a strict sense, is still an unsolved problem in fluid mechanics, the term "eddy diffusivity" is introduced to stand for the effect of turbulent mixing on the mean concentration of the diffused material (Bowden, 1967). In an estuary, this quantity varies from place to place and changes with time. For longitudinal eddy diffusivity it is primarily a function of x and t rather than a constant. Unfortunately, no tractable analytic solution can be obtained if K is assumed as a general function of x and t . In this case, a numerical analysis is preferable.

REFERENCES

Bowden, K. F. 1965. Horizontal mixing in the sea due to a shearing current. J. Fluid Mech., 21:83-95.

Bowden, K. F. 1967. Circulation and Diffusion, Estuaries, publication No. 83 of American Association for the Advancement of Science, 1967:15-36

Harleman, D. R. F. 1964. The significance of longitudinal dispersion in the analysis of pollution in estuaries. The Proc. of the Second International Water Pollution Research Conference, Tokyo, 1964:279-302.

Kent, R. E. 1958. Turbulent diffusion in a sectionally homogeneous estuary. Chesapeake Bay Inst., Johns Hopkins Univ., Tech. Report No. XVI.

Okubo, A. 1968. Some remarks on the importance of the "shear effect" on horizontal diffusion. J. of the Oceano. Soc. of Japan, 24:60-69.

Pritchard, D. W. 1954. A study of flushing in the Delaware model. Chesapeake Bay Inst., Johns Hopkins Univ., Tech. Report No. VII.

Taylor, G. I. 1954. The dispersion of matter in turbulent flow through a pipe. Proc. Roy. Soc. of London, 223:446-468.

Figure 14. The variation of $\frac{S}{a}$ vs. t at x = o, the dye release point (from equation (19).
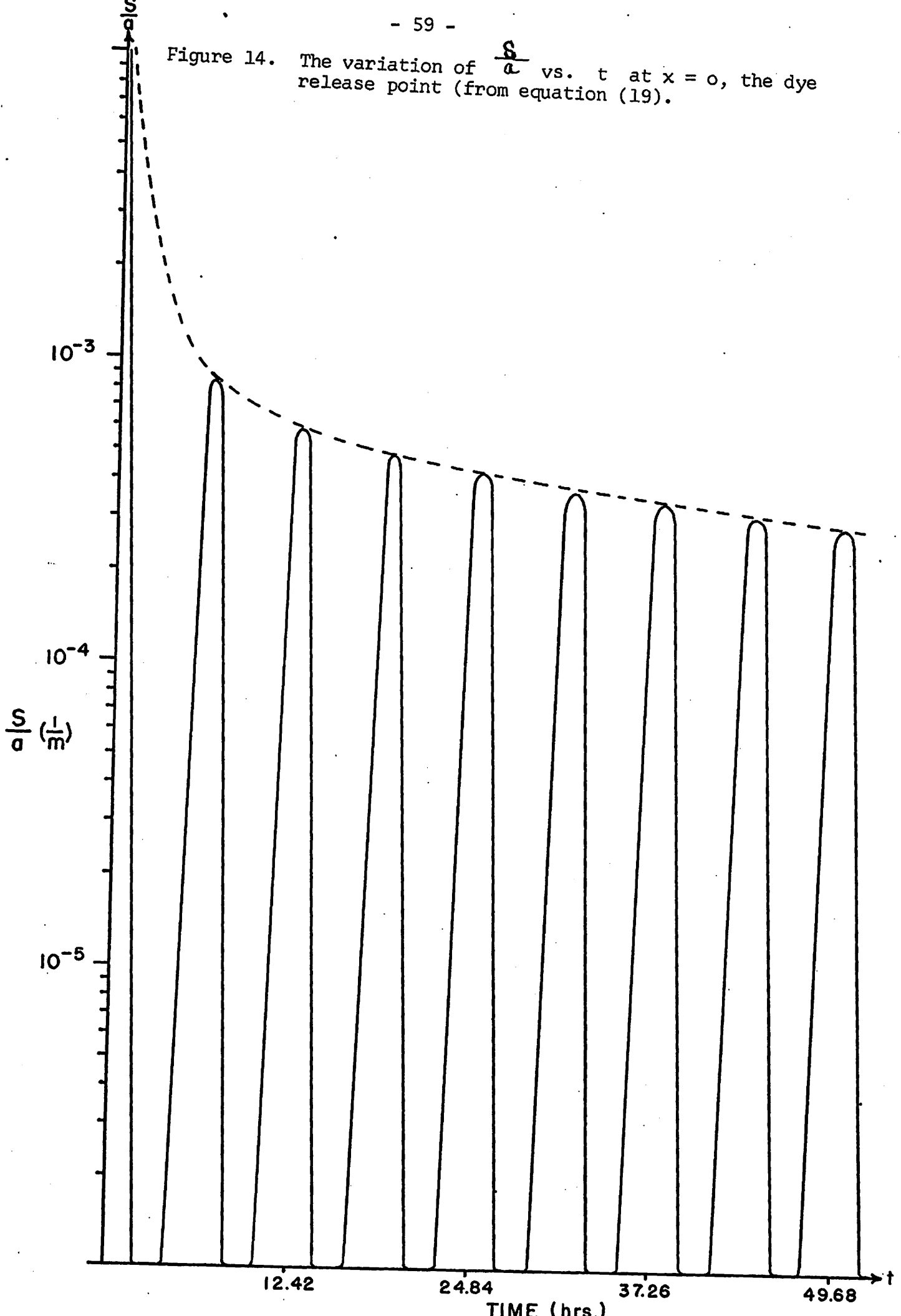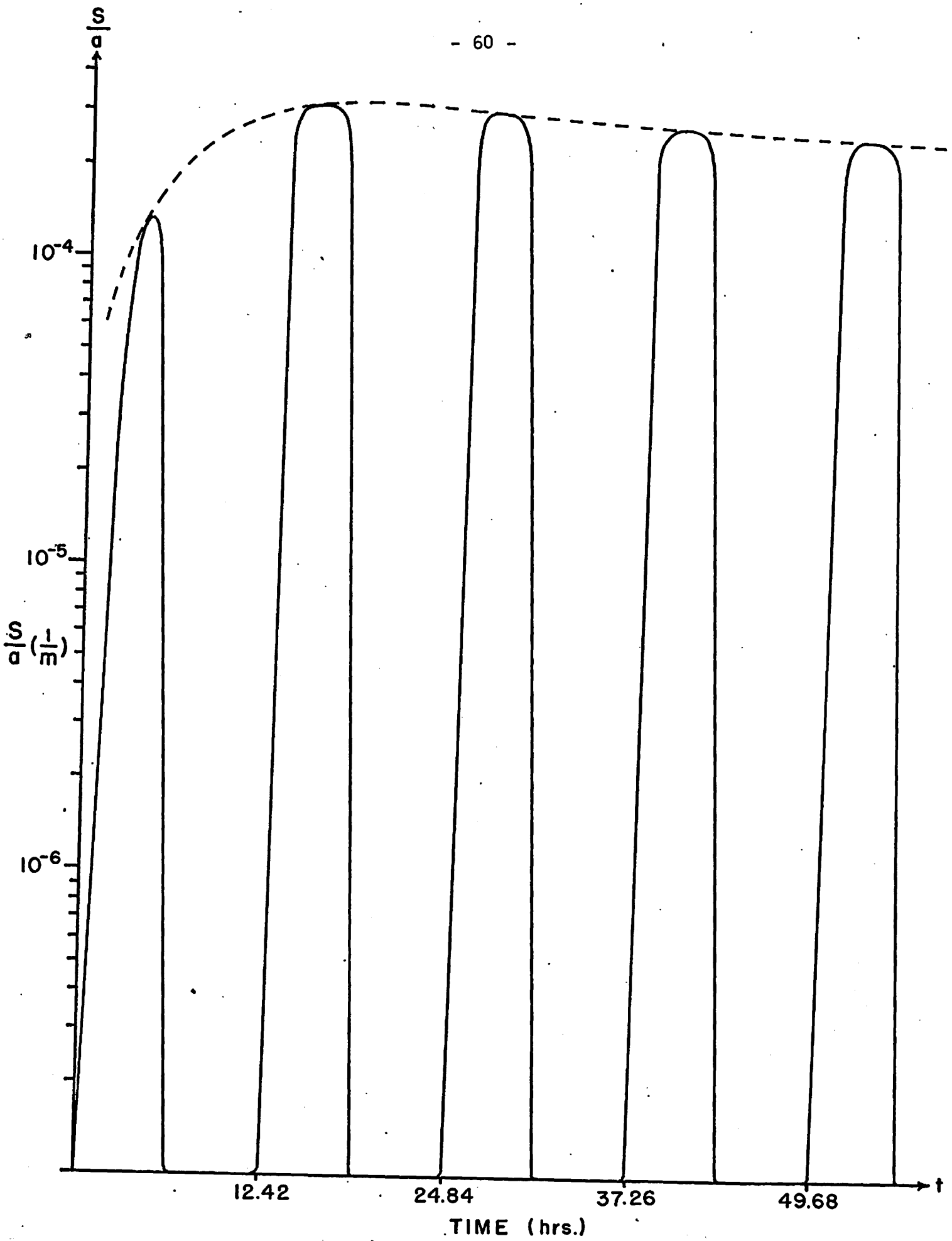
Figure 15. The variation of $\frac{S}{a}$ vs. t at x = 5400 m (from equation (19).
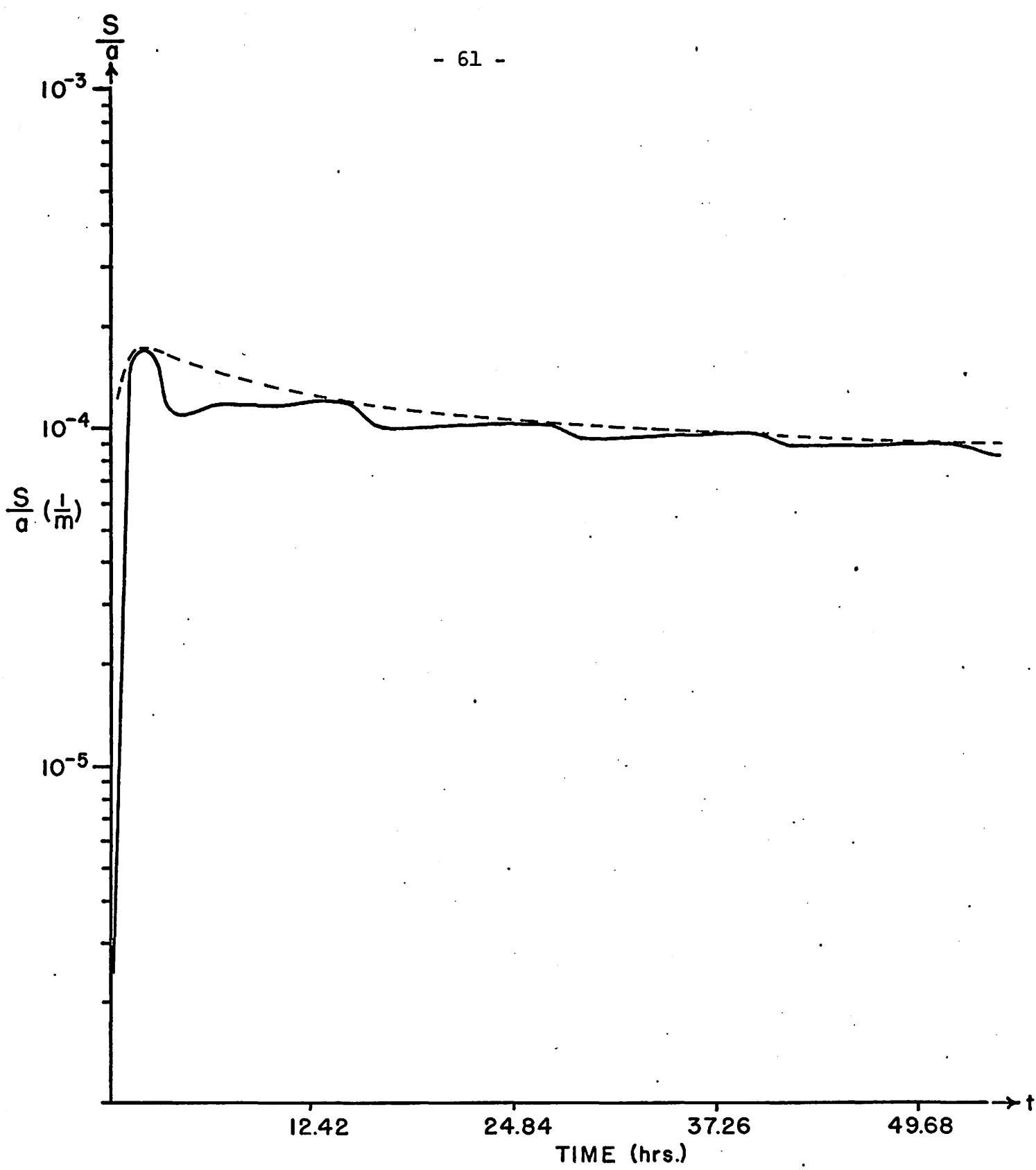
Figure 16. The variation of $\frac{S}{a}$ vs. t at x = 5400 m (from equation (20)).

The Integro-Differential Equations for Estuarine Flow

Yee-chang Wang

ABSTRACT

A system of integro-differential equations is obtained to determine the cross-sectional variations in mass, momentum and salt content along an estuary. Its application to estuarine studies is briefly discussed. The central mathematical problem of this integral approach - the Leibnitz rule for double integral is obtained formally.

INTRODUCTION

Even in the absence of fluctuating winds, estuarine flow is frequently random due to the turbulent mixing of salt and fresh water caused by tidal action. Because of the complexity of turbulent flow and the lack of field data, detailed scientific studies of most problems in estuarine hydrodynamics are still beyond our reach. However, if we content ourselves, from a pragmatic point of view, with knowing the changes in mass, momentum and salt content from cross-section to cross-section along the estuary, an integral approach to the governing equations of the above-mentioned quantities is indeed useful.

⁌This integral approach was first applied by Pritchard (1958) to the incompressibility condition and salt balance equation. Later, Arthur (1964) made a study on the equations of continuity for sea water and river water in estuaries by taking into account the process of diffusion between the two bodies of water. No report on the application of an integral approach to the momentum equation has been published. For estuarine study this approach would be incomplete should it not be applied to the momentum equation.

LEIBNITZ RULE FOR DOUBLE INTEGRALS

The central mathematical problem in this approach is to find the Leibnitz rule for the double integral when the limits of integration are functions of the variables of differentiation. This problem was first studied by Pritchard (1958) and later justified by Okubo (1965). Since there are a few minor errors in their results, the correct results are given below and a different, simpler derivation is given in the Appendix.

First, a Cartesian coordinate system is set up with its x_1-axis positive seaward, its x_2-axis positive toward the right, looking downstream and its x_3-axis positive downwards. With respect to these coordinates, an arbitrary cross-section $\sigma = \sigma(x_1, t)$ is shown in Figure 17. On a fixed cross-section at a fixed time, i.e. at fixed x_1 and t the boundary C of the cross-section can be represented as

$$X_3 = S(X_2 ; X_1, t)$$

or

$$X_2 = T(X_3 ; X_1, t)$$

provided the boundary C is smooth and simply connected. In a parametric representation with the arc length l as the parameter, the boundary C is described by

and

$$X_3 = \Psi(\ell ; X_1, t)$$
$$X_1 = \varphi(\ell ; X_1, t)$$

Then the Leibnitz rules for double integral of any function $f(\vec{X}, t)$ continuous in $\vec{X}$ and t are

$$(1) \quad \frac{\partial}{\partial X_1} \iint_\sigma f(\vec{x}, t) \, d\sigma = \iint_\sigma \frac{\partial f}{\partial X_1} \, d\sigma + \oint_C \left(\frac{\partial S}{\partial X_1}\right)_n f \, d\ell ,$$

$$(2) \quad \frac{\partial}{\partial t} \iint_\sigma f(\vec{x}, t) \, d\sigma = \iint_\sigma \frac{\partial f}{\partial t} \, d\sigma + \oint_C \left(\frac{\partial S}{\partial t}\right)_n f \, d\ell ,$$

Where the double integration is over the whole cross-sectional area, stands for the line integral along the boundary C in a counterclockwise direction, facing positive X_1 and the subscript n means the outward normal direction to the boundary C . Since it is evident that

$$(3) \quad \oint_C \left(\frac{\partial S}{\partial X_1}\right)_n f \, d\ell = \oint_C \left(\frac{\partial T}{\partial X_1}\right)_n f \, d\ell \, ,$$

$$(4) \quad \oint_C \left(\frac{\partial S}{\partial t}\right)_n f \, d\ell = \oint_C \left(\frac{\partial T}{\partial t}\right)_n f \, d\ell \, ,$$

the second terms on the right-hand sides of formulae (1) and (2) can be replaced by the right-hand sides of identities (3) and (4), respectively.

GOVERNING EQUATIONS AND BOUNDARY CONDITIONS FOR ESTUARINE FLOWS

Having derived formulae (1) and (2), we can obtain the integral momentum equation over an estuarine cross-section without any mathematical difficulty. Next we consider governing equations and boundary conditions for estuarine flows.

In the Cartesian coordinate system, the total velocity $u_i(\vec{X}, t)$ can be decomposed into the ensemble mean velocity $U_i(\vec{X}, t)$ and the turbulent velocity $u_i'(\vec{X}, t)$. Similarly, the total pressure and total density can be written as $p = p + p'$ and $\rho = \rho + \rho'$, respectively. In field work time averages are usually used, in particular, over a tidal period. For either temporal or ensemble averages the following results remain essentially the same except for the changes in definition. The continuity equation (Arthur, 1964) and Navier-Stokes equation are:

$$(5) \quad \frac{\partial \rho}{\partial t} + \frac{\partial (\rho u_i)}{\partial X_i} = 0 \, ;$$

$$(6) \quad \rho \frac{\partial u_i}{\partial t} + \rho u_j \frac{\partial u_i}{\partial X_j} + \frac{\partial P}{\partial X_i} - \nu \frac{\partial^2 u_i}{\partial X_j \partial X_j} - \rho g m_i = 0$$

where ν is the kinematic viscosity and $\vec{m}$ is a unit vector vertically downward.

Neglecting the ground water effect, the kinematic boundary condition that no flow passes through the boundary is expressed as

$$(7) \quad U_3 = U_1 \frac{\partial S}{\partial X_1} + U_2 \frac{\partial S}{\partial X_2} + \frac{\partial S}{\partial t}$$

Multiplying (7) by $\frac{\partial \varphi}{\partial \ell}$ and noting that $\left(\frac{\partial S}{\partial X_1}\right)\left(\frac{\partial \varphi}{\partial \ell}\right) = \left(\frac{\partial S}{\partial X_1}\right)_n$,

$$\left(\frac{\partial S}{\partial X_2}\right)\left(\frac{\partial \varphi}{\partial \ell}\right) = \left(\frac{\partial \psi}{\partial \ell}\right) \qquad \text{and} \qquad \left(\frac{\partial S}{\partial t}\right)\left(\frac{\partial \varphi}{\partial \ell}\right) = \left(\frac{\partial S}{\partial t}\right)_n ,$$

where $\left(\frac{\partial S}{\partial X_1}\right)_n$ and $\left(\frac{\partial S}{\partial t}\right)_n$ can be interpreted as the gradient and time

rate of change of S in the normal direction n , then the boundary condition (7) is rewritten as

$$(8) \quad U_3 \frac{\partial \varphi}{\partial \ell} = U_1 \left(\frac{\partial S}{\partial X_1}\right)_n + U_2 \left(\frac{\partial \psi}{\partial \ell}\right) + \left(\frac{\partial S}{\partial t}\right)_n$$

Evidently boundary condition (8) implies that

$$(9) \quad U_3 \frac{\partial \varphi}{\partial \ell} = U_1 \left(\frac{\partial S}{\partial X_1}\right)_n + U_2 \left(\frac{\partial \psi}{\partial \ell}\right) + \left(\frac{\partial S}{\partial t}\right)_n$$

for the mean velocities, and

$$(10) \quad U_3' \frac{\partial \varphi}{\partial \ell} = U_1' \left(\frac{\partial S}{\partial X_1}\right)_n + U_2' \left(\frac{\partial \psi}{\partial \ell}\right) + \left(\frac{\partial S}{\partial t}\right)_n$$

for the turbulent velocities.

Then taking ensemble averages of equation (5) and (6), we have:

$$(11) \quad \frac{\partial \bar{P}}{\partial t} + \frac{\partial (\bar{P} U_i)}{\partial X_i} + \left\langle \frac{\partial (P' u_i')}{\partial X_i} \right\rangle = 0$$

and (using the imcompressibility condition that $\frac{\partial U_i}{\partial X_i} = 0$):

$$\frac{\partial}{\partial t}\left\{\bar{P} U_i + \langle P' u_i' \rangle\right\}$$
$$+ \frac{\partial}{\partial X_j}\left\{\bar{P} U_i U_j + \langle P' u_i' \rangle U_j + \langle P' u_j' \rangle U_i + \langle u_i' u_j' \rangle \bar{P} + \langle P' u_i' u_j' \rangle\right\}$$
$$+ \frac{\partial \bar{P}}{\partial X_i} - \nu \frac{\partial^2 U_i}{\partial X_j \partial X_j} - \bar{P} g m_i = 0$$
$$(12)$$

where $\langle \ \rangle$ represents ensemble average.

THE INTEGRAL CONTINUITY AND MOMENTUM EQUATIONS FOR ESTUARINE FLOW

Having established the formulae (1) and (2), boundary conditions (9) and (10), the integral equations of continuity and momentum can be obtained readily. First let us integrate continuity equation (11) over a cross-sectional area σ and write down each term separately. By means of formula (2), the first term of (11) becomes

$$(13) \qquad \iint_\sigma \frac{\partial \bar{p}}{\partial t} \, d\sigma = \frac{\partial}{\partial t} \iint_\sigma \bar{p} \, d\sigma - \oint_c \left(\frac{\partial S}{\partial t} \right)_n \bar{p} \, d\ell$$

We separate the second term of (11) into two parts. The first part becomes

$$(14) \qquad \iint_\sigma \frac{\partial (\bar{p} U_1)}{\partial X_1} \, d\sigma = \frac{\partial}{\partial X_1} \iint_\sigma \bar{p} U_1 \, d\sigma - \oint_c \left(\frac{\partial S}{\partial X_1} \right)_n \bar{p} U_1 \, d\ell$$

and by means of the Green's theorem in the $x_2 - x_3$ plane the second part which consists of the x_2 - and x_3 - components becomes

$$(15) \qquad \iint_\sigma \left(\frac{\partial (\bar{p} U_2)}{\partial X_2} + \frac{\partial (\bar{p} U_3)}{\partial X_3} \right) d\sigma = \oint_c \bar{p} U_3 \, dX_2 - \oint_c \bar{p} U_2 \, dX_3$$

$$= \oint_c \left(\bar{p} U_3 \frac{\partial \phi}{\partial \ell} - \bar{p} U_2 \frac{\partial \psi}{\partial \ell} \right) d\ell$$

Combining equations (14) and (15) and using the boundary condition (9), we get

$$(16) \qquad \iint_\sigma \frac{\partial (\bar{p} U_i)}{\partial X_i} \, d\sigma = \frac{\partial}{\partial X_1} \iint_\sigma \bar{p} U_1 \, d\sigma + \oint_c \left(\frac{\partial S}{\partial t} \right)_n \bar{p} \, d\sigma$$

In the same manner we obtain from the last term of (11)

$$(17) \qquad \iint_\sigma \frac{\partial \langle p' u_i' \rangle}{\partial X_i} \, d\sigma = \frac{\partial}{\partial X_1} \iint_\sigma \langle p' u_i' \rangle \, d\sigma$$

noting that $\oint_c \left(\frac{\partial S}{\partial t} \right)_n \langle p' \rangle \, d\sigma = 0$ since $\langle p' \rangle = 0$ by definition.

Summing equations (13), (16) and (17), we have

$$(18) \qquad \frac{\partial}{\partial t} \iint_\sigma \bar{p} \, d\sigma + \frac{\partial}{\partial X_1} \iint_\sigma \left\{ \bar{p} U_1 + \langle p' u_i' \rangle \right\} d\sigma = 0,$$

the continuity equation integrated over a cross-sectional area.

From equations (14) and (16), the integral incompressibility condition can be readily obtained as:

$$(19) \quad \frac{\partial \sigma}{\partial t} + \frac{\partial}{\partial X_1} \iint_\sigma U_1 \, d\sigma = 0.$$

This equation (19) is a special case of (18), and was developed by Pritchard (1958). If we consider that the integration is over the same fluid particles passing through two cross-sections infinitesimally close to each other, from the definition of incompressibility that the density of a fluid particle is unchanged following its path, so $\frac{\partial}{\partial X_1} \iint_\sigma \langle \rho' u_1' \rangle d\sigma = 0$

and $\bar{\rho}$ can be taken out of the integration signs. Hence, equation (19) can be obtained from equation (18) as a special case.

As to the integration of the Navier-Stokes equation over a cross-sectional area, the essential operations are the same as before and the manipulations are cumbersome, so only the result is given here. After integration, the integral Navier-Stokes equation is

$$\frac{\partial}{\partial t} \iint_\sigma \{ \bar{\rho} U_i + \langle \rho' u_i' \rangle \} d\sigma$$

$$+ \frac{\partial}{\partial X_1} \iint_\sigma \{ \bar{\rho} U_1 U_i + \langle \rho' u_i' \rangle U_1 + \langle \rho' u_1' \rangle U_i + \langle u_1' u_i' \rangle \bar{\rho} + \langle \rho' u_1' u_i' \rangle \} d\sigma$$

$$+ \delta_{i1} \frac{\partial}{\partial X_1} \iint_\sigma \bar{P} \, d\sigma - g m_i \iint_\sigma \bar{\rho} \, d\sigma - \nu \frac{\partial^2}{\partial X_1^2} \iint_\sigma U_i \, d\sigma$$

$$+ \oint_c \left\{ \left(\frac{\partial S}{\partial t} \right)_n \langle \rho' u_i' \rangle - \delta_{i1} \bar{P} \left(\frac{\partial S}{\partial X_1} \right)_n - \delta_{i2} \bar{P} \left(\frac{\partial \psi}{\partial \ell} \right) + \delta_{i3} \bar{P} \left(\frac{\partial \varphi}{\partial \ell} \right) \right.$$

$$\left. + \nu \left(\frac{\partial S}{\partial X_1} \right)_n \left(\frac{\partial U_i}{\partial X_1} \right) + \nu \left(\frac{\partial \psi}{\partial \ell} \right) \left(\frac{\partial U_i}{\partial X_2} \right) - \nu \left(\frac{\partial \varphi}{\partial \ell} \right) \left(\frac{\partial U_i}{\partial X_3} \right) \right\} d\ell$$

$$- \nu \frac{\partial}{\partial X_1} \oint_c \left(\frac{\partial S}{\partial X_1} \right)_n U_i \, d\ell = 0$$

(20)

where δ_{ij} is a Kronecker delta such that $\delta_{ij} = 1$ if $i = j$ and 0 if $i \neq j$

It is noted that in many cases of estuarine flow the Reynolds stress terms are much larger than those terms associated with kinematic viscosity ν , and the integral equation (20) is then much simplified. Further, if we neglect the high-order terms $\oint_C <p' u_i'> \left(\frac{\partial S}{\partial t}\right)_n d\ell$ and

$\iint_\sigma <p' u_1'^2> d\sigma$, equation (20) in the X_1 - direction reduces to

$$\frac{\partial}{\partial t} \iint_\sigma \{\bar{p} U_1 + <p' u_1'>\} d\sigma$$

$$+ \frac{\partial}{\partial X_1} \iint_\sigma \{\bar{p} U_1^2 + 2<p' u_1'> U_1 + <u_1'^2> \bar{p}\} d\sigma$$

$$+ \frac{\partial}{\partial X_1} \iint_\sigma \bar{P} d\sigma = 0 ,$$

(21)

correct to the second order. This equation is of practical usefulness for the longitudinal variation of momentum across each cross-section of an estuary.

A SYSTEM OF INTEGRO-DIFFERENTIAL EQUATIONS FOR ESTUARINE FLOW

In this work the integral equations are obtained from the continuity equation and the Navier-Stokes equation. However, for most coastal plain estuaries in which tidal effect is strong enough to cause salt intrusion, an integral salt-balance equation is necessary to form a complete set of integro-differential equations for estuarine flow. This was derived by Pritchard (1958) and is written as follows:

$$(22) \quad \frac{\partial}{\partial t} \iint_\sigma \bar{S} d\sigma + \frac{\partial}{\partial X_1} \iint_\sigma \{\bar{S} U_1 + k_1 \frac{\partial \bar{S}}{\partial X_1}\} d\sigma = 0 ,$$

where $\bar{S}$ is the mean salt concentration and K_1 is the longitudinal diffusivity coefficient which is, in general, a function of $\vec{X}$ and t .

Altogether, equations (18), (20) and (22) form a complete set of equations governing the variations of mass, momentum and salt content across any cross-sectional area of an estuary.

For a sectionally homogeneous estuary, velocities, density and salt content are assumed constant over each cross-section, so that the integro-differential equations can be simply reduced to differential equations.

DISCUSSION

In the Navier-Stokes equation (6), the term of Coriolis force is omitted because it is a term of less importance compared to other terms in most estuarine flows. Among the three integro-differential equations, the equation (20) is most involved and may be too complicated for practical usefulness. But in most cases, it is essentially the equation (20) in the x_1-direction, i.e. equation (21) that needs to be taken into consideration.

For an hydraulic model to act like a corresponding estuary, the set of integro-differential equations should be satisfied in the model as it is satisfied in the estuary. Since a Froude model for an estuary with a basin of fairly large size usually cannot meet the requirement of Reynolds number similarity, (Von Arx, 1962) it is anticipated that in the Froude model this system of integro-differential equations will be satisfied in a manner different from that in the corresponding estuary. However, this set of equations should be the criterion for adjusting the flow in the Froude model in order to achieve a better simulation.

To verify the similarity of an hydraulic model of an estuary to that estuary from the point of view of conservation of mass, momentum and salt content, automated self-recording devices are necessary for instantaneous measuring of salinity, water depth and velocity. Better instruments

suitable for these "conservation tests" are being developed at VIMS. When these better instruments are available, detailed designs for the conservation tests will be established.

Appendix - On the Leibnitz Rule for Double Integral

First, the cross-sectional area σ (shown in Figure 17) can be represented in terms of S as follows:

$$(23) \quad \sigma = \int_c S \, dX_2 = \oint_c S \left(\frac{\partial \varphi}{\partial \ell} \right) d\ell$$

Then the quantity $\frac{\partial}{\partial t} \iint_\sigma f(\vec{X}, t) \, d\sigma$, the time rate of total sum of f over the cross-sectional area σ, can be summed up by two parts:

1. Due to time rate of change of f in the cross-section, i.e.

$$(24) \quad \iint_\sigma \frac{\partial f}{\partial t} \, d\sigma$$

and

2. Due to the time rate of change of the cross-sectional area σ, i.e.

$$(25) \quad \oint_c f \left(\frac{\partial S}{\partial t} \right) \left(\frac{\partial \varphi}{\partial \ell} \right) d\ell = \oint_c f \left(\frac{\partial S}{\partial t} \right)_n d\ell,$$

where $\left(\frac{\partial S}{\partial t} \right)_n$ means the time rate of change of S in the normal direction along C. Equation (25) is obtained in the same manner that equation (23) is derived. Therefore,

$$\frac{\partial}{\partial t} \iint_\sigma f \, d\sigma = \iint_\sigma \frac{\partial f}{\partial t} \, d\sigma + \oint_c f \left(\frac{\partial S}{\partial t} \right)_n d\ell.$$

Similarly, we have

$$\frac{\partial}{\partial X_1} \iint_\sigma f \, d\sigma = \iint_\sigma \frac{\partial f}{\partial X_1} \, d\sigma + \oint f \left(\frac{\partial S}{\partial X_1} \right)_n d\ell.$$

REFERENCES

Arthur, R. S. 1964. The equations of continuity for seawater and river water in estuaries. J. Mar. Res., 22:197-202.

Okubo, A. 1968. Private communication

Pritchard, D. W. 1958. The equations of mass continuity and salt continuity in estuaries. J. Mar. Res., 17:412-423.

vonArx, W. S. 1962. An Introduction to Physical Oceanography. Addision-Wesley, Reading, Mass., 422 pp.
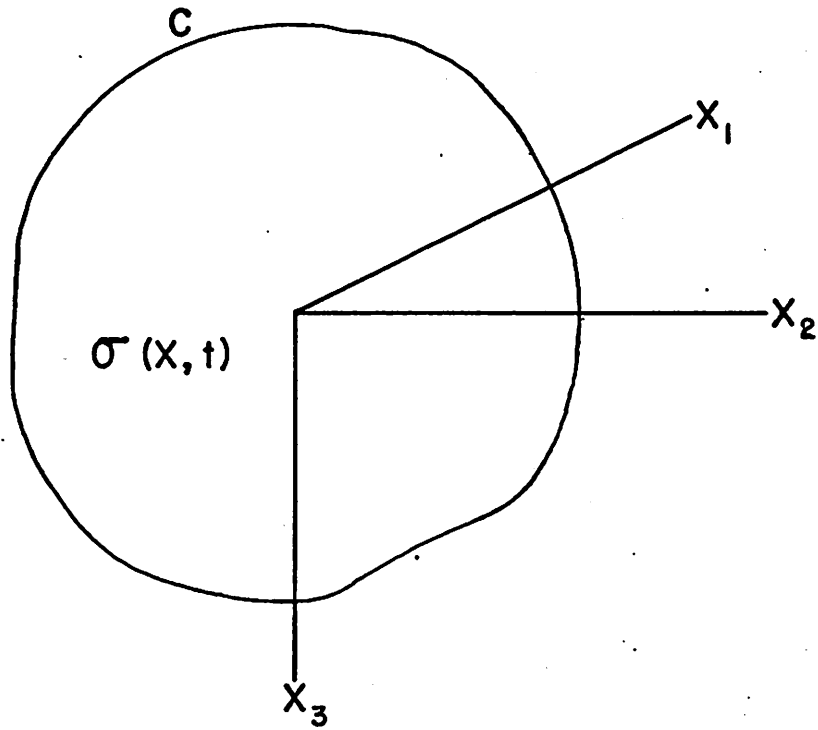
Figure 17. Arbitrary transverse cross-section.

Further Studies on the Integro-Differential Equations

for Estuarine Flow

Yee-chang Wang

In the previous report submitted to the Office of Water Resources Research (Hargis, 1969), a study on the integro-differential equations for estuarine flow in rectangular Cartesian coordinates. was made to find the cross-sectional variations of mass and momentum along an estuary with a fairly straight channel. In the present report, the application of the integrated continuity and momentum equations is studied further, and a set of integro-differential equations for estuarine flow in cylindrical coordinates is obtained for the purpose of studying the cross-sectional variations of mass and momentum along an estuary with a curved channel.

APPLICATION OF THE INTEGRO-DIFFERENTIAL EQUATIONS

The integrated continuity and momentum equations in rectangular Cartesian coordinates were obtained earlier (Wang, 1969). The integrated continuity equation is

$$(1) \quad \frac{\partial}{\partial t} \iint_\sigma \bar{\rho} \, d\sigma + \frac{\partial}{\partial X_1} \iint_\sigma \left\{ \bar{\rho} U_1 + \langle \rho' u_1' \rangle \right\} d\sigma = 0,$$

and the integrated longitudinal momentum equation is

$$(2) \quad \frac{\partial}{\partial t} \iint_\sigma \left\{ \bar{\rho} U_1 + \langle \rho' u_1' \rangle \right\} d\sigma$$

$$+ \frac{\partial}{\partial X_1} \iint_\sigma \left\{ \bar{\rho} U_1^2 + 2 \langle \rho' u_1' \rangle U_1 + \langle u_1'^2 \rangle \bar{\rho} \right\} d\sigma$$

$$+ \frac{\partial}{\partial X_1} \iint_\sigma \bar{P} \, d\sigma = 0$$

to the second order.

These two equations involve fluctuating quantities such as ρ' and u_1' which are assumed negligible in ordinary hydraulic equations for a stream tube. In the integrated continuity and momentum equations, two quantities that can indicate the turbulence of the estuarine flow are the correlation $\langle \rho' u_1' \rangle$ and the auto-correlation $\langle u_1'^2 \rangle$. The product of the auto-correlation $\langle u_1'^2 \rangle$ and the mean density $\bar{\rho}$ is twice the turbulent kinetic energy of the flow, and the quantity $\langle \rho' u_1' \rangle$ indicates the correlation between ρ' and u_1'. These two quantities can be expressed in terms of the mean values $\bar{\rho}, U_1$ and $\bar{P}$ of estuarine flow, under certain circumstances.

If the time averages over tidal periods are taken, then the integrated continuity equation and the integrated longitudinal momentum equation become

$$(3) \quad \frac{\partial}{\partial X_1} \iint_\sigma \left\{ \bar{\rho} U_1 + \langle \rho' u_1' \rangle \right\} d\sigma$$

and

$$(4) \quad \frac{\partial}{\partial X_1} \iint_\sigma \left\{ \bar{\rho} U_1^2 + 2\langle \rho' u_1' \rangle U_1 + \langle u_1'^2 \rangle \bar{\rho} + \bar{P} \right\} d\sigma = 0$$

where $\bar{\rho}, \bar{P}$ and U_1 are mean density, mean pressure, and mean longitudinal velocity averaged over tidal periods, and ρ', u_1' are turbulent fluctuations of density and longitudinal velocity relative to the time averages of density and longitudinal velocity. Equations (3) and (4) indicate that the total quantities in the integrands are conserved for each cross-section such that

$$(5) \quad \iint_\sigma \left\{ \bar{\rho} U_1 + \langle \rho' u_1' \rangle \right\} d\sigma = C_1$$

and

$$(6) \quad \iint_\sigma \left\{ \bar{\rho} U_1^2 + 2\langle \rho' u_1' \rangle U_1 + \langle u_1'^2 \rangle \bar{\rho} + \bar{P} \right\} d\sigma = C_2$$

These two equations involve fluctuating quantities such as ρ' and u_1' which are assumed negligible in ordinary hydraulic equations for a stream tube. In the integrated continuity and momentum equations, two quantities that can indicate the turbulence of the estuarine flow are the correlation $\langle \rho' u_1' \rangle$ and the auto-correlation $\langle u_1'^2 \rangle$. The product of the auto-correlation $\langle u_1'^2 \rangle$ and the mean density $\bar{\rho}$ is twice the turbulent kinetic energy of the flow, and the quantity $\langle \rho' u_1' \rangle$ indicates the correlation between ρ' and u_1'. These two quantities can be expressed in terms of the mean values $\bar{\rho}, U_1$ and $\bar{P}$ of estuarine flow, under certain circumstances.

If the time averages over tidal periods are taken, then the integrated continuity equation and the integrated longitudinal momentum equation become

$$(3) \quad \frac{\partial}{\partial X_1} \iint_\sigma \left\{ \bar{\rho} U_1 + \langle \rho' u_1' \rangle \right\} d\sigma$$

and

$$(4) \quad \frac{\partial}{\partial X_1} \iint_\sigma \left\{ \bar{\rho} U_1^2 + 2 \langle \rho' u_1' \rangle U_1 + \langle u_1'^2 \rangle \bar{\rho} + \bar{P} \right\} d\sigma = 0$$

where $\bar{\rho}, \bar{P}$ and U_1 are mean density, mean pressure, and mean longitudinal velocity averaged over tidal periods, and ρ', u_1' are turbulent fluctuations of density and longitudinal velocity relative to the time averages of density and longitudinal velocity. Equations (3) and (4) indicate that the total quantities in the integrands are conserved for each cross-section such that

$$(5) \quad \iint_\sigma \left\{ \bar{\rho} U_1 + \langle \rho' u_1' \rangle \right\} d\sigma = C_1$$

and

$$(6) \quad \iint_\sigma \left\{ \bar{\rho} U_1^2 + 2 \langle \rho' u_1' \rangle U_1 + \langle u_1'^2 \rangle \bar{\rho} + \bar{P} \right\} d\sigma = C_2$$

The quantity C_1 is the total mass flux through each cross-section and C_2 is proportional to the total energy of the flow across each cross-section.

The expression of $\iint_\sigma \langle \rho' u_i' \rangle d\sigma$ can be easily obtained from equation (5) in terms of $\bar{\rho}$, U_i, and constant C_1 as

$$(7) \quad \iint_\sigma \langle \rho' u_i' \rangle \, d\sigma = C_1 - \iint_\sigma \bar{\rho} U_i \, d\sigma$$

Eliminating the quantity $\iint_\sigma \langle \rho' u_i' \rangle U_i \, d\sigma$ from equation (6) by means of (7), an expression for $\iint_\sigma \bar{\rho} \langle u_i'^2 \rangle d\sigma$ can be obtained in terms of the constants C_1 and C_2. If the cross-sectional area σ changes slowly with time, the averages U_i and $\bar{\rho}$ can be expressed as

$$U_i = [U_i] + [U_i]'$$
$$\bar{\rho} = [\bar{\rho}] + [\bar{\rho}]'$$

where bracket $[\ ]$ represents the cross-sectional average of the time average, and $[\ ]'$ the deviation from this cross-sectional average. First let $U_i = [U_i] + [U_i]'$ in equation (5) and the second term in equation (6), so that equations (5) and (6) take the forms

$$(8) \quad \iint_\sigma \left\{ \bar{\rho} [U_i] + \bar{\rho} [U_i]' + \langle \rho' u_i' \rangle \right\} d\sigma = C_1$$

and

$$(9) \quad \iint_\sigma \left\{ \bar{\rho} U_i^2 + 2 \langle \rho' u_i' \rangle [U_i] + \langle u_i'^2 \rangle \bar{\rho} + \bar{P} \right\} d\sigma = C_2$$

where the high order term $\langle \rho' u_i' \rangle [U_i]'$ is neglected.

Equation (8), when multiplied by $2[U_i]$, becomes

$$(10) \quad \iint_\sigma \left\{ 2\bar{\rho} [U_i]^2 + 2\bar{\rho} [U_i][U_i]' + 2\langle \rho' u_i' \rangle [U_i] \right\} d\sigma = 2 C_1 [U_i]$$

Subtracting (10) from equation (9), we have

(11)
$$\iint_\sigma \bar{p} \langle u_i'^2 \rangle d\sigma = C_2 - 2C_1 [U_i] + \iint_\sigma \{\bar{p}[U_i]^2 - \bar{p}[U_i][U_i] + \bar{P}\} d\sigma.$$

In the integrand on the right-hand side the quantity $\bar{p}[U_i][U_i]$ is negligible compared with $\bar{p}[U_i]^2$ as long as $\dfrac{[U_i]}{[U_i]} << 1$.

Under these conditions, the integrated turbulent kinetic energy over a cross-sectional area becomes

(12)
$$\frac{1}{2}\iint_\sigma \bar{p} \langle u_i'^2 \rangle d\sigma = \frac{1}{2}\left\{ C_2 - 2C_1[U_i] + \iint_\sigma \{\bar{p}[U_i]^2 + \bar{P}\} d\sigma \right\}$$

Thus, the total turbulent kinetic energy over the cross-section $\frac{1}{2}\iint_\sigma \bar{p} \langle u_i'^2 \rangle d\sigma$ can be determined by the averaged quantities $[\bar{p}], [U_i]$ and $\bar{P}$, together with constants C_1 and C_2, which are the same for each cross-section.

With the constants C_1 and C_2 measured on one cross-section, the quantities $\iint_\sigma \langle p'u_i' \rangle d\sigma$ and $\frac{1}{2}\iint_\sigma \bar{p} \langle u_i'^2 \rangle d\sigma$ on other cross-sections can be determined from these constants together with the mean quantities $[\bar{p}], [U_i], \bar{p}$ and $\bar{P}$.

Under certain restriction, one can estimate the variations of $\iint_\sigma \langle p'u_i' \rangle d\sigma$ and $\iint_\sigma \bar{p} \langle u_i'^2 \rangle d\sigma$ owing to the change of the mean longitudinal velocity. If in a downstream part of an estuary where the tidal mean density does not change appreciably as the tidal mean velocity U_i changes slightly, the variation of the integrated correlations $\langle p'u_i' \rangle$ over the same cross-section can be obtained from equation (5). Let the mean velocity increases by ΔU, say $U_2 = U_{i1} + \Delta U$, then from equation (5)

(13)
$$\iint_\sigma \{\bar{p}(U_i + \Delta U) + \langle p'u_i' \rangle + \Delta \langle p'u_i' \rangle\} d\sigma = C_1$$

Then the difference in $\iint_\sigma \langle \rho' u_i' \rangle d\sigma$ due to the increase of mean velocity is

$$\delta \iint_\sigma \langle \rho' u_i' \rangle d\sigma \equiv \iint_\sigma \Delta \langle \rho' u_i' \rangle d\sigma$$

$$= -\iint_\sigma \{ \bar\rho (U_i + \Delta U) + \langle \rho' u_i' \rangle \} d\sigma$$

$$+ \iint_\sigma \{ \bar\rho U_i + \langle \rho' u_i' \rangle \} d\sigma$$

(14)

$$= -\iint_\sigma \bar\rho \Delta U d\sigma$$

Thus, the quantity $\iint_\sigma \langle \rho' u_i' \rangle d\sigma$ decreases by $\iint_\sigma \bar\rho (\Delta U) d\sigma$ if the mean velocity increases by ΔU. If the mean velocity U_i and its variation ΔU do not vary appreciably over a cross-section, the variation of $\iint_\sigma \langle u_i'^2 \rangle \bar\rho \, d\sigma$ can be estimated by equation (6) together with the result (14) as follows:

$$\delta \iint_\sigma \bar\rho \langle u_i'^2 \rangle d\sigma \equiv \iint_\sigma \bar\rho \Delta \langle u_i'^2 \rangle d\sigma$$

$$= -\iint_\sigma \{ \bar\rho (U_i + \Delta U)^2 + 2[\langle \rho' u_i' \rangle + \Delta \langle \rho' u_i' \rangle](U_i + \Delta U) \} d\sigma$$

$$+ \iint_\sigma \{ \bar\rho U_i^2 + 2 \langle \rho' u_i' \rangle U_i + \bar{P} \} d\sigma$$

$$= -\iint_\sigma \left\{ \begin{array}{l} 2\bar\rho U_i \Delta U + \bar\rho (\Delta U)^2 + 2\Delta \langle \rho' u_i' \rangle U_i \\ + 2 \langle \rho' u_i' \rangle \Delta U + 2 \Delta \langle \rho' u_i' \rangle \Delta U \end{array} \right\} d\sigma$$

$$= \iint_\sigma \Delta U \{ \bar\rho (\Delta U) - 2 \langle \rho' u_i' \rangle \} d\sigma$$

Thus, for a cross-section over which $\iint_\sigma \langle \rho' u_i' \rangle d\sigma$ is positive, if $\bar\rho (\Delta U) > 2 \langle \rho' u_i' \rangle$ then $\delta \iint_\sigma \bar\rho \langle u_i'^2 \rangle d\sigma$ increases as the mean velocity increases. On the other hand, if $\bar\rho (\Delta U) < 2 \langle \rho' u_i' \rangle$ then $\delta \iint_\sigma \bar\rho \langle u_i'^2 \rangle d\sigma$ decreases as the mean velocity increases.

It is noteworthy that for a cross-section over which $\iint_\sigma \langle \overline{\rho' u_i'} \rangle d\sigma$ is positive, when the mean velocity increases by an amount $2\langle \overline{\rho' u_i'} \rangle / \bar{\rho}$

then the turbulent kinetic energy of the flow begins to increase. For a cross-section over which $\iint_\sigma \langle \overline{\rho' u_i'} \rangle d\sigma$ is negative, the turbulent kinetic energy increases as the mean velocity increases.

THE INTEGRO-DIFFERENTIAL EQUATIONS FOR ESTUARINE
FLOW IN CYLINDRICAL COORDINATES

A set of integro-differential equations in rectangular Cartesian coordinates has been obtained for an estuary with a fairly straight channel in the previous report. Where the channel meanders, the estuarine flow is influenced by centrifugal force. For a meandering channel of circular arc, a set of integro-differential equations is obtained by integrating the conservation equations of salt, mass and momentum in cylindrical coordinates.

Let the center of cross-section of a part of the channel be along a circular arc with radius r , so that the cylindrical coordinates are set up with the origin at the center of curvature 0 , ϕ-axis along the tangent in the seaward direction, r-axis in the outward normal direction to the tangent and z-axis vertically upwards. In these coordinates, a typical cross-section $\sigma = \sigma(\phi, t)$ is shown in Figure 18. Since the free surface of the estuary fluctuates up and down with the tidal current, the free surface $-\eta$ is expressed as

$$\eta = -\eta(r, \phi, t)$$

the bottom $h = h(r, \phi, t)$, and two banks are expressed by $r_1(\phi, t)$ and $r_2(\phi, t)$. Combining $-\eta$ and h , the boundary C can be

expressed by $z = S(r; \phi, t)$ or $r = T(z; \phi, t)$; in parametric representation, $z = \psi(\ell; \phi, t)$ and $r = \phi(\ell; \phi, t)$, where ℓ is the arc length of the boundary C .

In these cylindrical coordinates, the Leibnitz rules for the double integrals are

(16)
$$\iint_\sigma \frac{\partial f}{\partial \phi} d\sigma = \frac{\partial}{\partial \phi} \iint_\sigma f d\sigma - \oint_C f \left(\frac{\partial S}{\partial \phi}\right)_n d\ell \ ,$$

$$\iint_\sigma \frac{\partial f}{\partial t} d\sigma = \frac{\partial}{\partial t} \iint_\sigma f d\sigma - \oint_C f \left(\frac{\partial S}{\partial t}\right)_n d\ell \ ,$$

(17)
where $\left(\frac{\partial S}{\partial \phi}\right)_n = \left(\frac{\partial S}{\partial \phi}\right) / \left(\frac{\partial \phi}{\partial \ell}\right)$ and $\left(\frac{\partial S}{\partial t}\right)_n = \left(\frac{\partial S}{\partial t}\right)\left(\frac{\partial \phi}{\partial \ell}\right)$

The continuity equation and the momentum equations (Goldstein, 1964) are

$$\frac{\partial \rho}{\partial t} + \frac{1}{r}\frac{\partial}{\partial r}(\rho r u) + \frac{1}{r}\frac{\partial}{\partial \phi}(\rho v) + \frac{\partial}{\partial z}(\rho w) = 0 \ ,$$

(18)
$$\frac{\partial}{\partial t}(\rho u) + \frac{\partial}{\partial r}(\rho u^2) + \frac{\partial}{\partial \phi}\left(\frac{\rho u v}{r}\right) + \frac{\partial(\rho u w)}{\partial z} + \frac{\rho(u^2 v^2)}{r}$$

(19)
$$= -\frac{\partial P}{\partial r} + u\left(\nabla^2 u - \frac{u}{r^2} - \frac{2}{r^2}\frac{\partial v}{\partial \phi}\right) \ ,$$

$$\frac{\partial}{\partial t}(\rho v) + \frac{\partial}{\partial r}(\rho u v) + \frac{\partial}{\partial \phi}\left(\frac{\rho v^2}{r}\right) + \frac{\partial}{\partial z}(\rho v w) + \frac{\partial \rho}{r}(v w)$$

(20)
$$= -\frac{\partial}{\partial \phi}\left(\frac{P}{r}\right) + u\left(\nabla^2 v + \frac{2}{r^2}\frac{\partial u}{\partial \phi} - \frac{v}{r^2}\right) \ ,$$

$$\frac{\partial}{\partial t}(\rho w) + \frac{\partial}{\partial r}(\rho u w) + \frac{\partial}{\partial \phi}\left(\frac{\rho v w}{r}\right) + \frac{\partial}{\partial z}(\rho w^2) + \frac{\rho u w}{r}$$

(21)
$$= -\frac{\partial P}{\partial z} + u \nabla^2 w$$

where ρ is density, P is pressure, μ is viscosity and u, v, w are velocity components in r, ϕ and z- direction, respectively. The conservation of salt is expressed by the equation

$$(22) \quad \frac{\partial(r\delta)}{\partial t} + \frac{\partial}{\partial r}(ru\delta) + \frac{\partial}{\partial\phi}(v\delta) + \frac{\partial}{\partial z}(rw\delta)$$
$$= \frac{\partial}{\partial r}\left(rk_r\frac{\partial\delta}{\partial r}\right) + \frac{\partial}{\partial\phi}\left(\frac{k_\phi}{r}\frac{\partial\delta}{\partial\phi}\right) + \frac{\partial}{\partial z}\left(rk_z\frac{\partial\delta}{\partial z}\right),$$

where δ is the averaged concentration of salt and K_r, K_ϕ, K_z are turbulent diffusivities defined as

$$(23) \quad \left. \begin{array}{l} K_r\frac{\partial\delta}{\partial r} = \langle u'\delta'\rangle \\[2mm] K_\phi\frac{1}{r}\frac{\partial\delta}{\partial r} = \langle v'\delta'\rangle \\[2mm] K_z\frac{\partial\delta}{\partial z} = \langle w'\delta'\rangle \end{array} \right\}$$

The kinematic boundary conditions are

$$w = \frac{\partial\eta}{\partial t} + u\frac{\partial\eta}{\partial r} + \frac{v}{r}\frac{\partial\eta}{\partial\phi} \qquad \text{on the free surface and}$$

$$w = -\frac{\partial h}{\partial t} - u\frac{\partial h}{\partial r} - \frac{v}{r}\frac{\partial h}{\partial\phi} \qquad \text{at the bottom.}$$

Summing up the above two boundary conditions, we have

$$(24) \quad w = \frac{\partial S}{\partial t} + u\frac{\partial S}{\partial r} + \frac{v}{r}\frac{\partial S}{\partial\phi}$$

Multiplying (24) by $\frac{\partial\phi}{\partial l}$, the boundary condition (24) becomes

$$(25) \quad w\frac{\partial\phi}{\partial l} = \left(\frac{\partial S}{\partial t}\right)_n + u\left(\frac{\partial\psi}{\partial l}\right) + \frac{v}{r}\left(\frac{\partial S}{\partial\phi}\right)_n$$

Similarly, the boundary condition for the turbulent velocities is

$$(26) \quad w' \frac{\partial \phi}{\partial \ell} = \left(\frac{\partial S}{\partial t}\right)_n + u' \left(\frac{\partial \psi}{\partial \ell}\right) + \frac{v'}{r} \left(\frac{\partial S}{\partial \phi}\right)_n \quad ,$$

where u', v' and w' are the turbulent velocities in r, ϕ and z directions. The boundary condition that no salt diffuses through the boundary due to the turbulent velocities is obtained as follows. Multiplying the boundary condition (26) by S', the turbulent fluctuation of salinity S', and taking ensemble averages, then the boundary condition becomes

$$(27) \quad \langle w'S' \rangle \frac{\partial \phi}{\partial \ell} = \langle u'S' \rangle \left(\frac{\partial \psi}{\partial \ell}\right) + \frac{\langle v'S' \rangle}{r} \left(\frac{\partial S}{\partial \phi}\right)_n \quad .$$

With the definitions of K_r, K_ϕ and K_z, the boundary condition (27) for salinity is

$$(28) \quad K_z \frac{\partial S}{\partial z} \left(\frac{\partial \phi}{\partial \ell}\right) = K_r \frac{\partial S}{\partial r} \left(\frac{\partial \psi}{\partial \ell}\right) + \frac{K_\phi}{r^2} \frac{\partial S}{\partial \phi} \left(\frac{\partial S}{\partial \phi}\right)_n .$$

Integrating the conservation equation of salt over any cross-section of an estuary, using the Leibnitz rule and the boundary condition, the resulted equation is

$$(29) \quad \frac{\partial}{\partial t} \iint_\sigma (rS) d\sigma + \frac{\partial}{\partial \phi} \iint_\sigma v S d\sigma = \frac{\partial}{\partial \phi} \iint_\sigma \frac{K_\phi}{r} \frac{\partial S}{\partial \phi} d\sigma$$

In this integrated conservation equation of salt (29), among the three turbulent diffusivities only K_ϕ appears. Thus, if the averaged concentration of salt S is known, K_ϕ can be calculated from the above equation.

Using the Leibnitz rule and the boundary conditions, the continuity equation and the momentum equations in cylindrical coordinates can also be averaged and integrated over any cross-sectional area along an estuary and are written as follows:

$$(30) \quad \frac{\partial}{\partial t} \iint_\sigma (r\bar{\rho}) d\sigma + \frac{\partial}{\partial \phi} \iint_\sigma \{ V\bar{\rho} + \langle \rho' v' \rangle \} d\sigma = 0 ,$$

and in the following integrated momentum equations, viscous terms are neglected since they are usually much smaller than Reynolds stress terms

$$\frac{\partial}{\partial t} \iint_\sigma \{ \bar{\rho} U + \langle \rho' u' \rangle \} d\sigma$$
$$+ \iint_\sigma \frac{1}{r} \{ \bar{\rho} U^2 + 2U \langle \rho' u' \rangle + \bar{\rho} \langle u'^2 \rangle - \bar{\rho} V^2 - 2V \langle \rho' v' \rangle - \bar{\rho} \langle v'^2 \rangle \} d$$
$$+ \frac{\partial}{\partial \phi} \iint_\sigma \frac{1}{r} \{ \bar{\rho} UV + \bar{\rho} \langle u'v' \rangle + U \langle \rho' v' \rangle + \langle \rho' u' \rangle V \} d\sigma$$
$$(31) \quad - \oint_c \bar{P} \frac{\partial \psi}{\partial \ell} d\ell = 0 ,$$

$$\frac{\partial}{\partial t} \iint_\sigma \{ \bar{\rho} V + \langle \rho' v' \rangle \} d\sigma$$
$$+ \frac{\partial}{\partial \phi} \iint_\sigma \frac{1}{r} \{ \bar{\rho} V^2 + 2V \langle \rho' v' \rangle + \bar{\rho} \langle v'^2 \rangle \} d\sigma$$
$$+ \iint_\sigma \frac{\partial}{\partial r} \{ \bar{\rho} UV + \langle \rho' u' \rangle V + \langle \rho' v' \rangle U + \bar{\rho} \langle u'v' \rangle \} d\sigma$$
$$(32) \quad + \frac{\partial}{\partial \phi} \iint_\sigma \frac{\bar{P}}{r} d\sigma - \oint_c \frac{\bar{P}}{r} \left(\frac{\partial S}{\partial \phi} \right)_n d\ell = 0 ,$$

and
$$\frac{\partial}{\partial t} \iint_\sigma \{ \bar{\rho} W + \langle \rho' w' \rangle \} d\sigma$$
$$+ \frac{\partial}{\partial \phi} \iint_\sigma \frac{1}{r} \{ \rho VW + \bar{\rho} \langle v'w' \rangle + W \langle \rho' v' \rangle + \langle \rho' w' \rangle V \} d\sigma$$
$$+ \iint_\sigma \frac{1}{r} \{ \bar{\rho} UW + \bar{\rho} \langle u'w' \rangle + W \langle \rho' u' \rangle + \langle \rho' w' \rangle U \} d\sigma$$
$$(33) \quad + \oint_c \bar{P} \left(\frac{\partial \phi}{\partial \ell} \right) d\ell = 0 ,$$

where $\langle \rangle$ denotes ensemble average $\overline{\rho}, \overline{P}, u, v, w$ are ensemble averages

of density, pressure, and velocities in r, ϕ and z directions.

REFERENCES

Hargis, W. J. Jr. 1969. Utilization of Physical and Mathemtaical Models in Marine Water Resources Research and Management. A report for the period 1 September 1967 - 31 December 1968. (OWRR Contract No. 14-01-001-1597, C-1214).

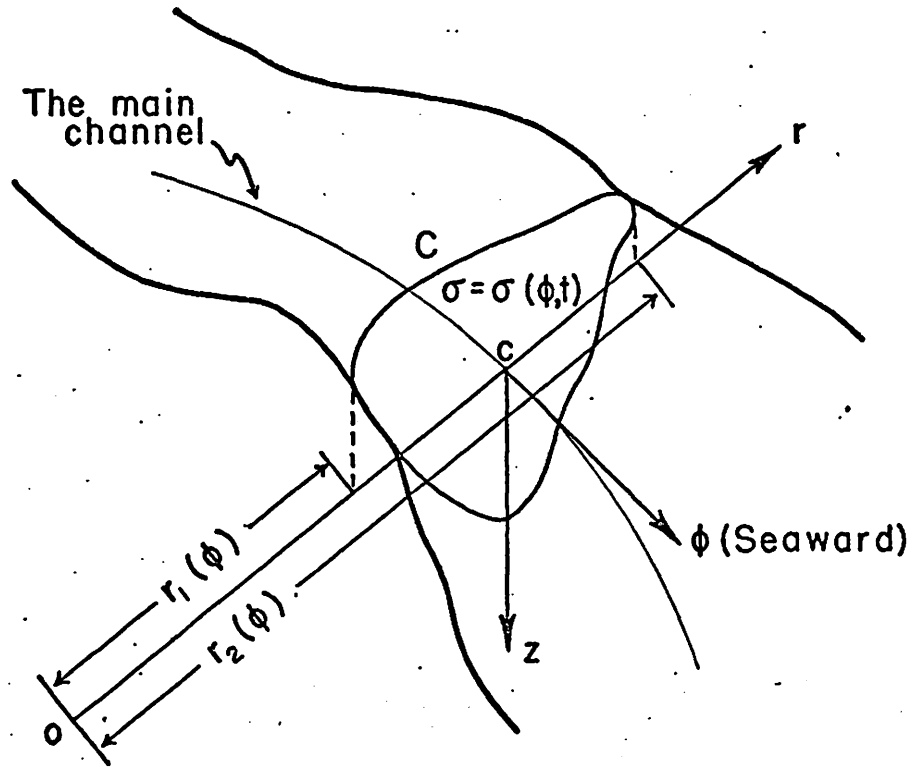Goldstein, S. 1964. Modern Developments in Fluid Dynamics. Dover.

Figure 18. A cross-section of an estuary in a cylindrical coordinate system.

Estuarine Computer Modeling:

A. A Two-Dimensional Computer Study of Estuarine Circulation and

B. One-Dimensional Analogue Simulation

Paul V. Hyer

A. A Two-Dimensional Computer Study of Estuarine Circulation

BACKGROUND

An estuary lies between the ocean, which is a reservoir of salt water, and a source of fresh water. In an estuary, therefore, a mixing of salt water and fresh water occurs. This mixing process is complicated by the fact that salt water is denser than fresh, so the mixing is accompanied by gravity-driven circulation.

One approach to the mathematical treatment of this advective diffusive system has been to treat the system as one-dimensional, with the molecular diffusivity replaced by a spatially varying dispersion coefficient (Ippen, 1966). Such an approach serves to mimic the gross features of the two-dimensional dynamics, but not to explain them.

A theoretical study of the two-dimensional processes occurring in estuaries has been made by Hansen and Rattray (1965). Their approach was to take the two-dimensional equations for momentum, mass conservation, and salt conservation, and derive from these a nonlinear pair of equations involving the stream function and salinity field. These equations are then solved analytically for various "regimes," i.e., sections of the system allowing specific approximations.

An attempt was made to solve these nonlinear equations numerically over the entire domain of interest, i.e., without breaking the system into a set of "regimes." From the equations, a set of finite difference equations was set up for a two-dimensional grid. These equations were solved as a boundary-value problem by the relaxation method (Shaw, 1953), also referred to as the implicit method (Fang, 1969).

DERIVATION

One chooses a coordinate system in which the z-axis points upward and the x-axis points downstream. These directions are opposite those used by Hansen (1965), but this difference affects only one arithmetic sign in the final equation. Keeping in mind this difference of coordinate system, the dynamic equations are:

$$(1) \quad \frac{1}{\rho} \frac{\partial P}{\partial x} = \frac{\partial}{\partial z}\left(A_v \frac{\partial u}{\partial z} \right),$$

$$(2) \quad \frac{1}{\rho} \frac{\partial P}{\partial z} = -g$$

In these equations A_v is the vertical eddy viscosity, P is the pressure, ρ the density, g the acceleration of gravity, and U the horizontal component of velocity. These equations apparently do not come from the quoted source (Pritchard, 1956), which treats the nonlinear terms as such. Equation (1) represents the horizontal balance of the pressure gradient against viscous drag. Equation (2) is the hydrostatic approximation. Cross-differentiating and combining to eliminate pressure, one obtains:

$$(3) \quad 0 = \frac{\partial \rho}{\partial z} \frac{\partial}{\partial z}\left(A_v \frac{\partial u}{\partial z} \right) + \rho \frac{\partial^2}{\partial z^2}\left(A_v \frac{\partial u}{\partial z} \right) + g \frac{\partial \rho}{\partial x}$$

It is assumed that density is a function of salinity only, so that one writes:

$$(4) \quad \rho = \rho_f \left(1 + \kappa S \right)$$

Since KS ≪ 1 , it can be shown that the first term in equation (3) is

much smaller than the second and that the equation becomes approximately

$$(5) \quad \frac{\partial^2}{\partial z^2} \left(A_V \frac{\partial u}{\partial z} \right) + g K \frac{\partial S}{\partial x} = 0$$

A stream function is introduced:

$$(6) \quad B w = \frac{\partial \psi}{\partial x}, \quad \text{and}$$
$$B u = -\partial \psi / \partial z, \quad \text{where}$$

B is the width of the stream. Equation (5) can then be written:

$$(7) \quad \frac{\partial^2}{\partial z^2} \left[A_V \frac{\partial}{\partial z} \left(\frac{1}{B} \frac{\partial \psi}{\partial z} \right) \right] - g K \frac{\partial S}{\partial x} = 0$$

The steady two-dimensional equation for salt conservation, including possible

variation of stream width, is

$$(8) \quad B \left(u \frac{\partial S}{\partial x} + w \frac{\partial S}{\partial z} \right) =$$

$$\frac{\partial}{\partial x} \left(B K_H \frac{\partial S}{\partial x} \right) + \frac{\partial}{\partial z} \left(B K_V \frac{\partial S}{\partial z} \right),$$

where K_H and K_V are the horizontal and vertical eddy diffusivities. Using

equations (6), this equation can be written:

$$(9) \quad \frac{\partial \psi}{\partial x} \frac{\partial S}{\partial z} - \frac{\partial \psi}{\partial z} \frac{\partial S}{\partial x} =$$

$$\frac{\partial}{\partial x} \left(B K_H \frac{\partial S}{\partial x} \right) + \frac{\partial}{\partial z} \left(B K_V \frac{\partial S}{\partial z} \right)$$

One assumes that B, Av, K$_H$, and Kv are constant, so that equations (7) and (9) become:

$$(10) \quad \frac{A_v}{B} \frac{\partial^4 \psi}{\partial z^4} - g K \frac{\partial S}{\partial x} = 0,$$

$$(11) \quad \frac{\partial \psi}{\partial x} \frac{\partial S}{\partial z} - \frac{\partial \psi}{\partial z} \frac{\partial S}{\partial x} = B K_H \frac{\partial^2 S}{\partial x^2} + B K_v \frac{\partial^2 S}{\partial z^2}$$

The equations are now nondimensionalized by introducing a set of scaling factors:

(12)   L = horizontal scale length;

H = vertical scale length;

So = characteristic salinity range;

R = river discharge.

Equations (10) and (11) then become:

$$(13) \quad \partial^4 \psi / \partial z^4 - N_1 \, \partial S / \partial x,$$

$$(14) \quad \frac{\partial \psi}{\partial x} \frac{\partial S}{\partial z} - \frac{\partial \psi}{\partial z} \frac{\partial S}{\partial x} = \left(N_2 \frac{\partial^2 S}{\partial x^2} + \frac{\partial^2 S}{\partial z^2} \right) N_3$$

where

$$(15) \qquad N_1 = \frac{g K S_0 H^4 B}{A_v L R},$$

$$N_2 = \frac{K_H H^2}{K_v L^2},$$

$$N_3 = \frac{K_v L}{H^2} \left(\frac{B H}{R} \right).$$

Hansen (1965, op. cit.) has noticed the similarity between N_1 and the Rayleigh number which appears in the theory of thermal convection (Rayleigh, 1916). The factor N_2 is an index of the relative importance of the horizontal and vertical diffusion processes. The remaining factor compares advection with diffusion. It can also be interpreted geometrically as the sine of the angle between isohalines and streamlines.

The boundary conditions to be satisfied by these equations are as follows:

i. No flux of salt or mass through the bottom and free surfaces;

ii. no slip at the bottom boundary;

iii. no stress at the free surface;

iv. no salt or vertical motion at the upstream limit of the system.

Mathematically, these conditions are:

$$(16) \quad \frac{\partial \psi}{\partial z} = \psi = \frac{\partial S}{\partial z} = 0, \quad at \ z = 0$$

$$\frac{\partial^2 \psi}{\partial z^2} = \frac{\partial S}{\partial z} = 0; \quad \psi = 1, \quad at \ z = 1$$

$$S = \frac{\partial \psi}{\partial x} = 0, \quad at \ x = 1$$

The pair of equations must be converted to difference equations in order to solve them on a digital computer.

$$(17) \quad \psi_{m,n-2} - 4\psi_{m,n-1} + 6\psi_{m,n} - 4\psi_{m,n+1} + \psi_{m,n+2}$$
$$- \frac{N_1 \Delta z^4}{2 \Delta x}\left[S_{m+1,n} - S_{m-1,n}\right] = 0, \quad and$$

$$(18) \quad \left(\psi_{m+1,n} - \psi_{m-1,n}\right)\left(S_{m,n+1} - S_{m,n-1}\right)$$
$$- \left(\psi_{m,n+1} - \psi_{m,n-1}\right)\left(S_{m+1,n} - S_{m-1,n}\right)$$
$$- \frac{4 N_3 \Delta x}{\Delta z}\left[S_{m,n+1} - 2S_{m,n} + S_{m,n-1}\right) = 0$$

The subscripts m and n denote the location of a point in a two-dimensional lattice. The vertical diffusion term has been neglected. The lattice spacings Δx and Δz are chosen to be 0.1. Extra lattice points are needed to express the boundary conditions. Hence, z = 0 corresponds to n = 2, z = 1 corresponds to n = 12, and x = 0 corresponds to m = 1, and x = 1 corresponds to m = 11. The boundary conditions are, in the finite difference formulation:

$$\psi_{m,3} = \psi_{m,1} \;\; ; \;\; S_{m,3} = S_{m,1} \;\; ; \;\; \psi_{m,2} = 0$$

$$(19) \quad S_{m,13} = S_{m,11} \;\; ; \;\; \psi_{m,13} = 2 - \psi_{m,11}$$

$$\psi_{m,12} = 1 \;\; ; \;\; S_{11,n} = 0 \;\; ; \;\; \psi_{12,n} = \psi_{10,n}$$

There is also a set of conditions demanded by the equations together with the boundary conditions. These conditions, once satisfied by the initial arbitrary fields, will continue to be satisfied.

$$(20) \quad \partial^4 \psi / \partial z^4 = \frac{\partial S}{\partial x} = 0 \; , \quad x = 1$$

$$\partial^2 S / \partial z^2 = 0 \; , \quad z = 0$$

Hence, far upstream the solution must be that occurring in the absence of salinity.

RESULTS

Typical values of the parameters N_1 and N_3 for the James River are (Hansen and Rattray, 1965; Bowden, 1967, p. 31):

$$(21) \qquad N_1 = 10^3$$

$$N_3 = 2$$

The program was tried with these values. It can be seen that the equations can be satisfied by the trivial solution:

$$(22) \qquad S \equiv 0$$

$$\psi = \frac{3z^2}{2} - \frac{z^3}{2}$$

In practice, this was the solution achieved by the computer program for a wide variety of initial conditions: In other cases, the solution tended to diverge. It is possible that point relaxation, or three-point simultaneous relaxation is unsatisfactory, and that the solution must be found simultaneous for all the points in a column. It is also possible that the value used for the parameter N_3 is outside the physically possible range. The salt conservation as used relate the Jacobean of the stream and salinity functions to a function of the salinity field. Hence, it might be the case that the factor N_3 must be of the order of magnitude of the trigonometric sine of the angle between a streamline and an isohaline, and so cannot be greater than unity.

The equations present a physically reasonable picture of the time-average behavior of an estuary. If salinity decreases going upstream and decreases vertically upward, then, according to equation (13), the fourth derivative of the stream function with respect to depth must be negative.

Given the bottom boundary condition, it follows that the stream function must be negative near the bottom (at least for $N_1 > 24$), i.e., there must be upstream motion along the bottom. Near the free surface, the isohalines tilt downwards with respect to the streamlines, looking up-stream. This process is opposed by vertical diffusion and by upstream transport along the bottom.

B. One Dimensional Analog Simulation

J. P. Schwar, of Lafayette College has adapted for use on the IBM 1130 computer an analog simulation program written by S. M. Morris (1967). This program is called LEANS, and is an attempt to bring to the user of a small computer a computing method which combines the convenience of analog programming and the accuracy of digital computing. The programmer can make the same sort of block diagrams that he would for use with a true analog computer, and quickly write a leans program from this diagram. Thereafter, "he need not concern himself with problems of convergence, stability, and other phenomena peculiar to digital computing. These factors are all compensated for automatically by the LEANS interpreter" (Morris and Schwar, op. cit. p. 2).

This program is presently being investigated to see if it can be used to solve one-dimensional time-independent estuarine problems involving salt balance, advection, and diffusion.

<div align="center">REFERENCES</div>

Bowden. 1967. Circulation and diffusion. In G. H. Lauff Estuaries, p. 15-36, Washington, D. C. (AAAS).

Fang, C. S., and M. Amein, 1969. Streamflow routing. Water Resources Research Institute, Tech. Report. No. 17, University of North Carolina.

Hansen, D. V., and M. Rattray, Jr. 1965. Gravitational circulation in straits and estuaries. Jour. Mar. Res., v. 23, no. 2, p. 104-122.

Ippen, A. T. 1969. Estuarine and Coastline Hydrodynamics, New York (McGraw-Hill).

Morris, S. M. and J. P. Schwar. 1967. The Lehigh Analog Simulator for the 1130. Misc. Publ., Computer Center, Lafayette College, Easton, Pa.

Pritchard, D. W. 1956. The dynamic structure of a coastal plain estuary. Jour. Mar. Res., v. 15, no. 1, p. 33-42.

Rayleigh, Lord. 1916. On convection currents in a horizontal layer of fluid, when the higher temperature is on the underside. Philosophical Magazine, Ser. 6, v. 32, In Barry Saltzmann, Theory of Thermal Convection, New York (Dover), 1962, p. 3-20.

Shaw, O. S., 1953. An Introduction to Relaxation Methods, New York (Dover).

INSTRUMENT AND TECHNIQUE DEVELOPMENT

Among the factors which severely limit the use of many estuarine hydraulic models, especially the family of estuarine models now in use at the Waterways Experiment Station, Vicksburg, Mississippi, in scientific and engineering research (and indirectly in planning and management activities) are a) lack of adequate instrumentation and b) lack of suitable hydraulic model-computer tie-in arrangements. Rectification of these shortcomings will greatly enhance chances of success in this program. The activities described below have been undertaken under this program.

Investigation of Progress in Automation of

Hydraulic Models at Other Centers

William J. Hargis, Jr., Paul V. Hyer and Maynard M. Nichols[8]

Though not likely to warrant preparation of a full-fledged report, this project will allow us to learn what has been done at other model centers toward improvement of hydraulic model systems, instruments and operating

---

[8]Associate Marine Scientist, Virginia Institute of Marine Science, Gloucester Point, Virginia

techniques. One of us (Hargis) has been associated with the models
developed at Alden Laboratories of Worcester Polytechnic Institute. Dr.
Nichols and others are in the process of studying techniques of instru-
mentation and control of hydraulic models developed in other countries.

A serious shortcoming at WES is the lack of in situ, multiple-
sensor recording instruments for use in salinity, temperature, current
and dye studies. Availability of such instrumentation would greatly
enhance scientific and engineering utility of these hydraulic scale
models.

Much of current sampling technique involves "destructive" sampling
in which a fairly large sample of water (in scale terms) is physically
removed from the system for analysis. Actual removal of the sample not
only eliminates a sizable part of the hydraulic system but it also causes
temporary disruption of stratification and salinity patterns which reduces
the resolution of the observations. Further, present manual sampling and
analysis techniques at WES require too many technicians and too much time
thus increasing the cost and making simultaneous collection of large numbers
of synoptically arranged samples, a very essential factor when one is deal-
ing with the shortened time spans that prevail in these Froude models in which
a complete tidal cycle requires only 7.4 minutes.

Multiple sensor recording units in use at Alden Laboratories,
for thermal studies, must be developed for other model parameters. A
report on instruments and control systems in use at the British Hydraulics
Research Station in Wallingford, England has been particularly enlightening.
Refinement in their systems include a) automatic recording instruments
which can accept over a hundred sensors and b) an automatic river-flow
control device which allows an annual hydrograph to be run without

attention. As indicated immediately below, we have made certain progress
toward development of more adequate sampling devices for use in the James
River hydraulic model.

An Automated Recording Salinometer for Use
in Hydraulic Scale Models

William G. MacIntyre[9]

INTRODUCTION

Experience with hydraulic models of estuarine areas at horizontal
scales of 1000:1 has shown that automated salinity measurement in these
models is desirable. Data rates and sampling sensities can be much
greater than with manual methods, and large models, like that proposed
for Chesapeake Bay, can be adequately sampled. The U. S. Army Corps of
Engineers is presently considering the use of automated systems for
hydraulic models.

THE SALINOMETER SYSTEM

Experiments were conducted to evaluate conductivity and temp-
erature sensors for use in hydraulic models. The conductivity sensor choice
was limited to platinum electrodes in various configurations, because
inductive sensors were necessarily so large as to impede water flow in the
model. The series cell of Holmes (1948) and the parallel cell of Hamon
(1956) were suitable. The former was selected because it had better
flushing, a higher cell constant, and lower flow resistance. Platinum
thermometers are ideal temperature sensors, but are prohibitively expensive.
Thermistors were used as an alternative and were found to be sufficiently
stable and accurate. Circuits like that designed by Hamon and Brown (1958),

---

[9]Associate Marine Scientist, Virginia Institute Marine Science,
Gloucester Point, Virginia

using thermistors for direct temperature compensation of conductivity and yielding salinity as an analog output, were considered. It was found most economical to use conductivity and temperature sensors that operate in a simple bridge circuit. Resulting temperature and conductivity readings can then be fed into a digital computer for the calculation of salinity. A simple bridge circuit has the further advantage that sensors are less complex and more reliable than those required for compensating circuits.

Commercial digitizing equipment was investigated and the Geodyne Corporation (Waltham, Mass.) was found to be the only manufacturer that directly digitizes the output of an A. C. bridge circuit. Geodyne digitizing electronics used in oceanographic equipment was suitable for use with hydraulic models. The manual digitizing bridge circuit shown in Figure 19 was built up with Geodyne components, producing the configuration shown in Figure 20. All components of the system except the digitizer unit were purchased or assembled at the Virginia Institute of Marine Science. The digitizer could not be purchased because funds were not available.

The phase-shift oscillator operates at $1KH_z$, and the bridge is transformer coupled to the oscillator and detection circuits to properly load the amplifiers.

Thermistor and conductivity-cell calibrations were made with a manual-balance digitizing ladder in place of the digitizer, and an oscilloscope was used to observe the bridge unbalance signal from the phase comparator. Electrical characteristics of the system were not altered by the absence of the digitizer. Table 6 gives a representative response for a conductivity cell in NaCl solution. Since NaCl is used in modeling

sea-water density, it must also be used in cell calibrations. Temperature response of the Fenwal (Framingham, Mass.) thermistor is given in Table 7.

Operation of the salinometer system is straightforward. Sensors are mounted in pairs so that temperature and conductivity are detected at the same points in the hydraulic model. Data from sensor pairs are required for calculation of salinity. The output of each sensor is balanced by a digitizing ladder network described by Perry (1965), and the digital word contained in the ladder is provided to a tape or computer interface with the digitizer. After all sensors are read, a gap is generated and the system recycles at a fixed rate. Fifty temperature-conductivity sensor pairs can be read in ten seconds at the standard rate of the Geodyne digitizer.

The cell constant of each cell must be determined by immersing it in a KCl solution of known conductance and measuring the cell resistance. The digital display monitor shown in Figure 20 facilitates cell constant determination by providing an instantaneous direct display of cell resistance.

Conductivity of water in the hydraulic model will be calculated by dividing the measured cell resistance by the cell constant. The resulting specific conductance will then be matched with the corresponding temperature and used in the equation of Weyl (1964) to give salinity. Weyl's equation applies to sea water, but will give consistent results for NaCl solutions. Later a table of specific conductances of high concentration NaCl solutions will be prepared and used in a similar equation applying to pure NaCl solutions

CONCLUSION

The system can be conveniently used in conjunction with sensors used for the automated measurement of tidal height or current speed and direction in hydraulic model. Control of tides and salinity at desired

levels could be achieved by using real time computer output to regulate
pumps and salt-addition devices supporting the model operation.

A ten sensor demonstration system has been proposed to the U. S.
Army Corps of Engineers. If the Corps, or other federal granting agency,
is able to fund fabrication of the system, it will be tested in the
hydraulic model of the James River estuary located at Vicksburg, Mississippi.

REFERENCES

Hamon, B. V. 1956. A portable temperature-chlorinity bridge for
    estuarine investigations and sea water analysis. J. Sci. Instrum.
    33, 329-

Holmes, J. F. 1948. Preliminary discussion of conductivity cells. WHOI
    Internal Report, July 7, 1948.

Perry, K. E., and Smith, P. F. 1965. Digital methods of handling
    oceanographic transducers. Marine Sciences Instrumentation 3,
    25-39.

Weyl, P.K. 1964. On the change in electrical conductance of sea water
    with temperature. Limnol. Oceanog. 9, 75-78.

Table 6   Cell Resistance Characteristics

Temperature 26°C

gm NaCl / liter	ohms
21.003	345
16.9940	414
15.035	463
13.004	528
10.983	614
8.993	728
7.000	917
5.038	1244

Cell constant   11.1

Table 7   Thermistor Resistance Characteristics

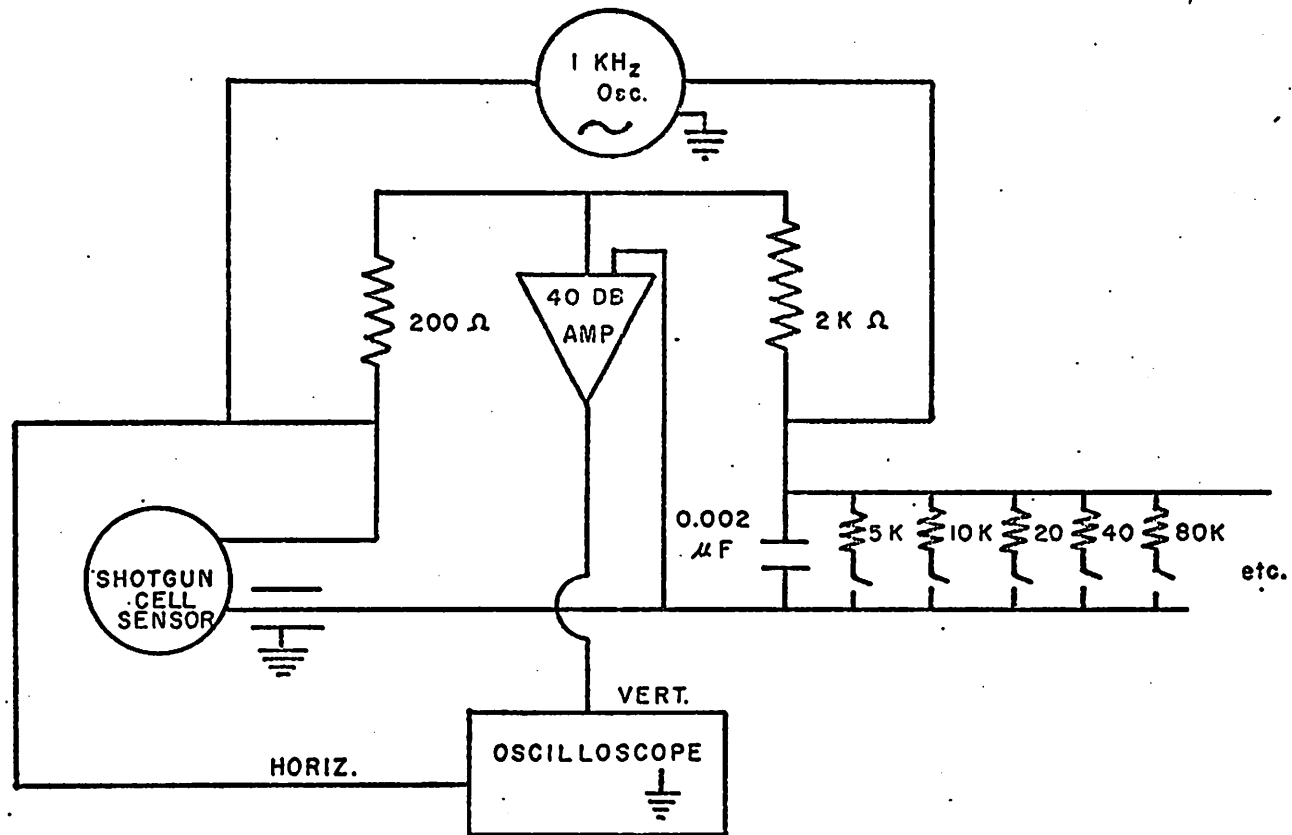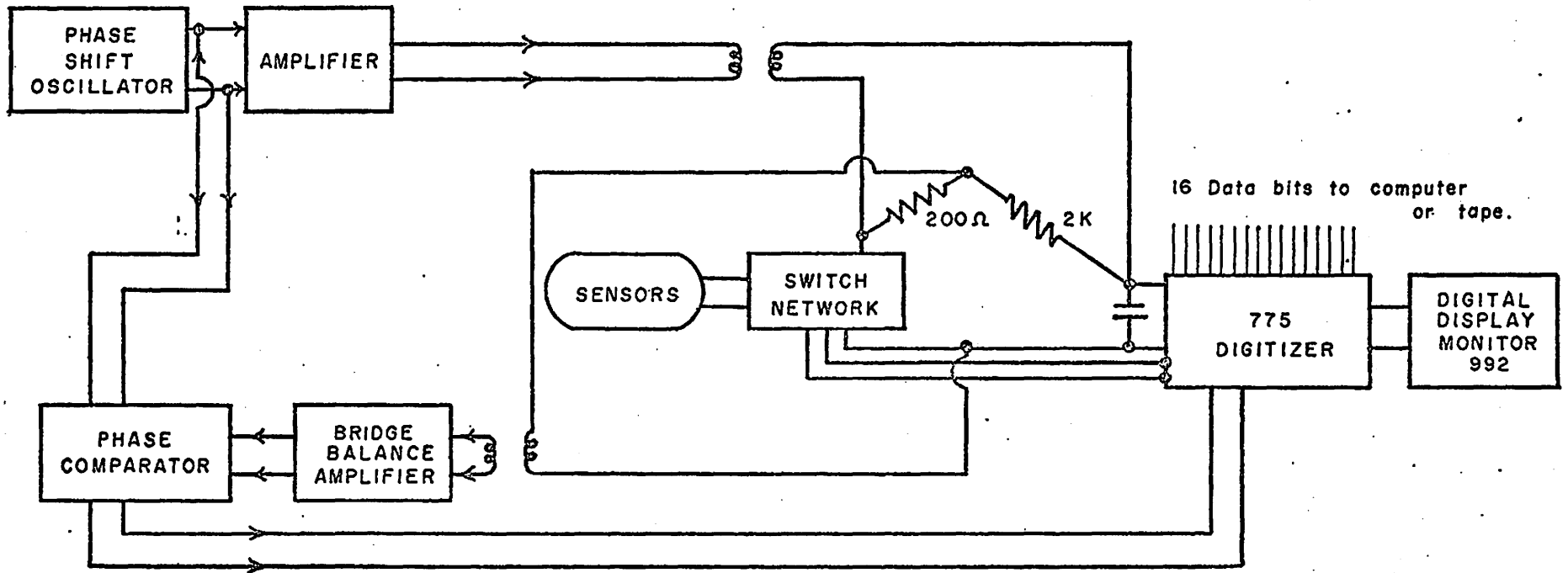| Temp. °C	ohms
0	1425
5	1141
10	919
15	746
20	609
25	500
30	413

Figure 19 · Salinometer Bridge Circuit.

Figure 20 Automated Multiple Sensor Salinometer System.

Development of a Miniaturized Current Meter for

Use in Hydraulic Scale Models

Evon P. Ruzecki

Present techniques of current speed and direction measurements now in use on the James River hydraulic model and similar estuarine models at WES are clearly inadequate. The instruments are physically large and therefore limited in resolution. They also disrupt the scaled system being studied. Worse, they require visual determinations in which the observer actually counts and manually records the rotations of a marked cup in a fixed time-period. Direction can be determined only grossly by recording rough observations of directional changes in the cup rotation or by visually observing or photographically recording dye and surface drifters.

To improve the quality and quantity of model current speed observations we have undertaken development of instrumented miniature current sensors capable of meeting the following criteria:

1. Sense current speed and direction <u>in situ</u> with accuracy and precision,

2. Allow frequent observation to give true indication of changing parameters,

3. Of smallest size possible to minimize disruption and allow use of many units,

4. Self-recording in digital format.

To meet these requirements, development studies undertaken with engineers and instrumentation specialists at NASA-Wallops have been moved

through two models or design series and are now in the third. These
are:

1. Savonius-type speed-sensor and vane direction sensor,
   abandoned because savonius sensor would not work due
   to insufficient size of rotor.

2. Price-type speed sensor and vane direction sensor.

3. Strain-gauge meter - present work is focused on a sphere
   suspended on a rigid rod. Deflection of the sphere by
   moving water is transmitted through the rod to a series
   of strain gauges. Strain gauge output is digitized.
   Sample rates can be as frequent as 100 per second,
   hence, a large volume of computer compatible data can
   be generated in a short time.

Adaptations of Computer Technology
to Hydraulic Model Systems

Paul V. Hyer, Richard Moncure and William G. MacIntyre

To increase capabilities of hydraulic scale models qualitatively
and quantitatively, VIMS has been engaged since 1966 in developing programs
for the computers at the model center WES (GE 2200) and at VIMS (IBM 1130
and 360) which will permit rapid processing of digital information and allow
graphical presentation directly from the computer. We hope, eventually,
to put computers on-line in model systems. This will obviously greatly
increase the scientific and engineering utility of hydraulic model systems
and particularly enhance development of mathematical models of estuarine
systems. Programs have already been developed here and elsewhere which allow:

1. Rapid reduction of model dye study data.

2. Production of displays for two-dimensional data by mapping directly from the computer.

3. Production of x-y graphs by local computer systems.

PRELIMINARY ANALYSIS OF THE UTILITY AND APPLICABILITY OF HYDRAULIC SCALE MODELS AND MATHEMATICAL MODELS TO SCIENTIFIC RESEARCH AND ENGINEERING DEVELOPMENT AND TO PLANNING AND MANAGEMENT

An objective implicit in this program as it has been developed is to examine and enhance the usefulness. Both techniques are undoubtedly valuable as tools for scientific research and engineering development. It is also clear that through the work proposed for this program as it continues and that going on elsewhere, the utility of these techniques can be improved markedly.

Review and analysis of the actual and potential utility of hydraulic and mathematical modeling techniques for planning and management of coastal and estuarine marine resources affirms that both are in actual use. Planning for development and use of marine environment and its resources and actual management thereof are now being aided by models, but their utility in these endeavors can be markedly improved, and this is an objective of this program.

In examining models and their utility and potential, we were impressed early by the partiality expressed by some individuals and/or organizations for one modeling technique over the other. Some claimed that mathematical models have eliminated or will soon do so, the necessity for hydraulic scale models (which are necessarily massive and costly) in work

on estuarine and coastal phenomena. Others contended that mathematical modeling techniques, especially when applied to the complexities of the four-dimensional estuarine circulation patterns were very limited in utility and would likely remain so.

Dispassionate analysis indicates that each has its weakness and good points. Each can be improved, but in all likelihood, neither will replace or eliminate the other due to their respective qualities and limitations. Though hydraulic scale models of estuarine and coastal areas are massive, requiring large sites and facilities and sizable investments of scientific and engineering talent, money and time to design, construct and operate, they are now capable of performing research and development work which is beyond the capability of the most sophisticated mathematical modeling operations. While mathematical modeling will undoubtedly be improved, it is unlikely that such models will ever develop to the point that they enable the detailed examination and manipulations which are possible in hydraulic scale models.

It is the opinion of this investigator that, rather than one technique pre-empting the other, both will be needed. Rather than any "startling" new developments arising in development of systems for planning, management and conservation of coastal and estuarine resources, we suspect that what will evolve or develop will be new arrangements of existing organizations and techniques.

For effective planning and management of the resources of the coastal zone, it seems to us that any effective management unit of each of the major segments of the coastal zone will have to be supplied with certain organizational arrangements for review and decision-making on

marine resource-use problems and that these review and decision-making units will require certain services. These services will involve readily accessible scientific and engineering advice and information and predictive capabilities. It will be necessary to supply the technological and scientific advisory entity with adequate tools. The most potent predictive tool will be "models systems" in which physical or hydraulic models (simplified and/or scale) will be used in conjunction with mathematical models.

With this in mind and our awareness of the weakness and strengths of both modeling techniques we hope that this program to develop and refine them will be continued by the Office of Water Resources Research.

ADVISORY ACTIVITIES

While this OWRR program has been underway, the Hydraulic Model unit and the oceanography section have been involved in certain advisory activities on scientific studies and practical matters.

Chiefly we have worked with the FWPCA in design of their hydraulic model diffusion and dispersal studies (related to pollution problems) on the reaches of the upper tidal James. Currently underway is preparation of an estimate of the computer requirements of the Chesapeake Bay model which was undertaken at the request of the Baltimore District of the Corps of Engineers.

SUMMARY

The program under consideration had several basic objectives. These were:

1. To examine and improve estuarine hydraulic modeling techniques.

2. To develop and improve mathematical concepts of estuarine and coastal phenomena.

3. To utilize each technique in comparison and developmental studies.

4. To evaluate and enhance, if possible, their utility in planning, development and conservation of marine resources.

Associated objectives have been a) to capitalize on the estuarine hydraulic model and the mathematical capabilities and the computer facilities at VIMS, and b) to recruit and train additional personnel.

Progress toward each of these objectives in the period between 31 December 1968 and the inception of the program in September 1967 has been noteworthy. Further the program is developing greater coherence as it progresses.

Operations in the early months of the program were restricted somewhat because of recruiting difficulties. However, during this period preliminary planning of the projected studies was possible.

HYDRAULIC MODEL STUDIES

During this period, Ruzecki and MacIntyre attempted development of an operable mathematical model of the tidal James using the Ketchum

technique, it was not entirely successful! More significantly, they undertook a study of the relationships between freshwater inflow and salinity in the estuarine portion of the James with a view toward developing the ability to predict salinity at a point or several points from appropriate freshwater inflow or even rainfall data. From this were developed certain concepts reported above. Further, the series of experiments involving pulsed-flow tests in the James River Model planned around this concept has been developed for this OWRR-supported program. We hope to be able to carry them out soon.

Recruiting efforts were finally successful in April of 1968, this research year when Hyer and Wang joined the group. Since that time marked progress has been made. Specifically, we have undertaken studies to determine the ability of the James River Hydraulic Scale Model (and others by analogy) to attain steady states and reproduce them. These basic characteristics had not been previously examined, only assumed. Preliminary indications are that steady states are attained within a certain definite number of tidal cycles for each level of freshwater inflow and reproducibility is good within certain reasonable limits. Additional studies to further examine these properties are required.

Another hydraulic model project involved an experiment with simultaneous point source releases of fluorescent and non-fluorescent dyes made at selected points in the model. These studies revealed details of circulatory patterns in the estuary of the tidal James which are quite interesting hydrographically. Previous concepts determined from studies of prototype data had indicated that water on the southerly side flushes more rapidly than that on the northerly side. This was confirmed in the

model studies. Unexpected was the comparative strength of this downstream southerly component. Of extreme interest are the unusual cross currents found in Burwell's Bay and the fact that in certain parts of Burwell's Bay the model indicates that flood predominates over ebb considerably; in fact, true ebb seems not to occur at some places. The significance of these results, if they also occur in nature, to movements of sediments and dissolved materials in Burwell's Bay is apparent. This series suggests other model studies and further, more careful studies in the James, itself.

A third model project involved utilization of the findings in the dye experiments reported above in attempts to evaluate earlier theories of factors affecting dispersion of oyster larvae in the James estuary (in narrative text above). Historically the most important seed area in the entire Chesapeake Bay area, sustaining 80 to 85 percent of all lower Bay oyster production, the James has fallen upon hard times. Well planned efforts are necessary to rebuild production there, if it is possible. We are attempting to apply hydraulic modeling techniques to this effort.

Preliminary results of the analyses of the significance of the results of the dye studies described above indicate that earlier notions of the importance of the upstream moving lower layer of saltier water as indicated by Pritchard in his work in 1953 may not be accurate and that other hydraulic mechanisms may be more important. Indications are that rehabilitative seedings of oyster larvae or establishment of colonies of adult brood oysters will be more productive if made at certain points along the northerly side than on the southerly. Surprisingly, the early analysis of model data indicates that releases made in the upper reaches of the estuary, the Burwell's Bay area, may be more successful. This is contrary to some earlier notions or models of the factors affecting distribution of oyster larvae in the James.

Preliminary results must be pursued with more detailed studies and further model and prototype work is indicated and planned for the next period of this program.

MATHEMATICAL MODELS AND COMPUTER STUDIES

Successful mathematical models of the structure and dynamics of estuarine waters and their circulatory and density patterns have not yet been developed here or elsewhere. Progress has been made toward this goal during this program.

Dr. Wang, one of the hydraulics specialists, has conducted theoretical studies of diffusion in estuaries since diffusion is a major component of estuarine hydraulics. In this work one-dimensional diffusion in a periodic current has been solved mathematically assuming a constant longitudinal eddy diffusivity using data from the model dye experiments described above.

Our hydraulics mechanics specialists have also conducted mathematical studies involving development of a system of integro-differential equations to determine the cross-sectional variations in mass, momentum and salt content along an estuary. The central mathematical problem of this integral approach--the Leibnitz rule for double integrals, has been obtained formally.

Dr. Wang's modeling studies have been fruitful, though somewhat preliminary, yielding refinements of and evaluations of earlier theoretical notions of estuarine circulation. Continuation and expansion is planned.

Dr. Hyer, our other hydraulics mechanics specialist, has undertaken development of a set of finite-difference equations to include salt advection (horizontal and vertical) and viscous dissipation factors in calculations of estuarine properties. This preliminary work must be continued as the program progresses.

Improvement in ability to deal mathematically with the factors involved in circulation of estuarine and coastal waters will depend upon continued involvement and improvement of high speed computers and development of analogue digital systems. To contribute we are studying the applicability of a computer program developed at Lehigh University which permits use of the IBM 1130 a digital machine, which we have, as an analogue device. It is hoped that this capability will aid in solution of complex problems involving partial differential equations so important in theoretical studies of estuarine circulation.

DEVELOPMENT OF IMPROVED INSTRUMENT CAPABILITIES AND TECHNIQUES FOR THE HYDRAULIC MODELS

To improve the quality and quantity of scientific and engineering studies on hydraulic scale models and enhance their use in planning and management and to permit future work in our mathematical and hydraulic model studies, we have undertaken a program to improve control and sensing systems in hydraulic models. This has involved 1) studies of advances in instrumentation and control systems of models at several stations in this country and abroad 2) development of projects to improve a) _in situ_ salinity observations and b) _in situ_ measurements of current speed and direction.

Work has also been undertaken in this OWRR program to develop
programs for several computers available here at VIMS and at Waterways
Experiment Station to put the computers "on-line" with the hydraulic models
and thus increase their capacities and capabilities and their utility in
science, engineering and marine resource management and planning.

ADVISORY ACTIVITIES

It is significant that the utility of both mathematical or
theoretical modeling and hydraulic scale modeling has been further demon-
strated by actual involvement of the members of this unit in efforts to
develop solutions of practical marine-resource use and development problems
even while the research program has progressed. Specifically, we have been
involved in a) preliminary evaluations of the effects of a proposed tidal
exclusion dam on the James estuary and b) development of studies of
dispersion and diffusion (with FWPCA-Charlottesville) of the upper tidal
reaches of the James for pollution purposes.

We have projected a series of future studies for the program.

CONCLUSIONS

In conclusion, we feel that this OWRR sponsored program has
made significant advances toward all its objectives and that the future will
see further advances.

Accomplishments can be indicated briefly as follows:

1. Have recruited and trained an increasingly competent team of
    fluid dynamicists and oceanographers who are capable of
    working with mathematical and hydraulic models and real
    problems.

2. Have made important contributions to critical evaluation and improvement of existing estuarine hydraulic scale model systems.

3. Have begun to improve on existing mathematical models of estuarine systems.

4. Have applied capabilities of scale models (by selves and with others) in development and evaluation of mathematical models of freshwater portions and estuarine portions of a classical, tidal tributary. This shows promise.

5. Have begun to improve instrumentation for automatic non-destructive, in situ sampling in hydraulic model systems.

6. Have actually applied these techniques to real marine resource use and coastal zone development problems.

7. Have plans for making scientific and engineering improvements in understanding of mechanics of estuaries and tidal tributaries and in development of techniques and suggestions for better planning and, use and management of the resources of these important parts of the coastal zone.

8. Stand excellent chance of bringing these plans off successfully, provided adequate support can be assured for the program.

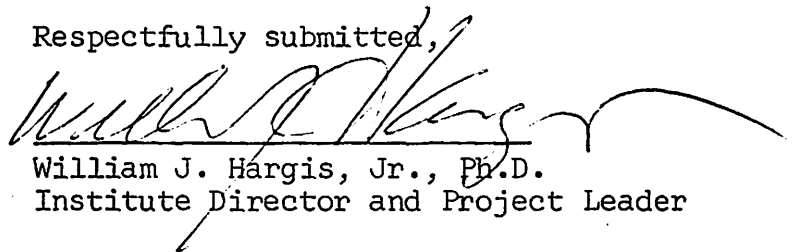FUTURE USES OF MODELING TECHNIQUES IN RESEARCH MANAGEMENT AND PLANNING

Of particular note are the emerging conclusions that both mathematical and hydraulic modeling techniques and, a newer concept, "mixes or systems of models" involving both will be important tools of those managers

and planners who will be involved in development, use and conservation
of important coastal and estuarine waters and the shorelines of the
coastal zone, especially those dealing with major sections of the environ-
ment such as bays and sounds and perhaps even coastal reaches of the sea.
The coherence of the various phases and projects of this program have
begun to emerge more clearly as the work has progressed!

Michelangelo contended that models were a most important part
of engineering development and well worth their costs.

There is little doubt that he would have agreed with us that
hydraulic models and mathematical models are extremely valuable tools for
PLANNING for and MANAGEMENT of the use and preservation of coastal marine
environments and their resources. That they can be improved and utilized
more fully is beyond question. Hopefully, the Office of Water Resources
Research will enable furtherance of this program.

<div align="right">

Respectfully submitted,

William J. Hargis, Jr., Ph.D.
Institute Director and Project Leader

</div>

BIBLIOGRAPHY

Hargis, William J., Jr. 1966. Final Report - Operation James River
An Evaluation of Physical and Biological Effects of the Proposed
James River Navigation Project. pp. 73. Special Sci. Rpt. in
Applied Marine Science & Ocean Engineering, No. 7, Virginia
Institute of Marine Science, Gloucester Point, Virginia

ACKNOWLEDGMENTS

Appendix I

Personnel Involved in Program

Period 1 September 1967 to 31 March 1968

Dr. W. G. MacIntyre, Physical and Chemical Oceanographer

Mr. E. P. Ruzecki, Physical Oceanographer

Dr. W. J. Hargis, Jr., Acting Head, Dept. of Physical and Chemical Oceanography and Project Director

Dr. Paul V. Hyer, Hydraulics Mechanics Specialist

Dr. Yee-chang Wang, Hydraulics Mechanics Specialist

Mr. Michael O'Brien, Graduate Research Assistant

Mr. David Tomb, Graduate Research Assistant

Mr. Harold N. Cones, Graduate Research Assistant

Mr. Richard W. Moncure, Computer Programmer

Mrs. Agnes D. Lewis, Oceanography Secretary

Other personnel participating have been a Key Punch Operator and an Illustrator.

Period 1 April 1968 to 31 December 1968

Dr. W. G. MacIntyre, Physical and Chemical Oceanographer

Mr. E. P. Ruzecki, Physical Oceanographer

Dr. W. J. Hargis, Jr., Acting Head, Dept. of Physical and Chemical Oceanography and Project Director

Dr. Paul V. Hyer, Hydraulics Mechanics Specialist

Dr. Yee-chang Wang, Hydraulics Mechanics Specialist

Mr. Michael Richardson, Graduate Research Assistant

Mr. Joseph T. DeAlteris, Graduate Research Assistant

Period 1 April 1968 to 31 December 1968 (Continued)

Mr. Richard Moncure, Computer Programmer

Mr. Walter Eanes, Laboratory Aide

Mr. W. C. Waddell, Laboratory Aide

Mrs. Agnes D. Lewis, Oceanography Secretary

Other personnel participating have been a Key Punch Operator and an

Illustrator.

Period 1 January 1969 to 30 September 1969

Dr. Wyman Harrison, Head, Dept. of Physical and Chemical Oceanography

Mr. E. P. Ruzecki, Physical Oceanographer

Dr. W. J. Hargis, Jr., Project Director

Dr. Paul V. Hyer, Hydraulics Mechanics Specialist

Dr. Yee-chang Wang, Hydraulics Mechanics Specialist

Dr. Ching Seng Fang, Hydraulics Mechanics Specialist

Mr. Joseph T. DeAlteris, Graduate Research Assistant

Mr. George Greer, Graduate Research Assistant

Mr. Richard Moncure, Computer Programmer

Mr. David Pinter, Laboratory Technician

Mr. James Sarver, Laboratory Aide

Mrs. Agnes D. Lewis, Oceanography Secretary

Other personnel participating have been a Key Punch Operator and an

Illustrator